

Index

SSC-105

WELD FLAW EVALUATION

MTRB LIBRARY

by

Samuel T. Carpenter

and

Roy F. Linsenmeyer

SHIP STRUCTURE COMMITTEE

SHIP STRUCTURE COMMITTEE

MEMBER AGENCIES:

BUREAU OF SHIPS, DEPT. OF NAVY
MILITARY SEA TRANSPORTATION SERVICE, DEPT. OF NAVY
UNITED STATES COAST GUARD, TREASURY DEPT.
MARITIME ADMINISTRATION, DEPT. OF COMMERCE
AMERICAN BUREAU OF SHIPPING

ADDRESS CORRESPONDENCE TO:

SECRETARY
SHIP STRUCTURE COMMITTEE
U. S. COAST GUARD HEADQUARTERS
WASHINGTON 25, D. C.

July 29, 1958

Dear Sir:

One phase of the research program of the Ship Structure Committee is directed toward improvement of methods of ship fabrication. An important element of such improvement is reduction of the size, number, and severity of flaws that may be introduced as a result of welding. The Ship Structure Committee has therefore sponsored a study at Swarthmore College aimed at establishment of criteria for evaluation of weld flaws. Herewith is the Final Report, SSC-105, of this project, entitled "Weld Flaw Evaluation", by Samuel T. Carpenter and Roy F. Linsenmeyer.

This project has been conducted under the advisory guidance of the Flaw Evaluation Advisory Group of the Ship Structure Subcommittee.

This report is being distributed to individuals and groups associated with or interested in the work of the Ship Structure Committee. Please submit any comments that you may have to the Secretary, Ship Structure Committee.

Yours sincerely,



K. K. Cowart, Rear Admiral
U. S. Coast Guard
Chairman, Ship Structure
Committee

Serial No. SSC-105

Final Report
of
Project SR-126

to the

SHIP STRUCTURE COMMITTEE

on

WELD FLAW EVALUATION

by

Samuel T. Carpenter and Roy F. Linsenmeyer

Department of Civil Engineering
Swarthmore College
Swarthmore, Pennsylvania

under

Department of the Navy
Bureau of Ships Contract NObs-72060
BuShips Index No. NS-011-067

Washington, D. C.
National Academy of Sciences-National Research Council
July 29, 1958

ABSTRACT

This is a detailed final report on a series of investigations made to determine a basis for the evaluation of the ability of weld flaws to initiate brittle fracture. The report is in four parts dealing successively with (1) brittle fracture mechanics based on the Griffith theory and on Irwin's strain-energy release rate adaptations, (2) static tests on flawed butt welds, (3) static and dynamic tests on small butt weld flaws with and without residual stress, and (4) static tests on weld flaws in a controlled field of high residual stress.

All welding flaws in selected materials were simulated flaws, varied to represent lack of penetration, porosity, lack of fusion, or sharp internal weld cracks.

The major objective was to examine the effect of given flaws in various environments, in order to determine the environment essential to initiate brittle fracture under low static stress conditions. Low temperature was generally an essential part of the environment, but low static stress initiation could not be procured below the nominal yield point unless the static stress was augmented by either a dynamic stress or a high previously-incurred residual stress. The residual stress environment proved to be most significant. Brittle fractures were initiated from short internal cracks with as small as 2000 psi of applied static stress at temperatures in the order of 0°F. If total brittle fracture did not result, arrested fractures occurred from small buried flaws, with the arrested crack forming a potential source of fracture initiation.

Finally, this report emphasizes the important bearing that residual stress has on the brittle fracture problem and the need for extended investigations in brittle fracture mechanics based on strain-energy release rates to furnish a complete engineering basis for flaw evaluation.

TABLE OF CONTENTS

	<u>Page</u>
Introduction	1
Part I - Crack and Flaw Propagation Theory	2
Part II - Flaws in Butt Welds	11
A - Incomplete-penetration butt welds	11
Specimens	13
Test set-up and instrumentation	13
Test results	15
Summary	19
B - Static strength of flawed butt welds	20
Cracks, internal and external, of varying lengths	20
Part III - Weld Flaws with Residual Stress - Static and Dynamic Stress Interaction	29
Introduction	29
Series "A" Specimens	31
Summary, Series "A"	38
Type "B" specimens	40
Dynamic stress studies - Type "B" Specimens	44
Summary - "B" Series	44
Analysis of Type B specimens by principle of strain-energy release rate	49
Type "C" Specimens	51
Discussion	51
Summary - Type "C" specimens	62
Summary of Part III	69
Part IV - Weld Flaws in Residual and Static Stress Fields	74
Introduction	74
Type of specimens	76
Test results - 50% buried flaw	81
Test results - 75% buried flaw	96
Test results - 100% (full thickness) flaw	103
Determination of force tendency - slotted plate	108
Overall Summary Statements	112
Acknowledgments	116
References	117

INTRODUCTION

This project has been directed toward an evaluation of weld flaws, their severity and effect in establishing conditions for fast brittle fracture, as well as the role of such flaws in impairing the strength of welded structures. The total environment of these weld flaws was also studied to explain, if possible, the low-nominal-stress fractures noted in service.

Part I of this report presents a theory based on strain-energy release rates, and its adaptations, so that subsequent discussion of test results may include analytical considerations.

Part II of the report first deals with the static tension tests made on butt welds, representing controlled but varied lack of penetration for the full length of weld. A second phase of this section presents the results of tests on internal flaws of variable length and penetration to represent lack of fusion, porosity, or internal and external weld cracks. These studies indicate that the effect of lack of fusion or penetration on strength is predictable on the basis of available weld area. While cleavage fractures may be initiated from such flaws by static tension, the test environment was not such as to initiate brittle fracture at low-nominal-stress values.

Part III describes extended experimentation with short full-thickness and buried flaws in which the flaws were subjected to a residual stress field. Initial experimentation to determine the effect of residual stress consisted of delivering a sledge-hammer impact to small-flawed tension specimens where the flaw was under an induced residual stress. Tests indicated that fracture initiation could occur at low tensile stress under these conditions. A refinement in inducing the impact was then introduced by using a drop-weight device to superimpose a dynamic effect on static axial tension. The results of these experiments all point toward a reduction in impact to initiate brittle fracture as the initial residual stress system surrounding the flaw is increased in intensity. Although the original goal

of obtaining interaction curves between static and dynamic stress was not obtained, it has been shown that it is possible with residual stress present to initiate a brittle fracture at a low-static stress without external dynamic loading.

Part IV returns to a discussion of static tension tests and experimentation on short buried flaws under controlled biaxial residual stress conditions. Brittle fracture initiation and propagation have been established by static means alone under superimposed tension of as low as 2500 psi, while the internal weld flaw has been as short as 1-1/2 in. Static tensions of about 10,000 psi have also induced initiation and propagation from flaws 3/4 in. in length.

Theoretical comparisons have been made throughout the report with the studies of A. A. Griffith¹ and G. R. Irwin^{2, 3} introduced in Part I, which deal with brittle fracture from crack-like flaws. The basis of the classical Griffith theory is that a flaw will be self-propagating when the available elastic strain energy is equal to or greater than the work required to extend the crack.

As an introductory summary, it appears that on the basis of this investigation, residual stress is one of the important factors in establishing the environment contributing to brittle-fracture initiation from flaws under the influence of low-applied static stress.

Part I

CRACK AND FLAW PROPAGATION THEORY

An understanding of the factors encountered in the study of initiation and propagation of brittle fracture will depend ultimately on a broad fundamental knowledge of fracture phenomena and related theory. While much is still to be learned, including the brittle strength of metals, the theory of brittle fracture dealing with initiation and propagation from sharp cracks stems from the basic considerations of A. A. Griffith.¹ G. R. Irwin^{2, 3} and others have refined and restated Griffith's concepts, but significant

improvements in the field have come only from elimination of some of the limiting assumptions of the original Griffith analysis. Experimental correlations and application of these theories have been made by A. A. Wells^{4, 5} and others and is continued in this report with an extension in application to the case of buried flaws.

The basic premise of the Griffith theory is that a sharp crack or crack-like flaw will induce and sustain a self-propagating brittle fracture when the elastic energy from the strained elements of the plate is equal to or greater than the brittle fracturing work rate required to fracture the material. Under this concept, two separate considerations are involved: first, it is essential to determine or account for the changes in strain energy that occur as a crack extends or grows; and second, the relevant properties of the material through which the crack extends must be determined. This second consideration logically deals with the rate of increase of the cracked surfaces' total surface energy and is associated with surface tensions. Although the total concept may be oversimplified, it merits recognition due to its basic fundamental energy approach.

The first consideration, the origin of the released strain energy, was demonstrated by Griffith as follows: consider an infinitely wide plate of thickness "t" with a central full-thickness sharp crack of length "x" oriented at right angles to the applied tension. If the axial tension force is such as to provide a unit stress of σ (based on the gross area of plate), the crack will open to an elliptically-shaped hole which has a volume of $\frac{\pi \sigma x^2 t}{2E}$ where E is Young's Modulus. Assuming that the pulling heads are fixed against movement and that a tensile stress can be applied along the boundary of the elliptical hole, then, as this stress builds up to a value of σ , the crack will close. This means that work has been done to close the crack equal to $\frac{\sigma}{2}$ times the volume of the crack opening. It is further assumed that, if this is the work done in closing the crack, it is also the total strain energy released as the crack grows from zero length to length x. Calling this strain energy W, then

$$W = \frac{\pi \sigma^2 x^2 t}{4 E}$$

To determine the strain energy dW released as the crack grows from a length x to a length $x + dx$,

$$\frac{dW}{dx} = \frac{\pi \sigma^2 x t}{2 E}$$

In order to determine when the energy released equals the work required to produce the incremental increase in crack surface, Griffith equated dW with the unit surface energy α times the new crack-surface area:

$$\frac{\pi \sigma^2 x t}{2 E} dx = 2 \alpha t dx$$

$$\sigma = \sqrt{\frac{4 \alpha E}{\pi x}}$$

This is called the Griffith equation.

G. R. Irwin³ suggests that $\frac{dW}{dA}$, the area rate of energy release, be termed "G" and interpreted as the force tendency tending to produce self propagation of the crack in the brittle mode. This can be found from the equation above for $\frac{dW}{dx}$ by substitution of $dA = t dx$, or

$$\frac{dW}{dA} = \frac{\pi \sigma^2 x}{2 E}$$

It will be recalled that the testing heads applying the stress were assumed fixed; hence, for this condition to apply, fast crack propagation is implied. It is also implied that the value of σ in effect at time of fracture is the critical stress for the given combination of "G" and crack length.

Irwin has expanded these views, incorporating stress functions of Westergaard⁶, to apply to a crack in a plate of finite width. The Irwin expression

for a single central full thickness crack is given as

$$G = \frac{\pi \sigma^2 a \tan (\pi a/b)}{E (\pi a/b)}$$

where a = one half of the crack length or x/2

b = finite width of the plate

or simplified

$$G = \frac{\sigma^2 b}{E} \tan \frac{\pi x}{2b}$$

In reading this section, it should be thoroughly understood that σ is the unit stress on the gross cross-section of the plate. In presenting subsequent test data, the gross stress σ is given instead of the stress on the reduced or net cross-section. This is thought to be justifiable since, in the nominal design situation, a flawless structure is postulated and gross stress evaluated.

The energy-release rate must at least equal the fracturing-work rate for fracture propagation to take place. Thus, in the redefining of the energy-release rate as a force tendency "G," it is apparent that "G" can also be thought of as the resisting force tendency of the material. If "G" varies with the material, experimental procedures may be used to determine its value, which in all probability is dependent on size as well as material. Accordingly, tests were made as will be described.

To determine "G" for weld metal, cracks of various percentages of plate width were made with a jeweler's hack-saw cut in butt welds joining plates 2-1/2-in. wide by 1/2-in. thick. The tensile loading was applied when the specimen was at a temperature of -80 F to insure a fast and complete brittle fracture. (The tests were also repeated with the crack being introduced in plate material instead of in a weld.) Using the formula $G = \frac{\sigma^2 b}{E} \tan \frac{\pi x}{2b}$, "G" was computed and is shown plotted in Fig. 1.1. Although "G" was not constant, the average of "G" for weld metal is 100 in.-lb per sq in., and for the plate, 80 in.-lb per sq in. A second brief set of tests

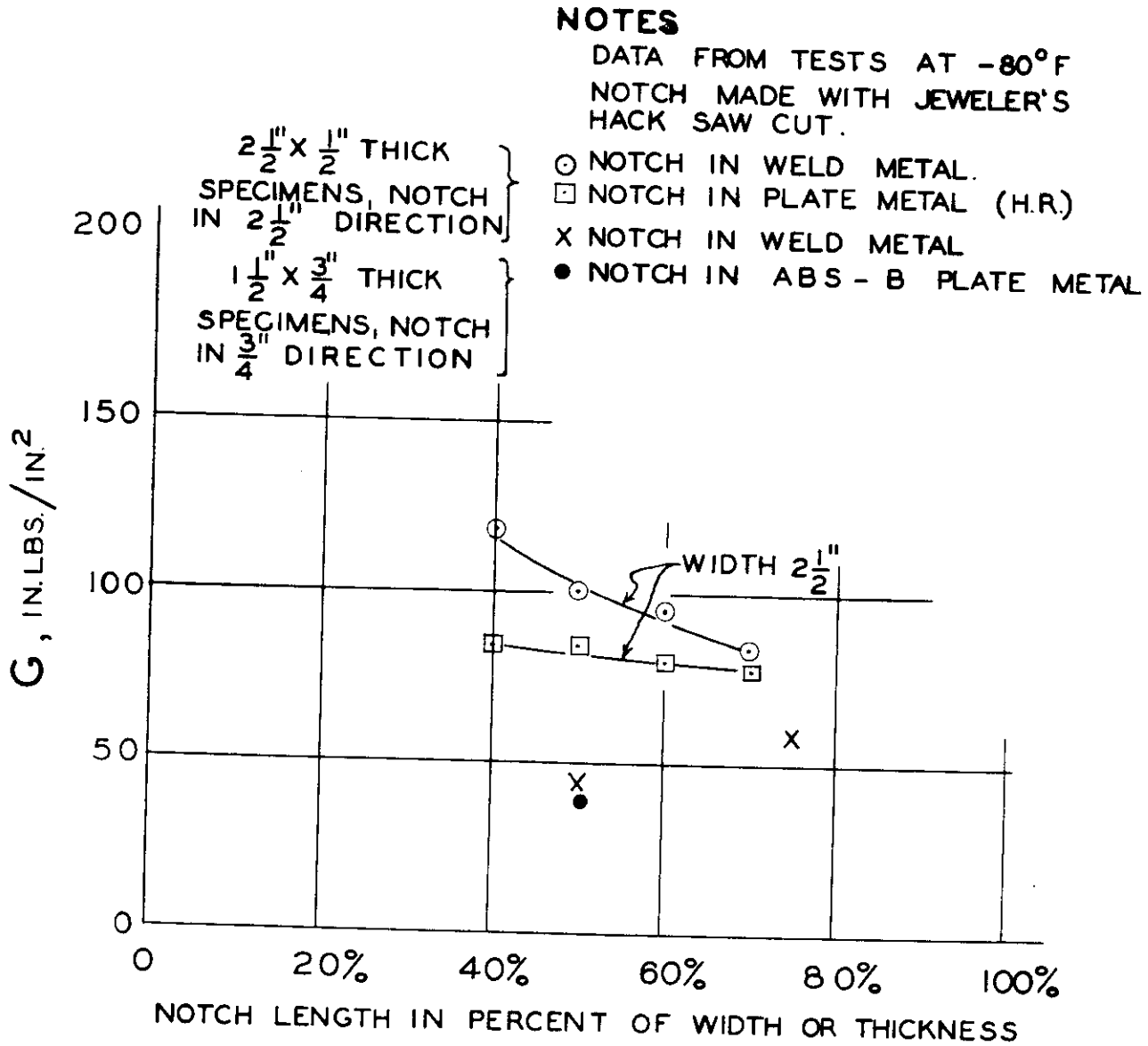
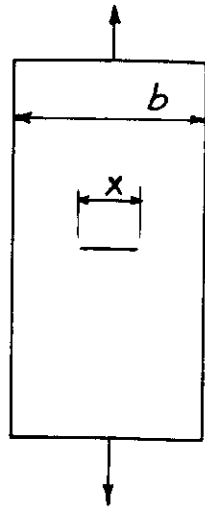


FIG. 11
"G" FACTOR TEST

was made using specimens 3/4-in. wide and 1-1/2-in. thick, with the full thickness crack sawed in and showing in the 3/4-in. dimension. The central cracks used were 3/8 in. and 9/16 in. in length, representing respectively 50% and 75% of the 3/4-in. dimension. In the formula, b now becomes 3/4 in. The results of tests at -80 F are shown in Fig. 1.1, the weld metal having an average "G" value of 50 in.-lb per sq in., and the plate 40 in.-lb per sq in. The variation in "G" between the two sets of tests may be due to size effects, which are not included in current theory.

To investigate width effects, tests were made in three series of 1/2-in. thick flat-plate specimens of hot-rolled steel, varying in width. The first series was planned to make $b \tan \frac{\pi x}{2b}$ equal to 2.5 and, in the second and third series, this parameter, termed "K," was made 5 and 7.5 respectively. The notch was made with a jeweler's hack-saw cut with notch lengths in each series representing, in consecutive specimens, a notch length 25%, 37.5%, 50%, 62.5% and 75% of the plate width. Plate widths ranged in the first series from 1.03 in. to 6 in., in the second series 2.06 in. to 12 in., and in the third series 3.09 in. to 18 in.; however, the latter 18-in. wide specimen was not tested. All tests were made at -100 F, and all fractures were brittle with no visible evidence of yielding at the notch. The average gross stress for fracture ranged from 20,400 psi to 41,300 psi as plate width increased.

It may be stated further that the gross stresses to fracture for the three series were nearly equal for equal ratios of notch width to plate width. The "G" values calculated from the test data and the Irwin equation are shown in Fig. 1.2. It is to be noted that width has a great effect on the calculated value of "G," which implies either that "G" has a changing value due to size effect, or that the theoretical equation may require modification. At this time, however, this phase has not been investigated further and must be considered as exploratory only. It must be established that all criteria associated with brittle fracture stemming from a sharp crack have been met by the experimentation.



$$G = \frac{\sigma^2 b}{E} \tan \frac{\pi x}{2b}$$
$$= \frac{\sigma^2}{E} (K)$$

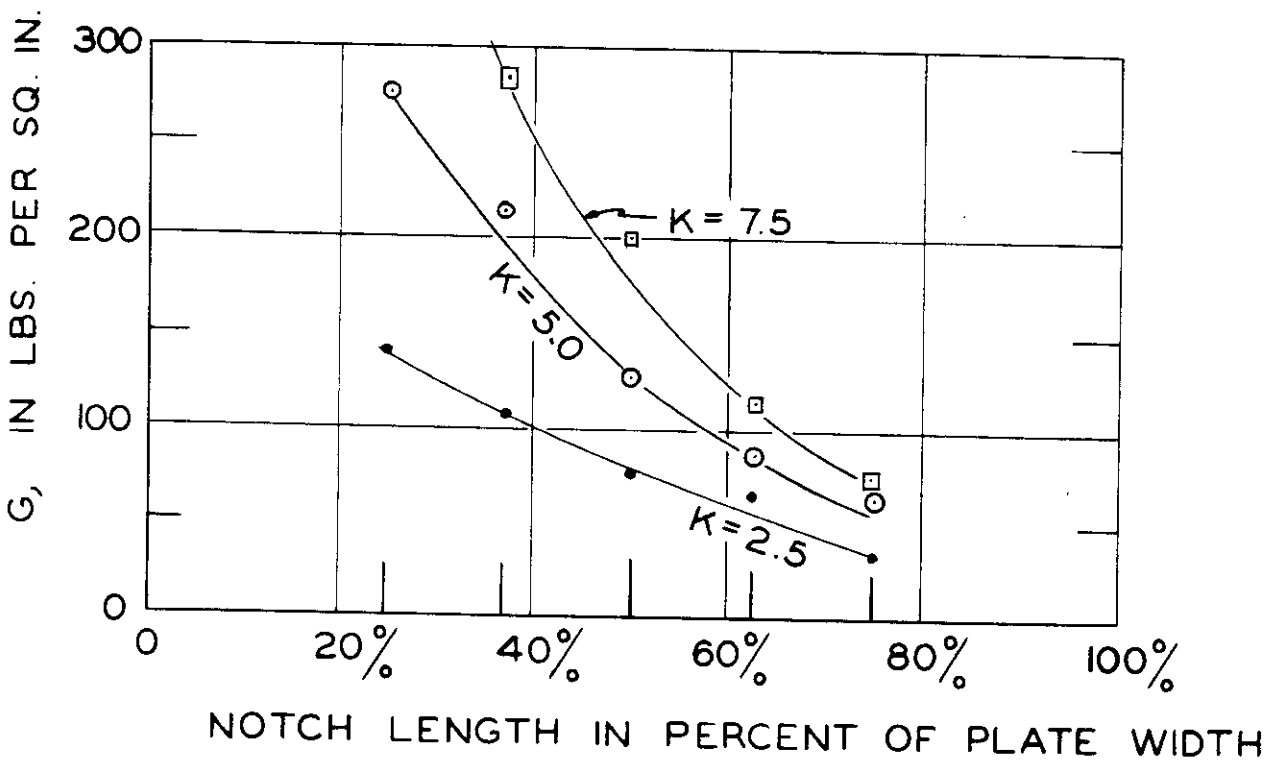


FIG. 1.2
"G" FACTOR TESTS

Studies by Brossman and Kies⁷, as well as interpretative studies on scattered observations of interrupted fractures in this laboratory, indicate that "G" (under current methods of evaluation) may have values ranging from 40 to 150 or 200 in-lb per sq in. Subsequent evaluation of interrupted fractures in this project has also shown the possibility of "G" obtaining a range from 40 to 150 or more.

The "G" value may be postulated as a statistical property of the material, and it must be assumed, under the present state of the theory, that the localized strain rate, although out of direct laboratory control, is at a rate favorable to brittle fracture initiation. Although it is easily agreed that close examination of the initiation zone may reveal small zones of ductile action, the basic separation appears in essentially all cases to be brittle.

While propagation of a brittle running crack may be explained by the above theory, it remains to explain the initial separation of the material that must occur before propagation. Initiation is definitely a complex problem, although it has been generally acknowledged that a separation of the material occurs when at the ends of the crack, the molecular bonds are broken or the temperature-dependent cohesive strength is exceeded. Since this separation must start on a small-scale basis and rapidly extend, it is highly probable that localized high strain rates are involved at the ends of the crack. This probable action establishes an environment difficult to measure physically and subject to laboratory control only by the form of the notch, applied rate of loading, and temperature.

The major deficiency in laboratory control is the lack of measurement of the localized high strain rates at the points of initial separation. Manjoine⁸ and others have demonstrated that, under extremely high strain rates, the yield point stress of mild steel may approach the ultimate stress. This means that brittle or non-ductile separation may occur at a high strain rate, and also means that a high strain rate may substitute for low temperature. Therefore, the experimenter has only general statistical control as established by external methods over the internal localized conditions at the most important of all points, the point of fracture initiation.

The preceding theoretical discussion has been limited to full-plate thickness cracks, whereas the latter part of this investigation has been concerned with small or short buried weld flaws. It is recorded that Sneddon⁹ approached the internal crack problem by considering a "disc-shaped" internal flaw cavity normal to the direction of tension. This theory led to the formulation of an equation for force tendency "G" for this type of flaw, while the internal flaw cavity extended in volume by first separating around the periphery of the flaw. It can be shown that, with the same force tendency "G", this type of flaw must have a larger radius to be as critical to a given applied stress as a full-thickness sharp crack.

Most of the internal weld flaws of this program took the form of an internal cavity, rectangular in shape but representing an internal sharp-edged flaw or crack of controlled length and width. Visual observations lead to the belief that the sequence of fracture initiation and propagation from a sufficiently long buried flaw was as follows: first, a separation occurs at the ends of an internal crack, as seen in the thickness direction of the plate, with a consequential rapid propagation of the fracture to the faces of the plate; second, once the faces of the plate are breached, the crack becomes a full-depth crack that rapidly opens to an elliptical shape. This rapid transformation from an internal flaw cavity to an open crack, characterized as a geometrical instability, is accompanied by a rapid release of strain energy and a rapid increase in stress at the ends of the open crack. Since the crack grows quickly, a high strain rate is established at its ends. This quick energy release may be likened to a dynamic or impact effect and may represent a distinguishing feature of buried flaws that can expand in this manner. It is thought, however, that if a flaw is too short, this mechanism will not describe the action for that reason the short or small buried flaw, like the "disc-shaped" flaw, does not establish the necessary environmental conditions for low-nominal stress initiation.

Initial experimentation on butt-weld flaws under static load did not provide brittle fracture from short internal flaws until the flaw was deliberately subjected

to a high residual stress. With the addition of residual stress, a low static applied-stress of from 2500 to 4000 psi could initiate a fracture that either grew into a complete fracture or was subsequently arrested.

Part II

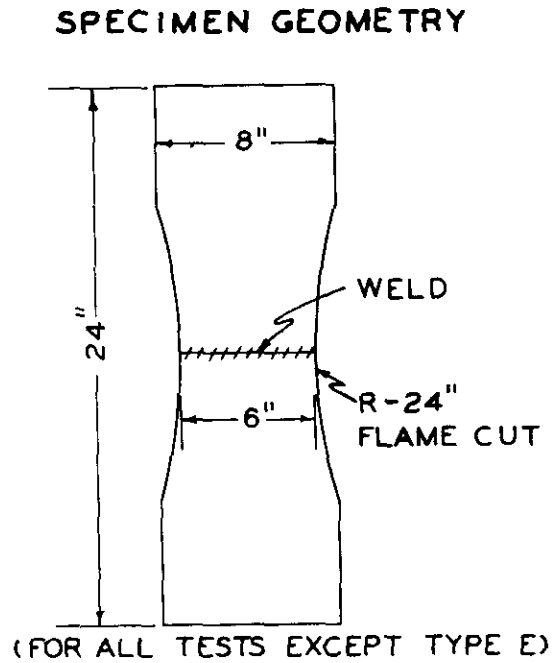
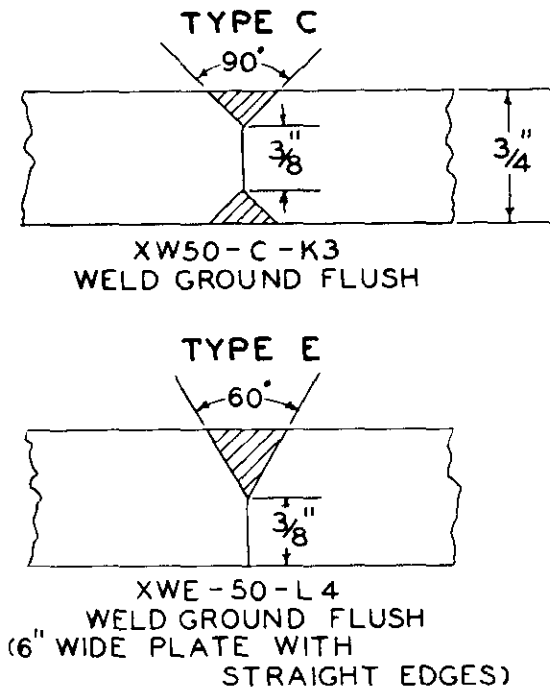
FLAWS IN BUTT WELDS

A. Incomplete-Penetration Butt Welds

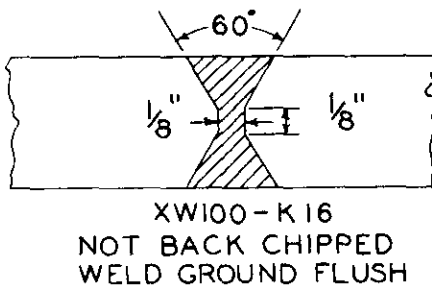
The static strength of incomplete-penetration butt welds intentionally made from E-6010 electrodes, with base plates of 3/4-in. thick ABS-Class B steel, were investigated by using laboratory specimens as shown in Fig. 2.1. It should be noted particularly that the penetration of the weld was controlled by regulation of the throat thickness as shown for Type C. The two halves of the specimens with machined bevels were butted tight and welded.

The degree of penetration is defined as the per cent of penetration, or alternatively, as the penetration ratio, wherein the thickness of the 3/4-in. base plate becomes the reference thickness. For example, if the unpenetrated throat thickness is 3/8 in., the weld penetration is taken as 3/8 in. or 50% of the plate thickness. For a 75% penetration weld, an unpenetrated 3/16-in. throat thickness is used; for a 100% penetration weld, the butt weld is fully welded. The penetration rating of the butt weld is the same for either a butt-welded joint ground flush or for a butt weld in which the reinforcement extends above the plate.

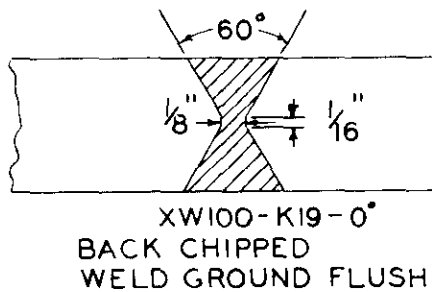
Specimens were fabricated and tested with per cent of penetration scheduled to vary from 50% to 100%. Inspection of fractured weld surfaces and measurement from photographs disclosed the true penetration, which may be plus or minus 5% from the intended penetration, except for the specimens with 100% penetration.



100% WELDED PLATES



MAXIMUM LOAD AT ROOM TEMPERATURE-278^K
 ELONGATION AT MAXIMUM LOAD-0.17 IN/1 1/2 IN



MAXIMUM LOAD AT 0°F - 313^K
 ELONGATION AT MAXIMUM LOAD-0.23 IN/1 1/2 IN

UNWELDED PLATES

XW-K14 MAXIMUM LOAD AT ROOM TEMPERATURE-281^K
 ELONGATION AT MAXIMUM LOAD-0.40 IN/1 1/2 IN

X-K20-0° MAXIMUM LOAD AT 0°F - 298^K
 ELONGATION AT MAXIMUM LOAD-0.31 IN/1 1/2 IN

FIG. 2.1 SPECIMEN TYPES

Specimens: The general shape of tensile specimens and the type of incomplete-penetration butt weld used throughout the initial test program are shown in Fig. 2.1. The 100% or completely penetrated butt welds that served as control specimens are also shown in Fig. 2.1. The Type "C" welds can be classified as double-vee butt welds with variable penetration, all fabricated with weld reinforcement; but for most specimens, the reinforcement was ground off to exercise a better control over the throat cross-section for experimental purposes.

In order to investigate the effects of weld eccentricity, a specimen hereafter referred to as Type "E" or single-vee was used, as is shown in Fig. 2.1.

The base plate of all specimens was Type ABS-Class B steel, and specimens were flame cut to external shape with all weld-groove bevels and lips machined to required dimensions. The welding was done with an E-6010 electrode with interpass temperatures of 80 F.

Fig. 2.1 also gives the test data for the control tests on solid plate or 100% welded plates with reinforcement removed. These results will be used later for determining load ratios.

Test Set-Up and Instrumentation: Specimens were cooled to test temperature by enclosing the welded specimen in an insulated box through which cooled air was circulated. Temperatures were held relatively constant throughout the test and were measured by means of copper-constantan thermocouples inserted in drill-holes in the plates. Tests were generally made at either 0°F, using the above technique, or at about 75 F, the average room temperature. A few tests were run at -40 F and others at 120 F, which gave results comparing favorably with the results at 0°F and 75 F, respectively.

The Type E, or single-vee weld types, created a special problem in instrumentation and analysis. Since the center of gravity of the weld metal was offset from the axis of loading at the beginning of the test, there was a definite

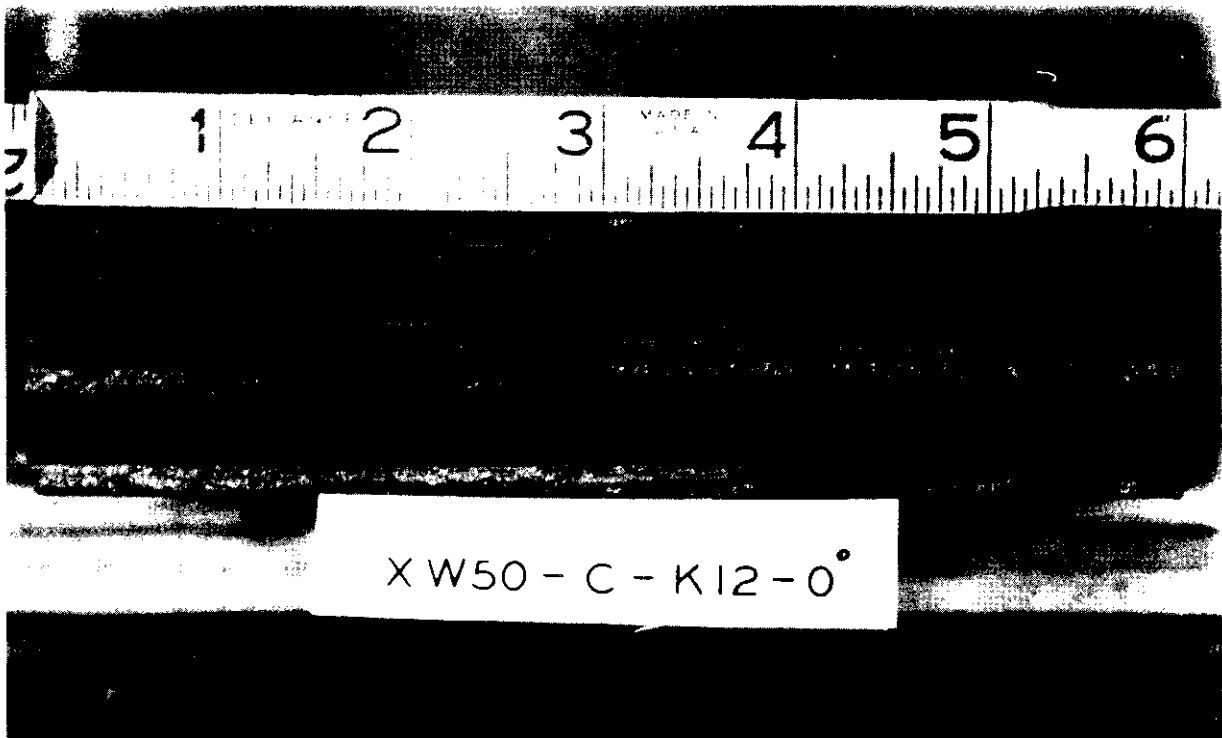


Fig. 2.2 - Photograph of fractured surface - Specimen C-K 12



Fig. 2.3 - Photograph of fractured surface - Specimen C-K 13

tendency for the plate to bend during the application of the load. The result of this bending was an excessive parting of the unwelded or unpenetrated portion of the weld section and a decrease in the deformations on the welded or beveled side of the plate.

Since it was impossible to control weld penetration during welding, the per cent of the welded or penetrated throat cross-section was determined from photographs of the fracture surfaces following the test. All failures occurred through the weld metal, leaving fractured weld metal exposed for photographing. The unwelded area was measured on the photograph, and this area, deducted from the original full-plate thickness cross-section, gave the original cross-section of the weld metal. It is believed that this method involved little error, since nearly all of the deformation and reduction in cross-section at the fracture surface occurred in the weld metal, leaving the unwelded portion in almost its original dimensions. Figs. 2.2, 2.3, & 2.4 represent views of the fractured surfaces for three of the specimens listed in Table 2-I.

Test Results: A tabulated summary of test results may be found in Table 2-I. It was thought that a satisfactory method for summarizing the results of this program would be the correlation plot shown in Fig. 2.5. Penetration ratio is defined as the ratio of the cross-sectional root area of weld metal between faces of the test plate to the original full-thickness area of the plate cross-section. By this definition, the area of weld metal that forms the reinforcing in a reinforced butt weld is not included in the computation of penetration ratio, but specimens that had a reinforced butt weld are distinctly marked on the plot. In Table 2-I, the load ratio has been computed on two bases: first, the maximum value of load found for a given weld-penetration ratio was divided by the maximum load value for an unwelded control plate at the same temperature to establish a criterion for overall joint efficiency; and second, the maximum load value for a given weld-penetration ratio was divided by the maximum load obtained for a 100% butt-welded control



Fig. 2.4 - Photograph of fractured surface - Specimen C-K 11

TABLE 2-I
SUMMARY OF RESULTS

Incomplete-penetration butt welds

Specimen No.	Temp. F	Actual penetration ratio	Maximum load kip	Load ratio	
				Unwelded plate	100% welded plate
<u>Weld Type "C"</u>					
XW50-C-K3	85	.456	162	.577	.583
XW75-C-K6	75	.708	211	.75	.759
XW90-C-K8	72	.880	235	.836	.845
XW50-C-K12	0	.520	170	.570	.543
XW75-C-K13	0	.720	207	.695	.662
XW90-C-K11	0	.835	257	.862	.822
XW90-C-K25	120	.9	243	--	--
XW75-K15	-40	.73	230	--	--

Weld Type "CR"

XW75-R-K24	75	.750	238	.85	.86
XW90-R-K23	75	.84	273	.97	.98
*XW100-R-K22	75	1.0	291	1.04	1.05
XW75-R-K28	0	.77	270	.93	.86
XW90-R-K26	0	.90	295	1.01	.94
*XW100-R-K27	0	1.0	315	1.08	1.01

Weld Type "E"

XWE-50-L4	77	.460	104	.370
XWE-75-L3	74	.680	162	.577
XWE-90-L1	74	.910	212	.755

Weld Type "ER"

XWE50R-L5	75		108	
-----------	----	--	-----	--

*Failed through plate.

Description of specimens

All specimens of 3/4-in. thick ABS-Class B steel
All welding done with E-6010 electrode
Specimens 24-in. long and 6-in. wide

Type "C"

90° double-vee, no root gap, not back chipped, ground flush, penetration ratio as stated in table

Type "CR"

Same as Type "C" except that weld reinforcement was left on

Type "E"

Eccentrically placed weld, welded from one side
Single-vee, no root opening, weld ground flush

Type "ER"

Same as Type "E" except weld reinforcement left on

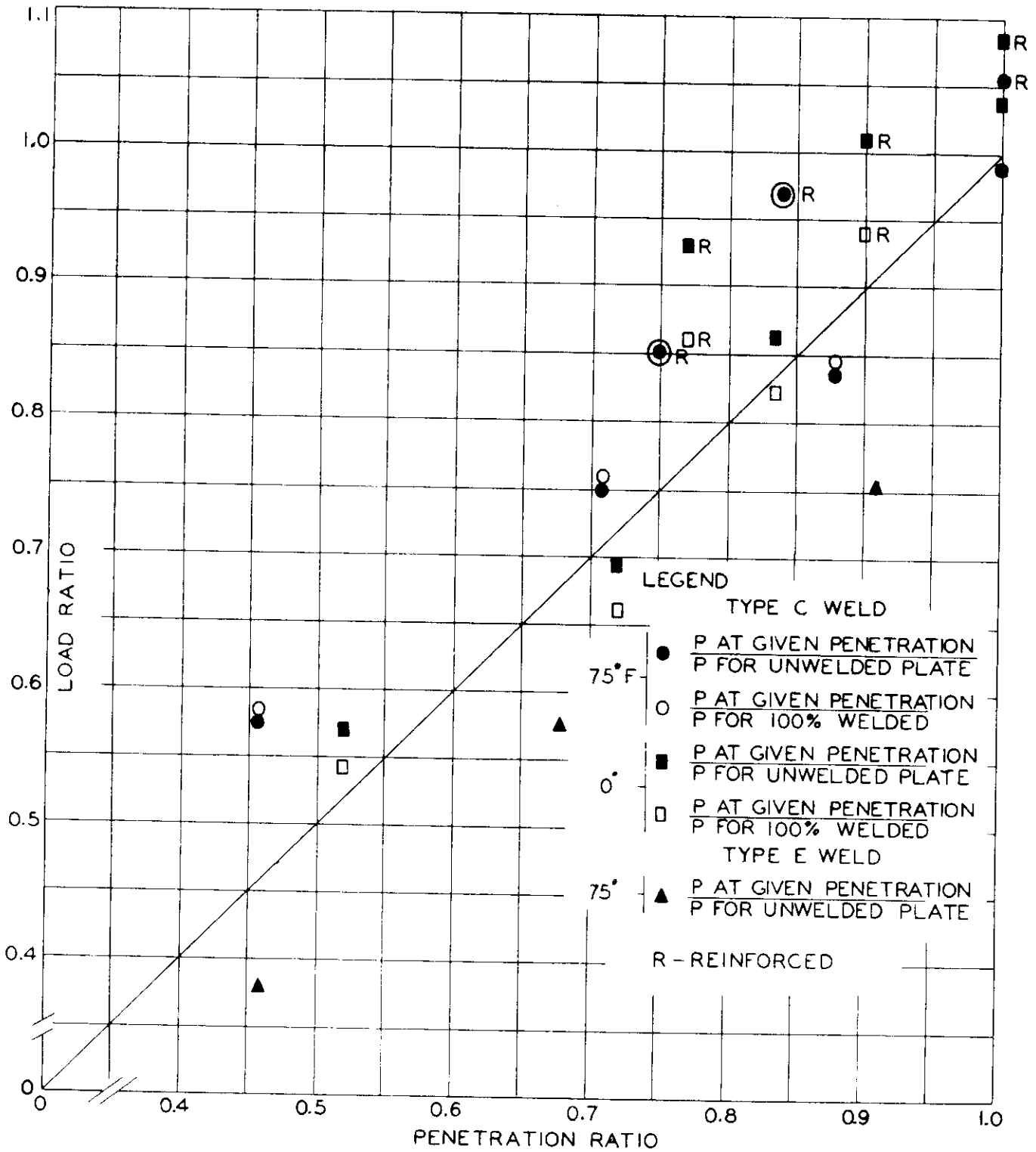


FIG. 2.5
LOAD RATIO VS. PENETRATION RATIO

plate at the same test temperature to establish a criterion for weld-metal efficiency. Fig. 2.5 is a plot of the ratios.

The correlation line is drawn at a 45° angle in Fig. 2.5 and serves as a guide for comparing the maximum loads at two temperatures, 0°F and 75 F. For example, it might be expected that if the penetration ratio were doubled, the maximum static load would be doubled if the varying notch sensitivity and unavoidable weld variations were neglected. The general trend of the test results parallels the correlation line as may be noted in Fig. 2.5. The butt-weld reinforcement definitely strengthened the welds so that, at 90% penetration, the butt welds had a strength which nearly equaled that of the unwelded plate. A comparison of the incompletely-penetrated welds with the 100% welded joints shows, for all but two specimens, that the proportional strength was exceeded. While this is true for the double-vee butt welded joints, the single-vee butt weld, with incomplete penetration and load eccentricity at the weld throat, possessed much less than proportional strength based on its comparison with a fully penetrated single-vee weld.

Summary: The intentionally-controlled incomplete-penetration butt welds used in this test program do not simulate any particular weld flaw as it occurs in actual welded construction. They were chosen because of the simplicity with which penetration could be controlled. For that reason, the results obtained cannot be utilized in their present form for direct evaluation of incomplete penetration as may be found in faulty welded construction. However, certain trends that are of value are indicated by the test results from these simplified, weakened butt welds.

The static strength of an intentionally-made, incompletely-penetrated butt weld appears to be predictable. That is, the static strength of a welded joint of this nature can be estimated by multiplying the penetration ratio by the expected strength of the full unwelded plate. The reinforcement of a butt weld is effective and can practically make up for loss in strength when the penetration ratios are

in the order of 90%. However, rather than count on this added strength, the reinforcement should be considered as a way of introducing an additional factor of safety when joints are under static load.

The tests on the incomplete-penetration welds were made at 0°F and at 75 F. However, there was no significant difference in the load-carrying capacity at the two temperatures. The fracture appearance for the specimens at 0°F appeared to be of the cleavage nature, although some evidence of a small shear lip was apparent in about 50% of the specimens.

B. Static Strength of Flawed Butt Welds

This section reports on the static tensile tests of butt welds that had been flawed to study the effect of internal cracks, external cracks, slag inclusions and porosity. The general specimen was 3/4-in. thick, 10-in. wide and 24-in. long, of ABS-Class B steel. The 90° double-vee welds, made with the E-6010 electrode as described subsequently, were all reinforced. Weld reinforcements were left on for all tests. All tests except those noted were made at 0°F. The general type of specimen employed is shown in Figs. 2.6, 2.7, and 2.8. The flaws were varied in length from 5/8 in. to 6-1/4 in.

For purposes of flaw classification, the depth of internal flaw is stated as a percentage of the original plate thickness. For example, a flaw 3/8 in. in depth and located centrally would be termed a 50% flaw. A 100% flaw on this basis would be a full thickness flaw, although no tests of this percentage are reported in this section.

Cracks, Internal and External, of Varying Lengths. Cracks were established in a brittle weld made by depositing the E-6010 weld metal into iron filings previously placed in the butt-weld groove. The length of this brittle deposit was controlled to the length of flaw required, and the depth in the groove controlled to the

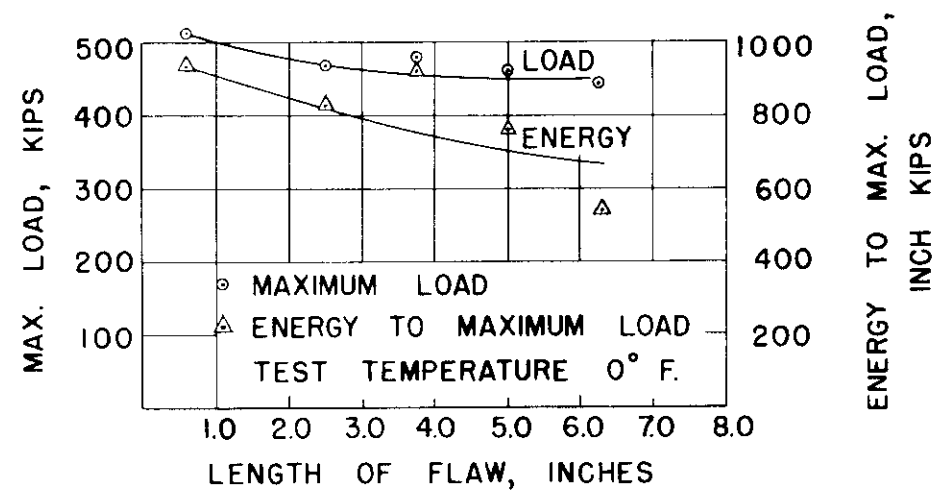
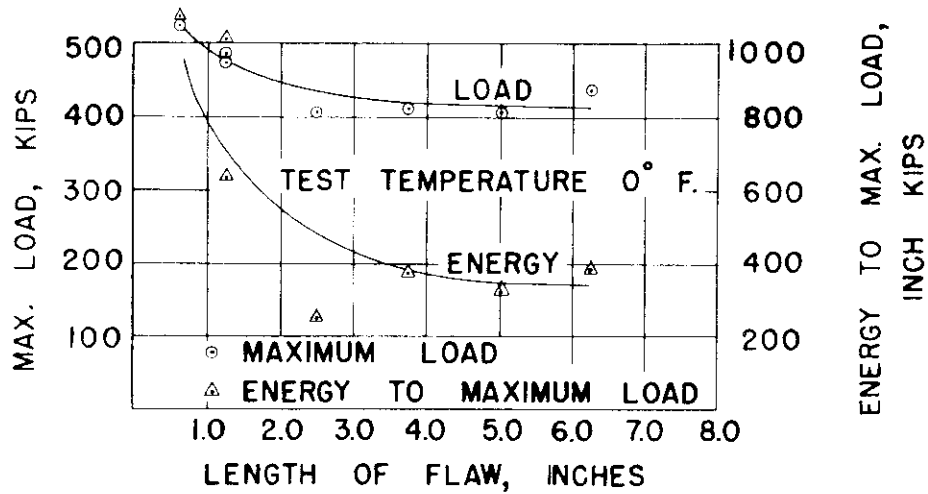
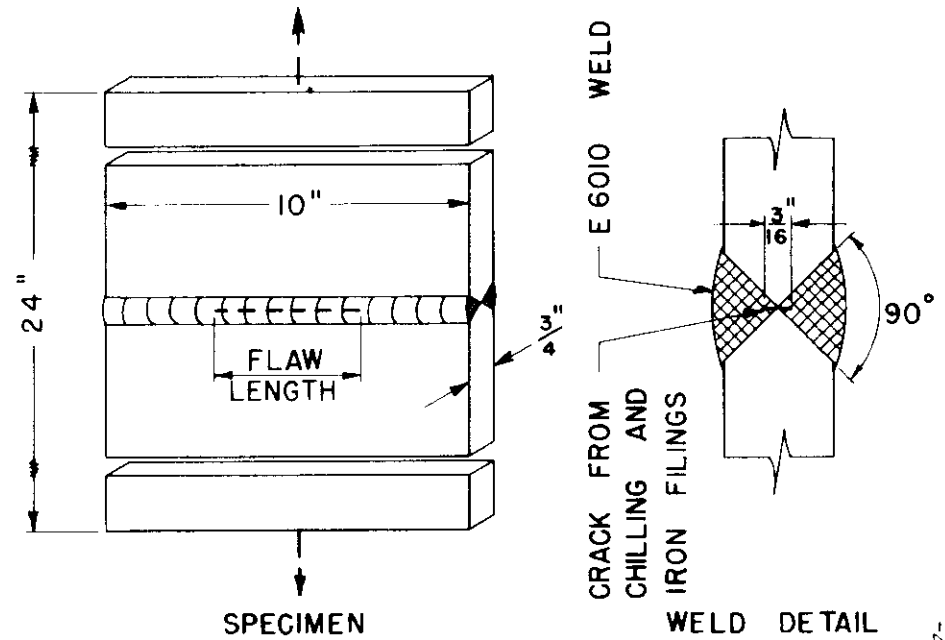
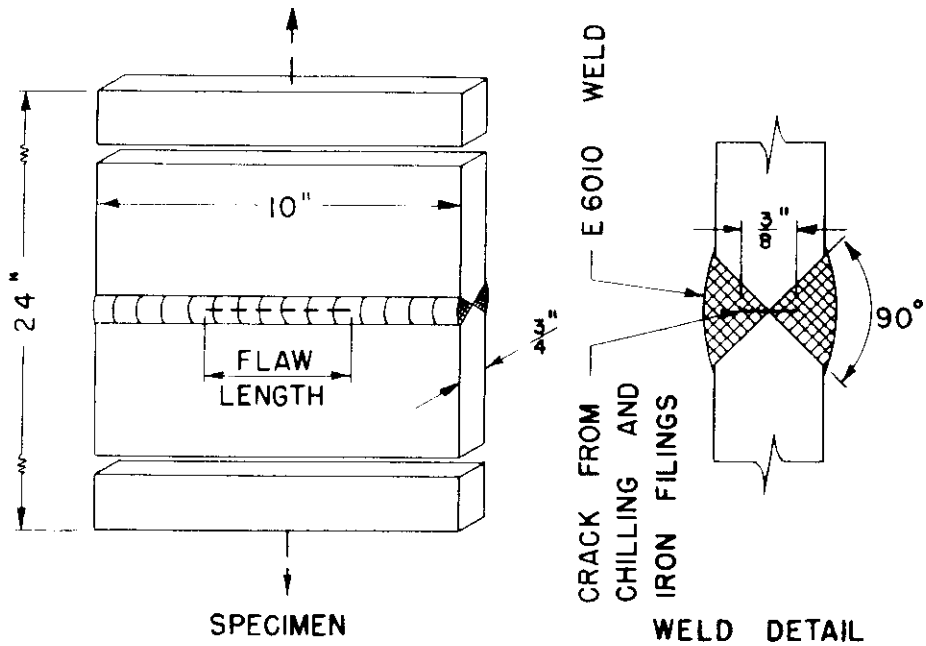


FIG. 2.6 BUTT WELD TESTS - INTERNAL FLAW

FIG. 2.7 BUTT WELD TESTS - INTERNAL FLAW

desired depth to represent the per cent of flaw. This brittle metal was then rapidly chilled by compressed air, which formed a crack of nearly microscopic thickness and of the stated length and depth. The butt weld was then completed using only the E-6010 electrode. External cracks were made by the same general method with the E-6010 and iron-filing combination used externally. Fig. 2.9 shows the general appearance of fractured specimens.

Tables 2-II, 2-III, and 2-IV present the test data, and Figs. 2.6, 2.7, and 2.8 plot the maximum load and the energy to maximum load, based on elongations measured over the 24-in. specimen length versus length of flaw. It may be noted from plotted data that, as the crack length increased, both load and energy decreased for each of the three types of flawed specimens. The mode of fracture for the majority of specimens was a fast cleavage fracture (zero per cent shear), and the reduction in thickness rarely exceeded 2%.

As might be expected, the internal 25% flaws were slightly better than the 50% flaw in strength and energy to maximum load. The external flaws showed results similar to the 50% flaw.

The flaws may also be considered in terms of the fracture stress computed on the gross section of weld. As previously explained, σ , the unit stress on the gross section of weld metal, was thought to be a better index than stress on the net cross-section, in view of all other complicating factors. These unit stresses, in nearly every case, show that there is a general impairment in strength caused by the notch effect of the flaw. These static unit stresses vary from 60,000 psi for short flaws to a stress of about 45,000 to 48,000 psi for most of the long flaws. One flaw of 3-3/4-in. length permitted fracture at 39,000 psi, the lowest observed.

To check on the severity of the flaws or cracks described above, six tests were made on the internal 2-1/2-in. long weld crack, which had been made with a jeweler's hack saw. The results are given in Table 2-V, and these results indicate that the crack previously made is about as severe as the jeweler's saw cut. It is

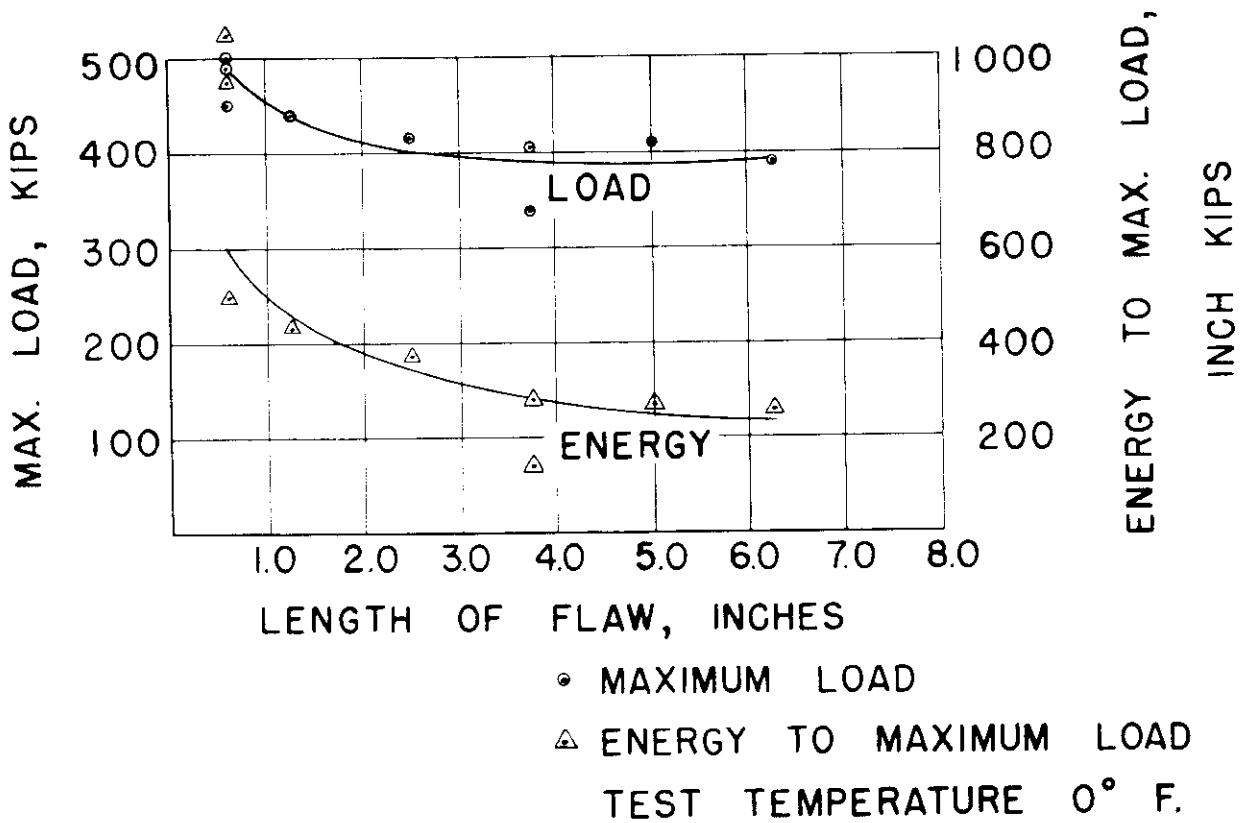
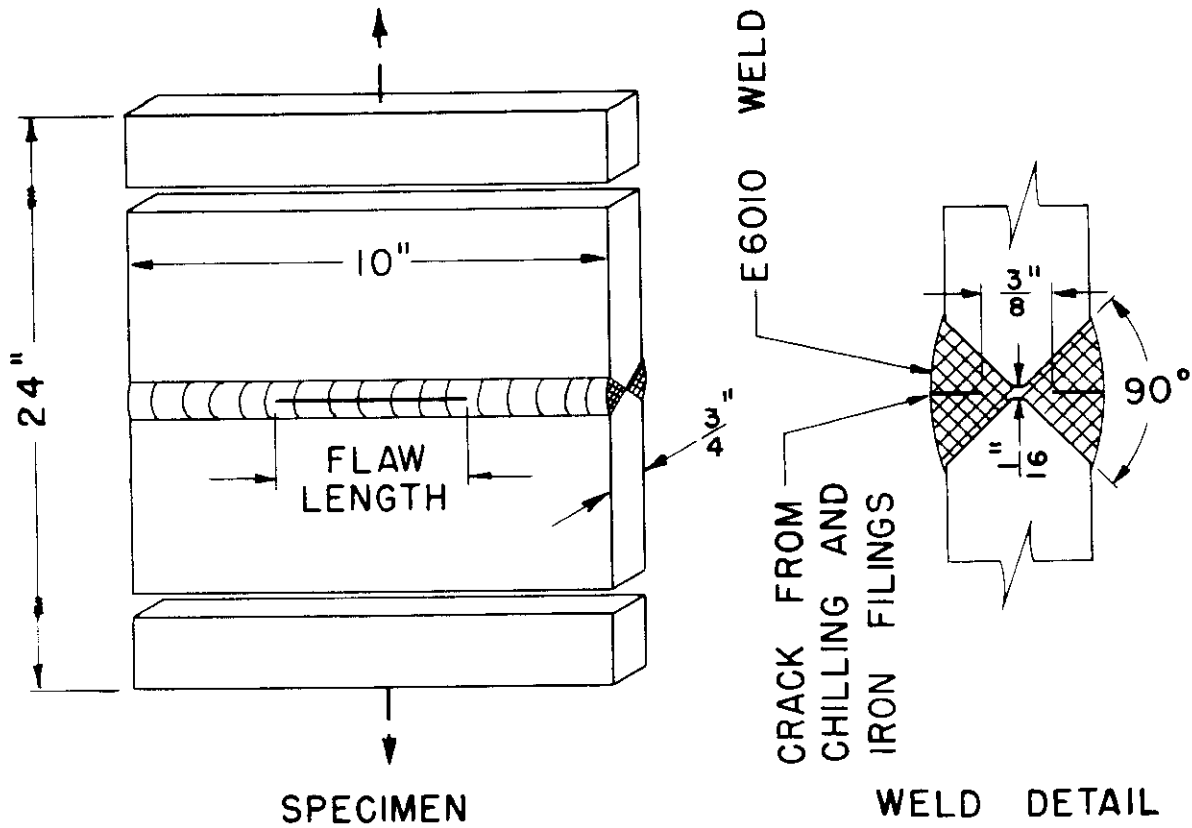


FIG.2.8 BUTT WELD TESTS - EXTERNAL FLAW

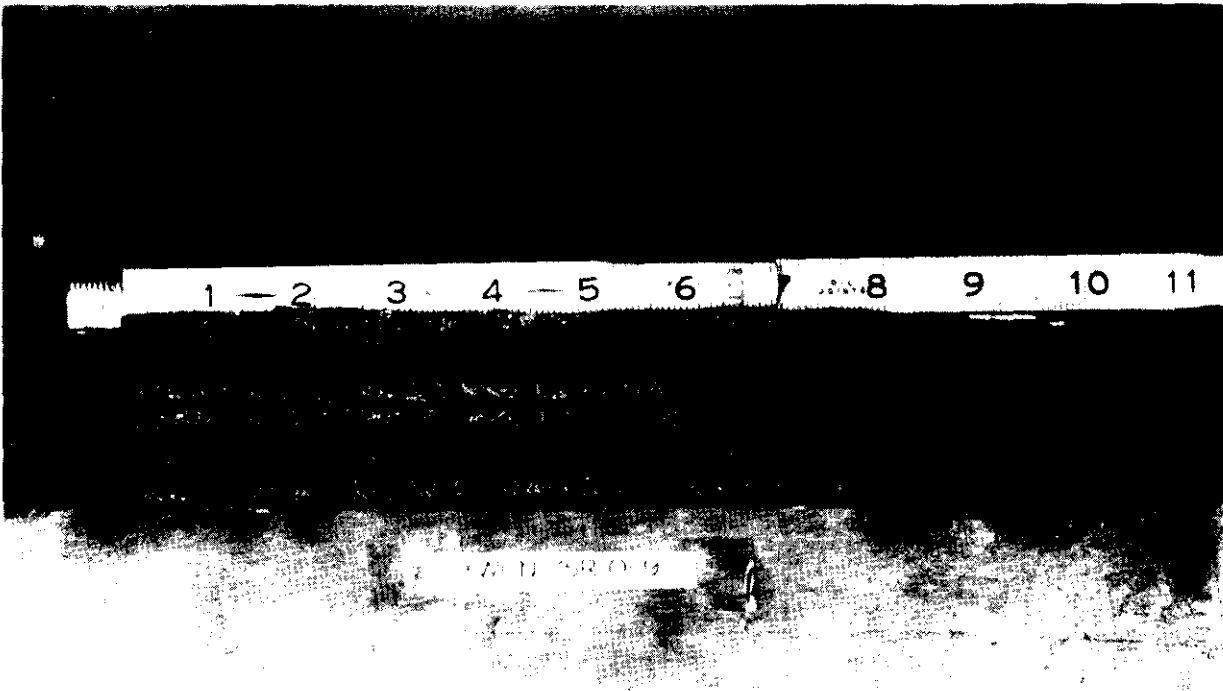


Fig. 2.9 - Fractured specimen - Type "CR"

TABLE 2-II

Butt-weld tests with internal crack

Flaw: Incomplete internal penetration of varying length (50% flaw)

(See Fig. 2.6)

Specimen No.	Length of flaw, in.	Temp. F	Mode of fracture in % of Shear	Maximum load, kip	Energy to max. load, in.-kip	Fracture load, kip	Energy to fracture load, in.-kip	psi on gross cross-section	Remarks
N 26	5/8	0	0	525.0	1161	-	-	60,000	Fractured through weld
N 25	1-1/4	0	0	483.0	636	-	-	55,200	" " "
O 13	1-1/4	0	90	490.5	1010	170	1160	56,000	" " "
N 24	2-1/2	0	0	408.0	256	-	-	46,600	" " "
O 2	3-3/4	0	0	412.0	371	-	-	47,200	" " "
O 1	5	0	0	408.0	338	-	-	46,600	" " "
O 6	6-1/4	0	0	434.5	395	-	-	49,700	" " "

General Remarks: Specimens of ABS-B steel, 3/4 in. x 10 in. x 24 in. long. Reinforced butt welds, double vee 90° angle, no lip or root opening, E-6010 electrode. Energy reported for 24-in. length of specimen.

TABLE 2-III

Butt-weld tests with internal crack

Flaw: Internal crack of varying length, (25% flaw)

(See Fig. 2.7)

Specimen No.	Length of flaw, in.	Temp. F	Mode of fracture in % of shear	Maximum load, kip	Energy to max. load, in.-kip	Fracture load, kip	Energy to fracture load, in.-kip	psi on gross cross-section	Remarks
N 27	5/8	0	45	506.0	968	470	985	58,000	Fracture through weld
O 10	2-1/2	0	10	472.5	844	445	870	54,000	" " "
O 9	3-3/4	0	0	480.0	954	-	-	55,000	" " "
O 8	5	0	0	465.0	750	-	-	53,200	" " "
O 7	6-1/4	0	15	446.5	528	430	545	51,100	" " "

-26-

General Remarks: Specimens of ABS-B steel, 3/4 in. x 10 in. x 24 in. long. Reinforced butt welds, double vee 90° angle, E-6010 electrode. Energy reported for 24-in. length of specimen.

TABLE 2-IV

Butt-weld tests with external cracks

Flaw: External cracks of varying length, leaving central 3/8 in. intact. (See Fig. 2.8)

Specimen No.	Length of flaw, in.	Temp. F	Mode of fracture in % of shear	Maximum load, kip	Energy to max load, in -kip	Fracture load kip	Energy to fracture load, in -kip	psi on gross cross-section	Remarks
O 14	5/8	0	0	451.0	505	-	-	51,600	Fracture through weld
O 19	5/8	0	0	492.0	950	-	-	56,300	" " "
O 20	5/8	0	-	499.5	1050	260	-	57,100	" " "
O 15	1-1/4	0	0	440.5	433	-	-	50,600	" " "
O 11	2-1/2	0	0	419.5	372	-	-	48,000	" " "
O 16	3-3/4	0	0	341.0	140	-	-	39,000	" " "
O 21	3-3/4	0	0	409.5	280	-	-	46,900	" " "
O 17	5	0	0	411.0	273	-	-	47,000	" " "
O 18	6-1/4	0	0	396.5	263	-	-	45,400	" " "

-27-

General Remarks: Specimens of ABS-B steel, 3/4 in. x 10 in. x 24 in. long. Reinforced butt welds, double vee 90° angle, E-6010 electrode. Energy reported for 24-in. length of specimen.

TABLE 2-V

Butt-weld tests with internal cracks

Flaw. 2-1/2 in. long internal jeweler's saw-cut notch over central 50% of weld (50% flaw)

Specimen No.	Temp. F	Mode of fracture in % of shear	Maximum load kip	psi on gross cross-section	Remarks
M 1	-40	0	359.0	41,000	Fracture through weld
M 2	+75	100	347.5	39,800	" " "
M 3	-40	0	351.5	40,200	Disregard - fractured at header
M 4	-30	0	475.0	54,400	Fracture through weld
M 5	-40	0	476.0	54,500	" " "

General Remarks: Specimens of ABS-B steel 3/4 in. x 10 in. x 24 in. long. Reinforced butt welds, double vee 90° angle, E-6010 electrode, 1/8-in. root opening, 1/16-in. lip.

interesting to note, however, that a test at 75 F gave the lowest fracture stress of this group, 39,800 psi, although fracture was completely ductile. Such occurrences as these extreme values of strength are vitally important if the factor of safety and the probability of failure are to be considered.

One test was made with a weld flaw representing a slag inclusion and one test with weld porosity. The results are given in Table 2-VI. For the specimen with slag inclusions, fracture occurred through the plate outside of the weld. The flaw representing porosity permitted fracture to take place through the weld at a gross stress of 51,500 psi. No further tests with these types of weld defects were made, since it was thought that they were not the most serious flaws. Furthermore, they were difficult to make and control.

It was concluded from these tests that the overall test environment was not effective in providing a laboratory test that simulated conditions for low-stress service fracture or brittle fracture. Reflection at this point in the program led to the view that an attempt should be made to study flaws in the presence of residual stresses. The next two parts of the report deal with this added feature.

Part III

WELD FLAWS WITH RESIDUAL STRESS--STATIC AND DYNAMIC STRESS INTERACTION

Introduction

After the static tests of butt-welded specimens containing welding flaws, it became apparent that fracture could not be initiated from flaws at nominal stresses below the static yield point of the plate or of the welding material. Ship fractures, however, had been reported as initiating from welding flaws at static applied stress values of about one half the static yield point in magnitude. Reproducing these low-applied-stress fractures in the laboratory seemed to require

TABLE 2-VI

Butt-weld tests with slag and porosity

Flaws: Slag inclusions*
Porosity**

Specimen No.	Length of flaw, in.	Temp. F	Mode of fracture in % of shear	Maximum load, kip	Energy to max. load in.-kip	Fracture load kip	Energy to fracture load, in.-kip	psi on gross cross-section	Remarks
N 23	2-1/2 slag	0	50	533	1431	500	2010	61,000	Plate fractured 3 in. above butt weld, no distress at weld
N 12	2-1/2 porosity	0	100	450	545	125	638	51,500	Fractured through weld, initiation in zone of porosity

General Remarks: Specimens of ABS-B steel, 3/4 in x 10 in. x 24 in. long. Reinforced butt welds, 90° bevels, E-6010 electrode. Energy reported for 24-in. length of specimen.

*Slag inclusions created by not brushing slag from several root passes deposited by E-6010 electrode before subsequent welding.

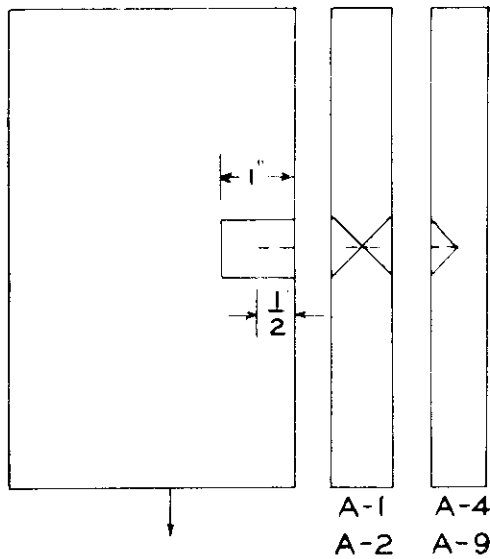
**Porosity created by mixing floor sweeping around welders' bench with powdered slag (screened to pass No 20 sieve). This mixture was put in weld groove before each pass.

a procedure which would augment the applied static tensile loading. The Series A tests represent a search for such a procedure, as well as a qualitative examination of the variables associated with low-stress brittle fracture initiation.

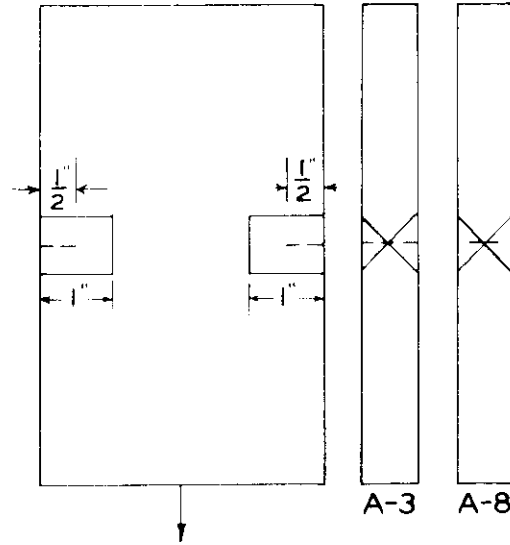
Type-A Specimens: The variables examined in this phase of the program included combinations of cyclic loading, impact loading, flaw location, residual stress systems surrounding the weld flaw, and lowered temperatures. The specimens are shown in Fig. 3.1, and a brief description of their fabrication and testing techniques is given in Table 3-I.

The welding flaws were prepared for specimens A-1 through A-6 by laying beads of E-6010 weld metal over cast-iron filings. Upon examination after fracture, it appeared that this technique gave a well defined crack-like flaw. The method adopted for specimens A-7 through A-16 was to lay root passes of a high-carbon hard facing rod, and to complete the surface welding with E-6010 welding material. Upon the cooling and shrinking of the hard facing rod, the root passes cracked. This gave an internal flaw of the approximate dimensions desired. The location of the cracked welds was varied so that a number of combinations could be considered. The crack locations are described in Table 3-I and shown in Fig. 3.1. The specimens of this Series A were tested at temperatures ranging from -20 to -80 F. These low temperatures were selected to give the specimen every opportunity to fracture in the brittle mode.

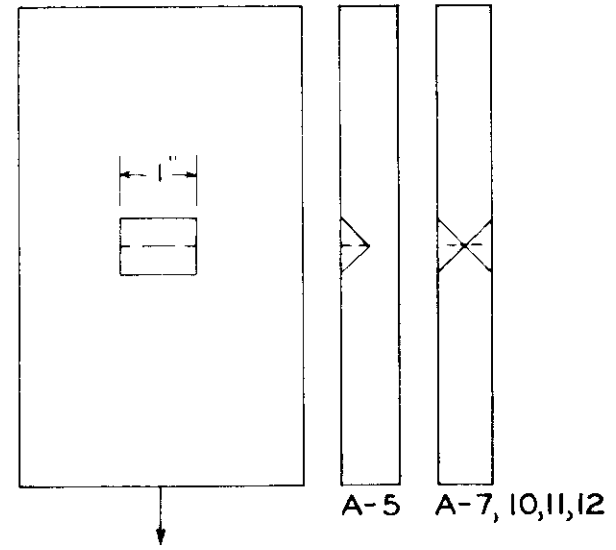
In an effort to encourage low static tensile-stress cleavage fracture, the loads on specimens A-1 through A-5 were cycled in the post-yield point tensile range. The effect of the load cycling on these specimens is inconclusive because of variable lengths and locations of the flaws in the specimens. In general, it appears that load cycling, as it was performed in these experiments, had little effect in reducing the static tensile stress required for cleavage fracture. The fracture surfaces of specimen A-5 are shown in Fig. 3.2.



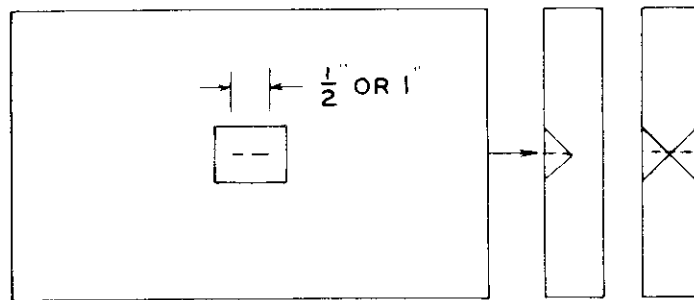
SPECIMENS A-1 & A-2
 FLAW $\frac{1}{2}$ " X $\frac{3}{8}$ " IN C.I. FILINGS
SPECIMEN A-4
 FLAW $\frac{1}{2}$ " X $\frac{1}{2}$ " IN C.I. FILINGS
SPECIMEN A-9
 FLAW $\frac{1}{2}$ " X $\frac{1}{2}$ " IN TOOLWELD



SPECIMEN A-3
 FLAW $\frac{1}{2}$ " X $\frac{3}{4}$ " IN C.I. FILINGS
SPECIMEN A-8
 FLAW $\frac{1}{2}$ " X $\frac{3}{8}$ " IN C.I. FILINGS



SPECIMEN A-5
 FLAW 1" X $\frac{1}{2}$ " IN C.I. FILINGS
SPECIMENS A-7, 10, 11, 12
 FLAWS 1" X $\frac{3}{8}$ " IN TOOLWELD
 WITH NORMAL WELD REINFORCE



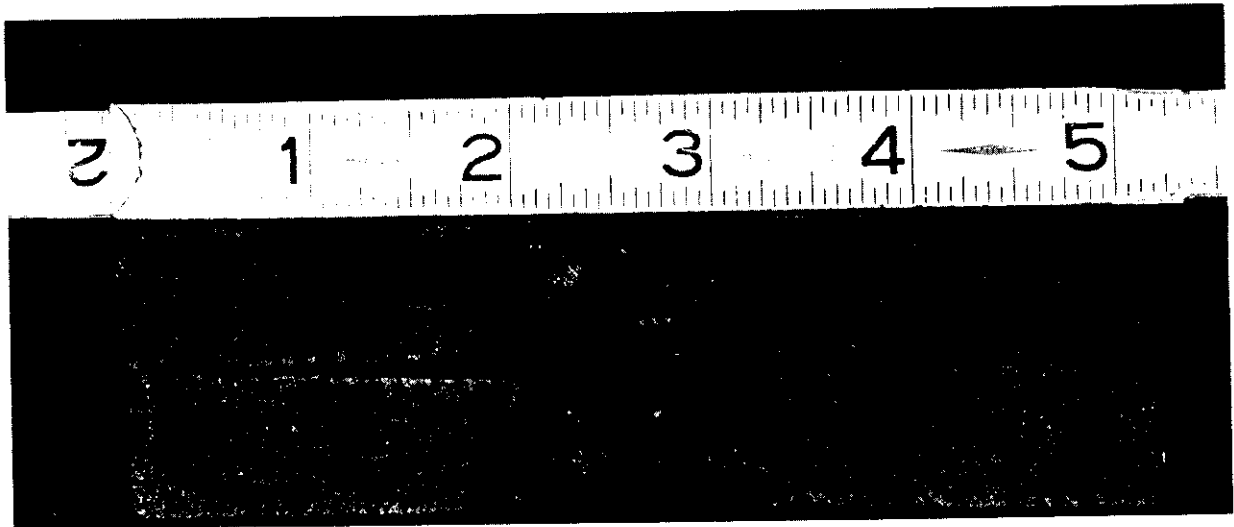
SPECIMEN A-6
 FLAW $\frac{1}{2}$ " X $\frac{1}{2}$ " IN C.I. FILINGS

A-6 A-13, 14, 15, 16
SPECIMENS A-13, 14, 15, 16
 FLAW 1" X $\frac{3}{8}$ " IN TOOLWELD
 WITH NORMAL REINFORCE.

GENERAL NOTES

ALL SPECIMENS $5\frac{1}{2}$ " X 8" X $\frac{3}{4}$ " DN STEEL
 WELD REINFORCEMENTS GROUND FLUSH
 UNLESS NOTED.
 WELDING OF E6010 ELECTRODE
 DIRECTION OF STATIC TENSION
 INDICATED BY ARROWS.

FIG. 3.1
SPECIMENS OF
"A" SERIES



A-5

Fig. 3.2 - Photograph of fracture of Specimen A-5

TABLE 3-I

Data summary - "A" series

Specimen size - 5 1/2 in. wide, 8 1/2 in. long, 3/4 in. DN Steel

Specimen	Specimen description (See Fig. 3-1)	Test temp F	Testing technique	Static tensile stress at fracture (gross area) psi
A-1	50% flaw in C I filings, 9/16 in. long on edge of specimen at mid- depth	-63	Loaded to 100 ^{kip} Load cycled from 100 ^{kip} to 140 ^{kip} 6 times, 2 sec/cycle Load cycled from 140 ^{kip} to 170 ^{kip} with cleavage fracture at 170 ^{kip} on 3rd cycle	39,600
A-2	As A-1	-50	Load cycled 10 times each between 80 ^{kip} -- 100 ^{kip} , and 10 cycles repeated for each 10 ^{kip} load increase. After 140 cycles specimen hit with 8-lb sledge at each 10 ^{kip} load increment, with cleavage frac- ture at 173 ^{kip}	40,600
A-3	100% flaws in C.I. filings, 1/2 in. long on both edges	-50	Load cycled 5 times between 100 ^{kip} and 120 ^{kip} and 5 cycles repeated for each 10 ^{kip} load increase to 150 ^{kip} . Specimen struck re- peatedly with sledge as load slowly ad- vanced. Cleavage fracture at 154 ^{kip}	36,800
A-4	Flaw in C I. filings from face to 50% of plate thickness. 1/2 in. long on one edge	-50	Load cycled from 100 to 120 ^{kip} 5 times, 5 cycles repeated for each 10 ^{kip} of load increase to 140 ^{kip} . Load lowered to 120 ^{kip} and advanced slowly while speci- men was struck with 8-lb sledge. Cleavage fracture at 132 ^{kip}	31,700

TABLE 3-I - Data summary - "A" series (continued)

Specimen	Specimen description (See Fig. 3-1)	Test temp. F	Testing technique	Static tensile stress at fracture (gross area) psi
A-5	Flaw 1 in. long. 50% of plate thickness at mid-width and mid-depth of plate in C. I. filings	-60	Load advanced slowly to 118 ^{kip} where flaw became 100% of thickness. Load advanced to 164 ^{kip} , lowered to 130 ^{kip} , then advanced slowly while specimen was struck with 8-lb sledge at 5 ^{kip} intervals. Cleavage fracture at 223 ^{kip}	53,500
A-6	Vertical crack, 1/2 in. long, from face to 50% of thickness in C.I. filings	-57	Load slowly advanced to 160 ^{kip} , lowered to 130 ^{kip} . Struck with sledge, cleavage fracture	31,600
A-7	Specimen loaded in compression to 140 ^{kip} . Then mid-thickness flaw, 50%, 1 in. long, prepared with hard facing rod. Welding completed with E-6010	-80	Load advanced slowly to 160 ^{kip} , lowered to 62 ^{kip} . Struck with 8-lb sledge. Cleavage fracture	15,400
A-10	As specimen A-7	-57	Loaded slowly to 4 ^{kip} , struck with sledge hammer at 8 ^{kip} intervals thereafter. At 25 ^{kip} , flaw fractured through to surface. Complete cleavage fracture at 57.5 ^{kip}	13,700
A-11	Prepared as specimen A-7 except no compressive preload was used	-38	Loaded slowly, struck with sledge at 8 ^{kip} intervals. Cleavage fracture at 133.6 ^{kip}	31,600

TABLE 3-I - Data summary - "A" series (continued)

Specimen	Specimen description (See Fig. 3-1)	Test temp. F	Testing technique	Static stress stress at fracture (gross area) psi
A-8	50% edge flaws at mid-thickness of plate 1/2 in. long in hard facing rod	-28	Struck with 8-lb sledge at 10 ^{kip} load increments. Cleavage fracture at 170 ^{kip}	41,600
A-9	As specimen A-4	-50	Struck with 8-lb sledge at 10 ^{kip} load increments. Cleavage fracture at 112 ^{kip}	28,800
A-12	Prepared as specimen A-7 with compressive load of 110 ^{kip}	-60	Specimen slowly loaded statically to fracture at 196 ^{kip}	48,800
A-13	Vertical 50% flaw at mid-depth of plate, 1 in. long in hard facing rod with E-6010 for remainder. Welded under transverse compressive load of 150 ^{kip}	-80	Struck with sledge at 8 ^{kip} intervals to 114.5, when partial cleavage fracture occurred in a vertical direction above and below weld flaw and partially curving into direction perpendicular to maximum longitudinal stress. Fracture complete at 113 ^{kip}	28,400
A-14	As specimen A-13	-34	As specimen A-13. Partial cleavage fracture at 122.4 ^{kip}	31,700
A-15	As specimen A-13	-38	Loaded slowly to cleavage fracture at 238 ^{kip} transverse across end of flaw	57,700
A-16	Prepared as specimen A-13, except no compressive load was used	-22	Loaded slowly to cleavage fracture at 250 ^{kip} , transverse across end of flaw	60,600

In a further effort to bring about low static-stress brittle fracture, a combination of cyclic tensile loading and shock effects was employed. The shock was applied by striking the specimen on the face with an 8-lb sledge hammer. If the results from tests on specimens A-1 (without shock) and A-2 (with shock) are compared, it can be seen that the sledge-hammer shocks as applied were not effective in reducing the static tensile stress required for specimen fracture.

At this point in the investigation, measures were adopted to introduce a high residual tensile stress at the flaw. The first attempt was made with specimen A-7 to develop full yield-point residual stress, such as might be expected in full-scale welded fabrication. After a groove was cut in the plate, it was compressed axially in a testing machine to shorten the groove opening. While the axial load was maintained, the flaw was prepared by laying root beads of hard high-carbon facing rod in the one-inch long groove. Upon chilling with an air blast, the root beads cracked and exhibited a well defined flaw in the mid-thickness of the plate. Welding was completed with the E-6010 electrode. After the specimen had cooled to room temperature, the compressive load was removed. As a result of this preparation, the tensile stress at the welding flaw was of yield-stress magnitude, as measured on other specimens with SR-4 gages.

The first specimen of this type, A-7, was loaded to 15,000 psi, and struck on the face with a single blow of the 8-lb sledge hammer; it exhibited a brittle fracture. This was the first of the Series A specimens to fracture at a tensile stress significantly below the yield point of the base material. A second test was made on A-8, fabricated in the identical manner of specimen A-7. This specimen was struck repeatedly with the 8-lb sledge hammer as the static load was increased, with brittle fracture occurring at 13,700 psi applied stress. To obtain a measure of the effect of the sledge-hammer blows, specimen A-12, identical to specimen A-7, was fabricated with residual stresses and loaded statically to fracture. This specimen fractured at the post-yield point stress of

48,800 psi. This indicated the importance of the dynamic load applied by the sledge hammer.

The magnitude of the residual stress seemed a factor to be considered. To obtain a lower residual stress, specimen A-11 was prepared in the same manner as A-7, except that no compressive pre-load was used. As the static tensile stress was increased, the specimen was repeatedly struck with the sledge. The lowered residual stress was reflected in the higher static stress required for brittle fracture, 31,600 psi.

As a part of this phase of the investigation, specimens A-13 through A-15 were prepared with welding flaws that were parallel to the axis of loading. These were loaded slowly and struck repeatedly on the face with the 8-lb sledge as the load increased. The first specimen of this type, A-13, exhibited an arrested brittle fracture, which after initiation at the ends of the vertical flaw, ran in a vertical direction until it curved toward a transverse orientation before stopping. Specimens A-14, 15 and 16 fractured brittly in a transverse orientation from an end of the vertical flaw.

Summary, Type-A Specimen Tests: The objective of this series of tests on Type-A Specimens was to establish a testing technique by which brittle fractures could be initiated in the laboratory at static applied stresses of approximately the same magnitude as reported for the ship fractures that originated from welding flaws. This series demonstrated qualitatively that low-static applied stress systems could superpose on high residual stress systems under certain conditions to bring about brittle fracture. On the basis of these tests, the conditions believed to be required for specimens containing welding flaws in the presence of yield-point residual stresses are: (1) sufficiently low temperatures and (2) sufficiently high strain rates. The testing temperatures for the specimens of this series were all in the sub-zero range, as low as -80 F.

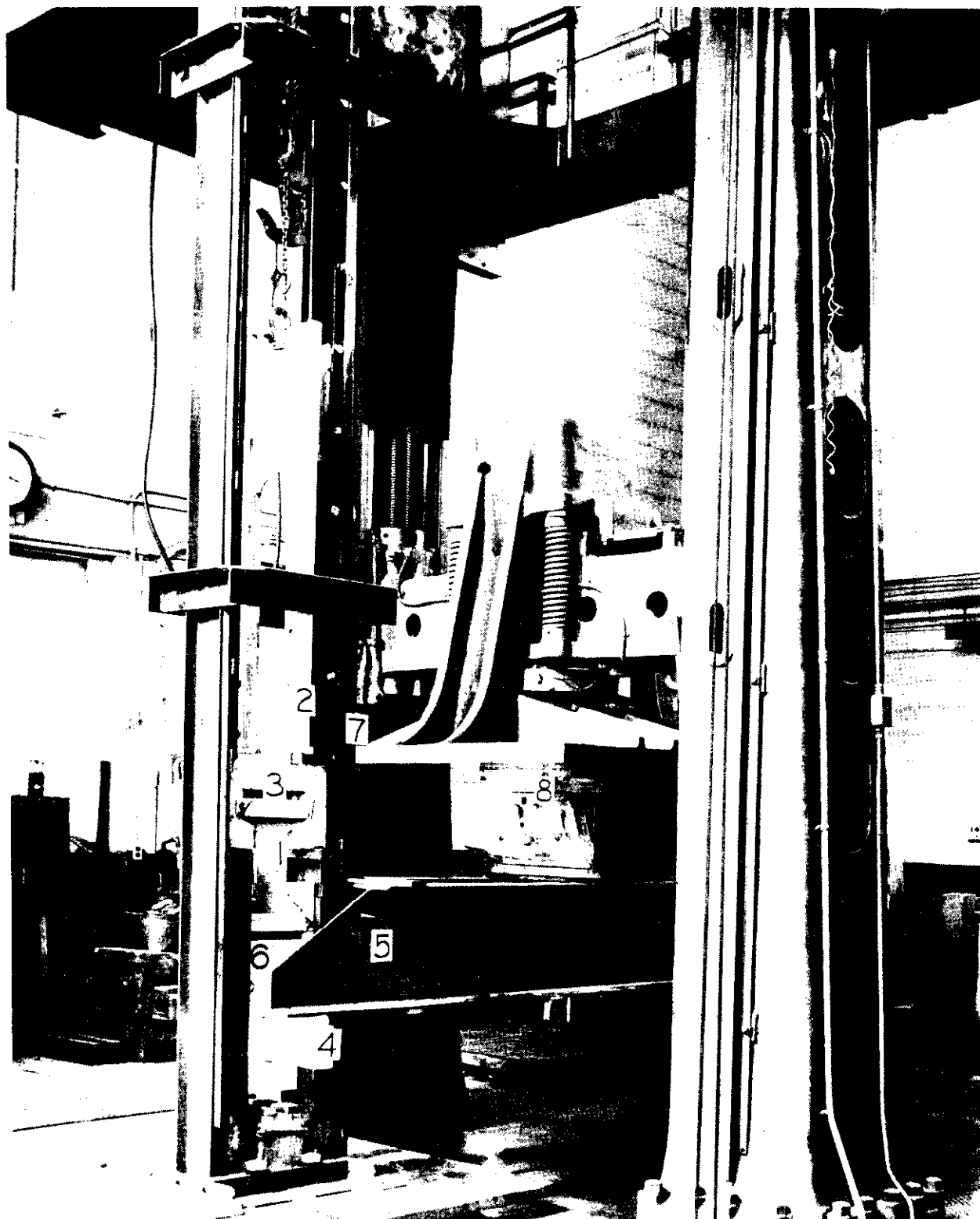


Fig. 3.3 - Drop-weight testing device

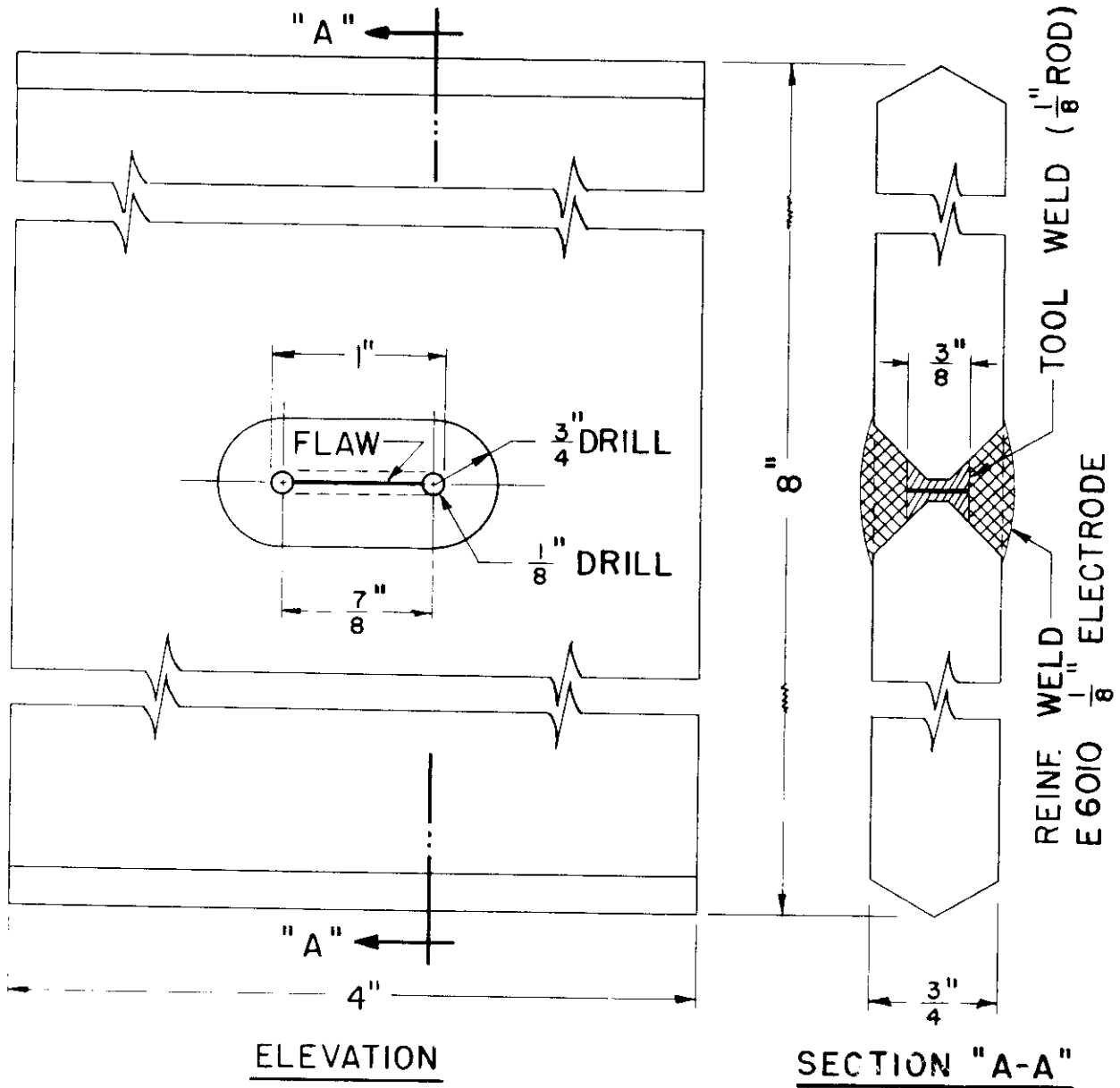
1. Specimen
2. Drop-weight
3. Top specimen grip
4. Striking anvil
5. Beam for applying static load
6. Lower specimen grip
7. Drop-weight testing frame
8. Static-loading knife edge

These preliminary tests suggested that the next phase of study should incorporate welding flaws in a natural environment of residual stress to determine the relative magnitudes of static and dynamic stresses required for brittle fracture.

Type-B Specimens. To accomplish the study of the effect of dynamic loading on specimens containing welding flaws, the drop-weight testing device pictured in Fig. 3.3 was fabricated. With this arrangement, it was possible to apply tensile impact loading to the specimens with or without additional static loading. The maximum height of the drop of the hammer was 12-1/2 ft, and the hammer weight varied from 175 lb to 475 lb. The data from the Series B tests are shown in Table 3-II and plotted in Fig. 3.5 and 3.6.

The Type-B specimen design is shown in Fig. 3.4. The flaws were 1-in. long and 50% of the plate thickness at the mid sections. They were prepared by laying root passes of hard facing rod and the welding was completed with an E-6010. The welding reinforcement was ground flush.

The first group of Type-B specimens considered in this discussion are those that were fractured by a drop-weight of 308 lb, without superposition of applied static stress. These specimens contained residual stresses in the region of the weld flaw of approximately yield-point magnitude. The data plot of Fig. 3.5 indicates that a hammer drop between 3 and 4 ft was sufficient to cause brittle fracture at 0°F. To determine the effectiveness of this high residual stress in promoting cleavage fracture, several additional specimens were stress relieved for one hour at 1100 F and furnace cooled. The data for these specimens are also shown in Fig. 3.5, with the notation "S.R." None of the stress-relieved specimens fractured on the first blow, although they did fracture on subsequent higher blows. It is apparent that the normal residual stress resulting from weld-metal shrinkage is sufficient, when combined with dynamic loading, to cause brittle fracture. A photograph of a typical fracture of a Type-B specimen is given in Fig. 3.7.



GENERAL NOTES:

1. REINF. GROUND FLUSH ON SOME SPECIMENS, SEE TABLE
2. TOOL WELD CRACKED BY CHILLING.
3. 90° TAPERED POINT ON 3/4" DRILL.
4. EXCESS METAL BETWEEN 3/4" HOLES TO BE CHIPPED OUT.

FIG. 3.4 TYPICAL "B" SERIES SPECIMEN

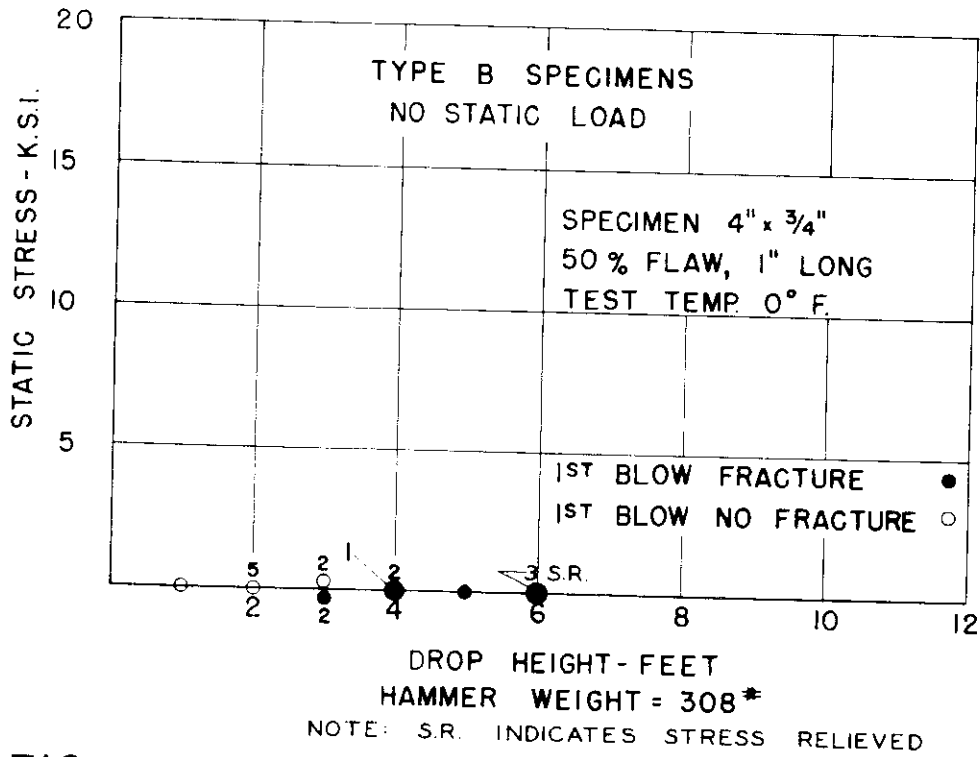


FIG. 3.5 DATA SUMMARY TYPE "B" SPECIMENS

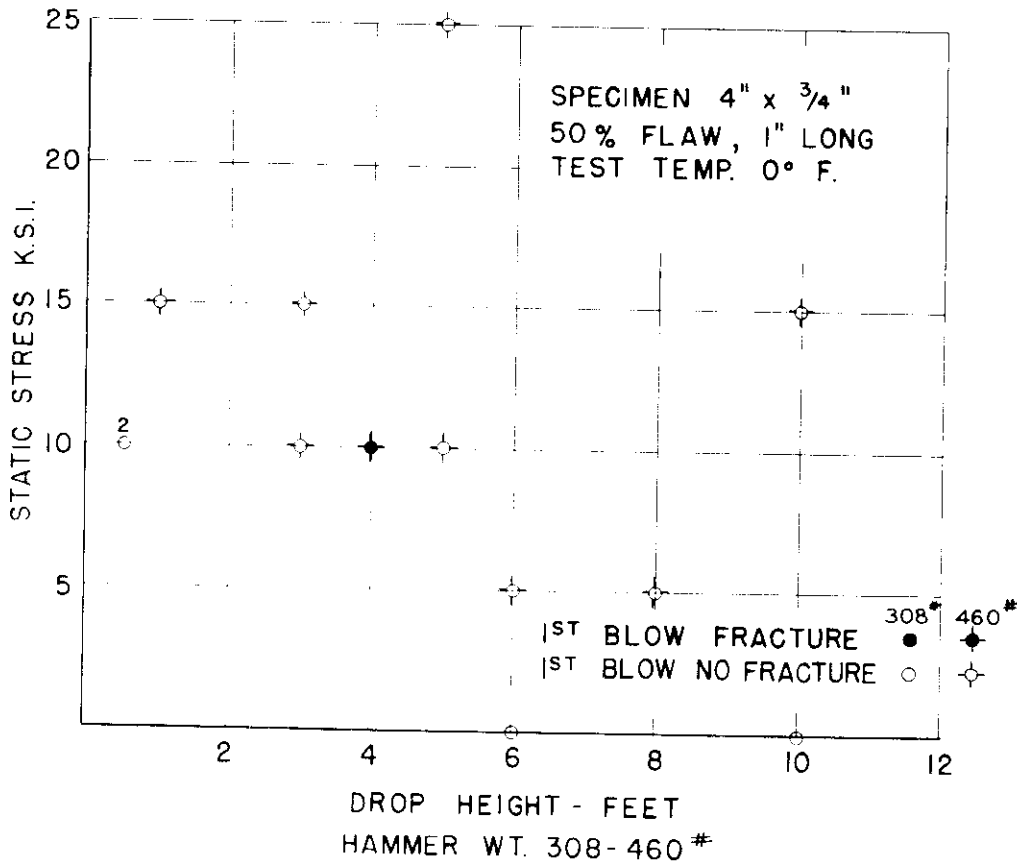


FIG. 3.6 DROP WEIGHT TESTS, TYPE "B" SPECIMENS WITH STATIC LOAD

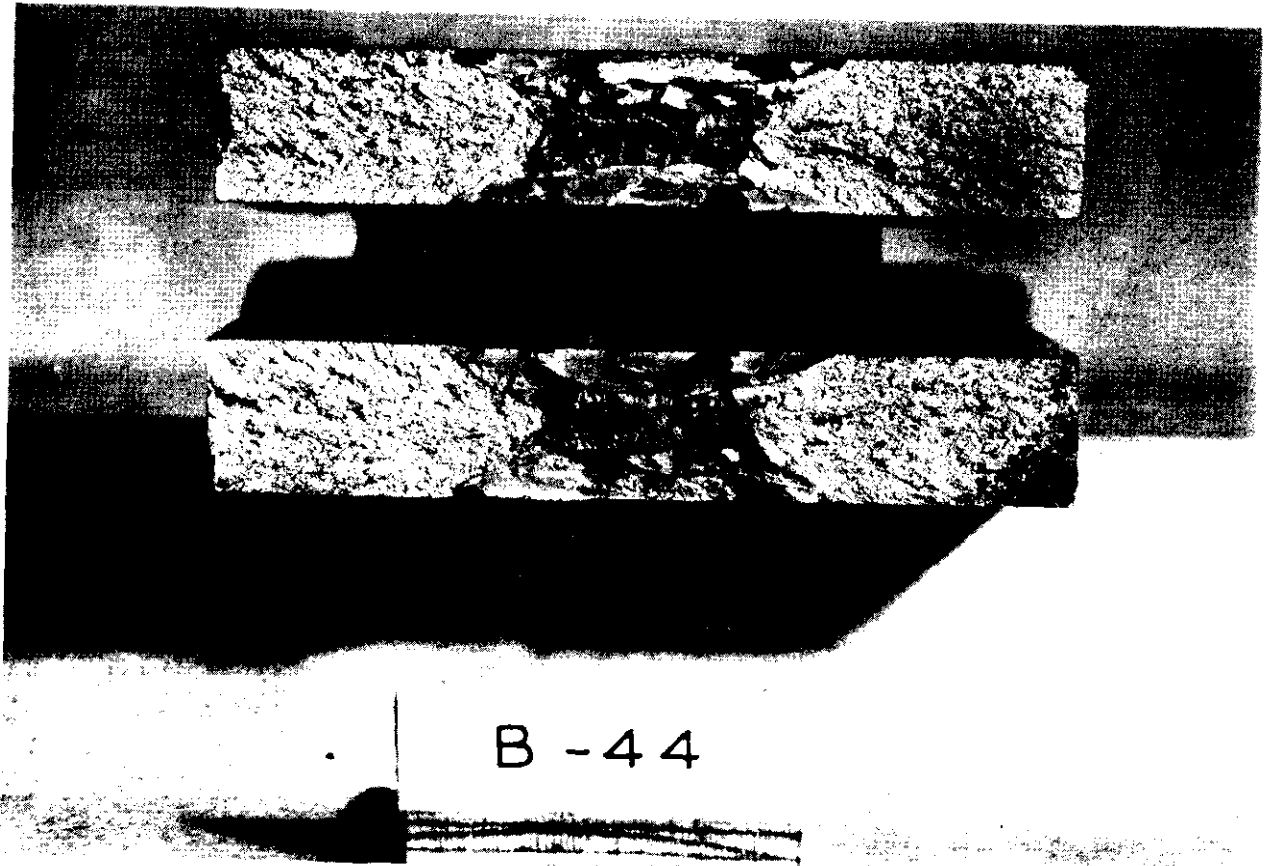


Fig. 3.7 - Photograph of fracture of Specimen B-44

The next group of Type-B specimens with residual stress were those that had dynamic effects superposed on various static stress levels. These data are plotted in Fig 3.6. It is interesting to note that none of these specimens fractured, even when the hammer weight was increased from 308 to 460 lb. It is believed that the energy losses incurred in the system while applying the static and dynamic loads were so great that insufficient dynamic energy reached the specimen. The loading beams that were used to apply the static loads were in place for all of the tests indicated in Fig. 3.6, whereas they were not used in the tests of Fig. 3.5.

Dynamic Stress Studies--Type-B Specimens: To measure the dynamic stresses that resulted from the tensile impact of the falling weight, specimens 3-in. wide and 7-in. wide (representative of the Series C tests, a discussion of which follows, were prepared without weld flaws and instrumented with SR-4 strain gages. The dynamic strains were measured with the aid of a Brush-type recording oscillograph. The dynamic stresses were calculated from the recorder data and are shown graphically in Fig 3.8. Pronounced permanent set was observed at the 4-ft drop of a 316-lb hammer on the 3-in. wide specimen, and at a 6-ft drop on the 7-in. wide specimen.

Strain rates were also estimated from the recorder data and appear to be about 0.20 in./in./sec in magnitude for the 3-in. wide specimens with a 3-ft drop of the hammer. The calculated strain rate values for this specimen are shown in Fig 3.9.

Summary, Type-B Specimen Tests. The Series B specimens led to several interesting observations and suggestions for further experimentation.

Considering Fig. 3.5, the minimum height of drop required to cause brittle fracture is approximately 3-1/2 ft. From Fig. 3.8, a 3-1/2-ft drop on a 4-in. wide specimen would correspond to a dynamic stress of approximately 22,500 psi.

TABLE 3-II

Data summary - Type B specimens

Specimen size: 4 in. x 8 in. x 3/4 in. ; weld flaw: 1 in. long buried crack in double-V slot. All tests at 0°F.

Specimen	Static stress psi	1st blow drop height ft	1st blow fracture		Total blows	Ht. of last blow ft	Fracture		Hammer weight lb	Remarks
			yes	no			yes	no		
B-4	0	2		x	2	4	x		308	Tested at -50 F
B-7	0	2		x	3	4	x		308	
B-8	0	4	x		1	4	x		308	
B-10	0	4		x	4	7	x		308	Stress relieved at 1100 F.
B-9	0	6		x	5	10	x		308	" " " "
B-6	0	1		x	7	7	x		308	Welded under compression load, 70 ^{kip}
B-5	0	2		x	3	6	x		308	Welded under compression load, 70 ^{kip}
B-13	0	3		x	2	4	x		308	
B-11	0	7	x		1	7	x		308	
B-12	0	5	x		1	5	x		308	Welded under compression load, 70 ^{kip}
B-14	0	3		x	3	5	x		308	
B-15	0	3	x		1	3	x		308	
B-16	0	6		x	4	10	x		308	Stress relieved at 1100 F.
B-17	0	6		x	2	8	x		308	" " " "
B-18	0	2		x	2	3	x		308	1 in. vert. flaw intersecting trans. flaw
B-22(a)	0	4		x	5	13		x	308	Solid weld metal--no flaw
(b)	0	6		x	4	12		x	460	Tested with 290-lb hammer: retested with 460-lb ham- mer. Flaw detail B.

Notes: All weld reinforcements ground flush, unless noted.
Loading beams not in place for specimens B-4--B-28

TABLE 3-II (continued)

Data summary - Type B specimens

Specimen	Static stress psi	1st blow drop height ft		1st blow fracture		Total blows	Ht. of last blow ft		Fracture		Hammer weight lb	Remarks
		ft	ft	yes	no		yes	no	yes	no		
B-23	0	6		x		1	6		x		308	
B-26	0	2			x	5	6		x		308	
B-27	0	4		x		1	4		x		308	
B-20	0	3		x		1	3		x		308	
B-28	0	2			x	4	5		x		308	
B-29(a)	10,000	0.5			x	7	3			x	308	Tested at 10,000 psi. No fracture
(b)	15,000	2			x	4	4			x	308	Retested at 15,000 psi. No fracture
(c)	20,000	4			x	2	5			x	308	Retested at 20,000 psi. No fracture
B-32(a)	10,000	0.5			x	6	4			x	308	Tested at 10,000 psi. No fracture
(b)	15,000	3			x	3	5			x	308	Retested at 15,000 psi. No fracture
B-34(a)	0	6			x	4	13			x	308	Tested with 308-lb hammer. No fracture
(b)	0	8			x	2	13			x	460	Retested with 460-lb hammer. No fracture
B-33	0	10			x	2	13			x	460	
B-21	10,000	4		x		1	4		x		460	
B-41	10,000	3			x	2	4		x		460	
B-40	5,000	6			x	2	10		x		460	
B-39	5,000	8			x	2	10			x	460	
B-38	15,000	1			x	8	10			x	460	

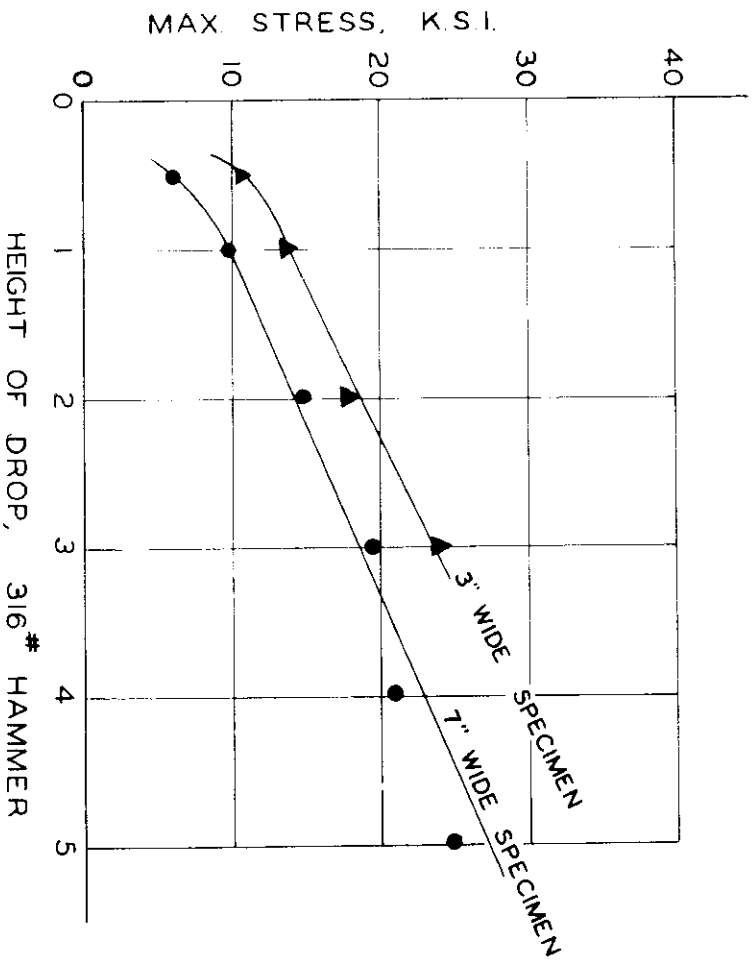
Notes: All weld reinforcements ground flush, unless noted.
Loading beams not in place for specimens B-4--B-28.

TABLE 3-II (continued)

Data summary - Type B specimens

Specimen	Static stress psi	1st blow drop height ft	1st blow fracture		Total blows	Ht. of last blow ft	Fracture		Hammer weight lb	Remarks
			yes	no			yes	no		
B-37	10,000	5		x	2	8		x	460	Reinforcing not ground flush.
B-36	15,000	10		x	2	13		x	460	" " " "
B-44(a)	15,000	3		x	2	4		x	460	Tested at 15,000 psi. No fracture
(b)	20,000	5		x	1	5		x	460	Retested at 20,000 psi. No fracture
(c)	25,000	10	x		1	10	x		460	Retested at 25,000 psi. Fracture
B-45	50,000	0	x		0	0			---	Static tensile test.
B-35(a)	25,000	5		x	1	5		x	460	Stress relieved at 1100 F. No fracture at 25,000 psi
(b)	30,000	5		x	2	8		x	460	Retest at 30,000 psi. No fracture
(c)	38,000	8		x	2	12	x		460	Retest at 38,000 psi. Fracture

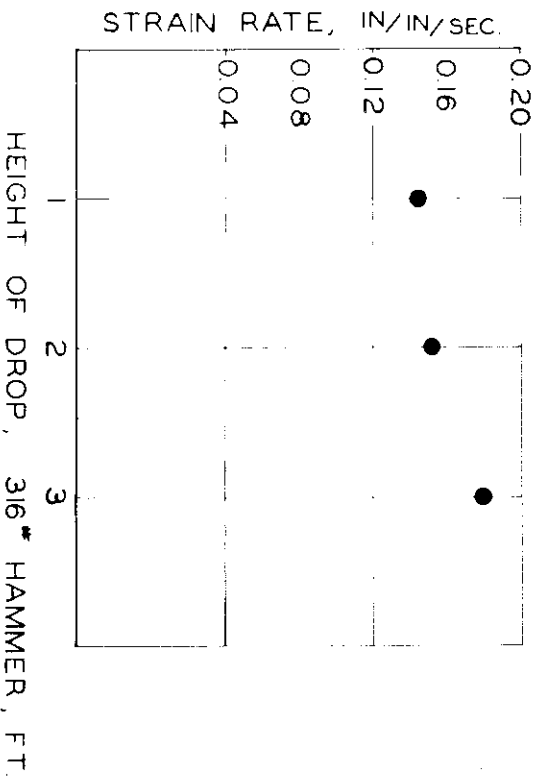
Notes: All weld reinforcements ground flush, unless noted.
Loading beams not in place for specimens B-4--B-28.



DYNAMIC STRESS VS. HEIGHT OF DROP FOR 316# HAMMER AT ROOM TEMPERATURE

DYNAMIC STRESSES

FIG. 3.8



STRAIN RATES MEASURED ON 3" x 3/4" UNNOTCHED SPECIMEN AT ROOM TEMPERATURE

STRAIN RATE MEASUREMENTS

FIG. 3.9

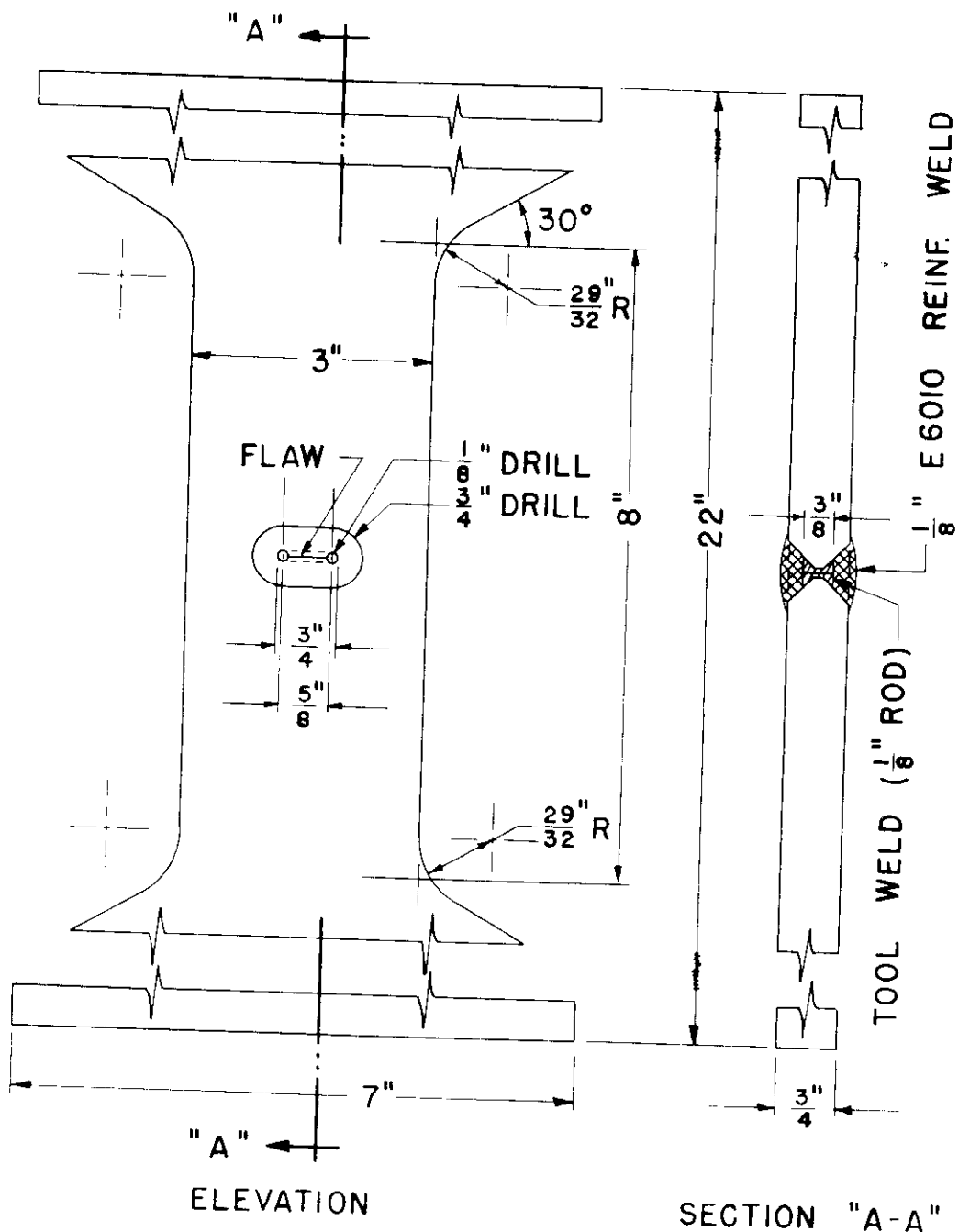
at the flaw. The longitudinal residual stress measured at the center of a 4-in. wide specimen was 44,500 psi. The sum of these two values is 67,000 psi. One specimen of Type B was tested to fracture in static tension at 0°F to determine the stress required for brittle fracture without the addition of a dynamic effect. This specimen fractured at a static stress of 50,000 psi. This stress level would suggest that there was perhaps partial, but not complete, superposition of static stress and mid-width residual stress of 44,500 psi.

The strain rates as estimated from the recorder data are low in comparison with the strain rates required to give appreciable increases in the yield-point at room temperature, according to published research data. However, it is felt that with the lowered temperatures of testing in this program, increased resistance to slip could come about at these strain rates. This effect is discussed further in the summary of Part III

The beneficial effect of stress relief in providing resistance to dynamic fracture was demonstrated by the data shown in Fig. 3.5. These specimens were struck repeatedly with the 308-lb drop hammer at drop heights of from 8 to 10 ft and plastically deformed before exhibiting cleavage fractures.

The results of the tests as shown in Fig. 3.6 are inconclusive. Only one specimen fractured on the first blow of either a 308-lb hammer or a 460-lb hammer. The specimen design for this group was the same as that for those specimens whose values are plotted in Fig. 3.5. The testing technique was undoubtedly affected by the addition to the testing system of the beams used to apply static tensile load. It is believed that less dynamic energy reached the specimen because additional energy was dissipated in the loading mechanism; thus fracture could not be produced.

Analysis of Type-B Specimens by Principle of Strain-Energy Release Rate.
At the suggestion of G. R. Irwin, specimens of Series B were tested to determine typical "G" values for E-6010 weld metal and ABS-Class B plate.



GENERAL NOTES:

1. REINF. GROUND FLUSH ON SOME SPECIMENS, SEE TABLE
2. TOOL WELD CRACKED BY CHILLING.
3. 90° TAPERED POINT ON 3/4" DRILL.
4. EXCESS METAL BETWEEN 3/4" HOLES TO BE CHIPPED OUT.

FIG. 3.10 TYPICAL 3" WIDE "C" SERIES SPECIMEN

The "G" value determined for a 50% mid-thickness flaw in E-6010 weld metal was about 100 in.-lb per sq in. in magnitude.

It is assumed that fractures from buried flaws take place in two stages. The first stage constitutes the "crash through," when a buried flaw of a given length suddenly breaks completely through the plate thickness without appreciable change of flaw length. The second stage of the fracture is the transverse fracture across the plate width.

Irwin³ has shown that the value of strain-energy release rate for crack propagation in a finite width of plate is given by the expression $G = \frac{\sigma^2 b}{E} \tan\left(\frac{\pi C}{2b}\right)$, where "G" is strain-energy release rate, σ is stress on gross area, b is the width of plate, and C is the crack length. This relationship may be applied to a Type B specimen, where b is now interpreted as plate thickness and $C = 3/8$ in., with the assumption of a strain-energy release rate value of 100 in.-lb per sq in. Considering the "crash through" or first stage of fracture, the stress on the gross area is calculated to be 63,400 psi, which closely approximates the estimated superposed residual and dynamic stress of 67,000 psi. According to the theoretical expression, if a strain-energy release rate of 100 in.-lb per sq in., as determined by specimens of Series B, is used, the second stage of the fracture should proceed at a stress level of 42,500 psi. It is to be expected then that the fracture would continue in its transverse propagation following the "crash through" at a 63,400 psi stress level.

Strain-energy release rates for specimens containing buried welding flaws are discussed at greater length in Part IV of this report.

Type-C Specimens--Discussion: Specimens of Type-C were 3-in. wide, 8-in. long, and of 3/4-in. thick ABS-Class B steel, as shown in Fig. 3.10 and in the photograph, Fig. 3.11. A later modification of the Type-C specimen was 7-in. wide at the test section, as shown in Fig. 3.12 and in the photograph, Fig. 3.13. The purpose of introducing the Type-C specimens into the program

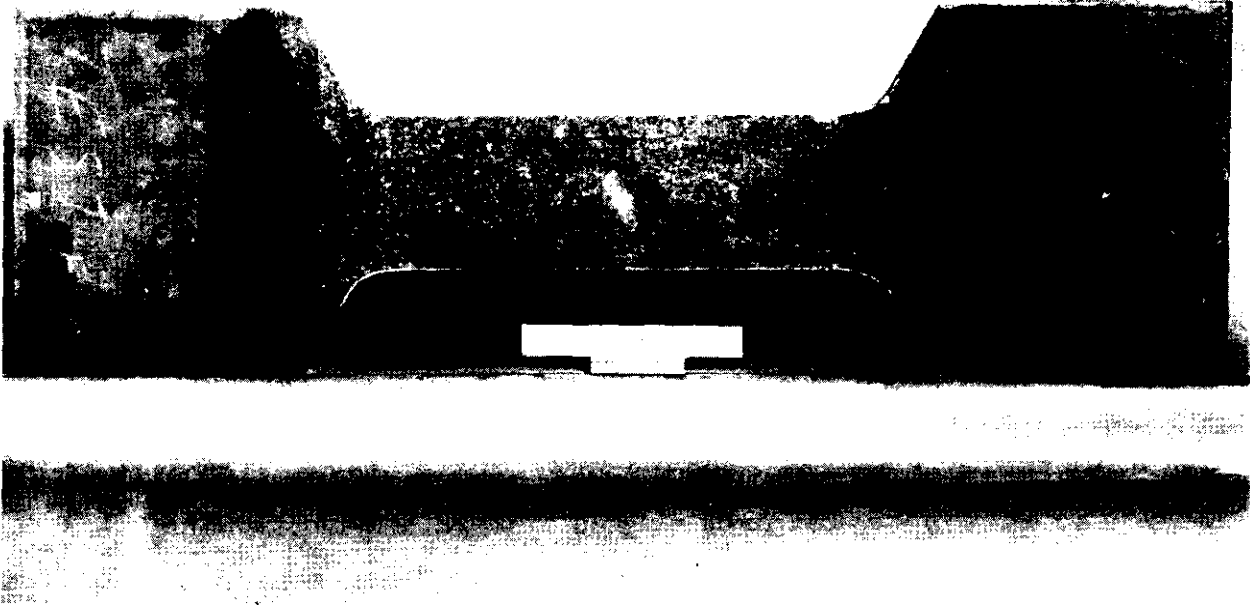
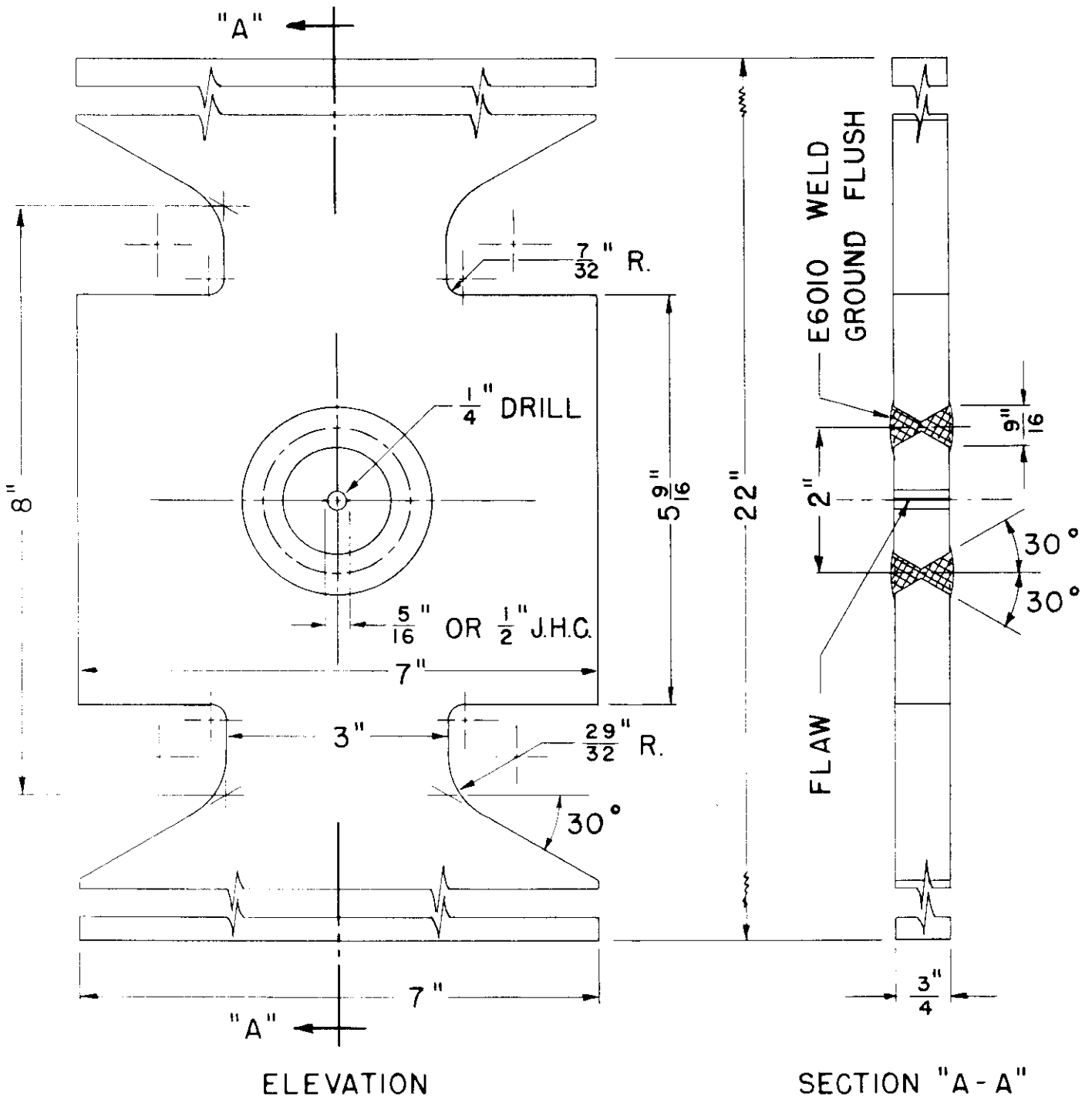


Fig. 3.11 - Photograph of 3-in. wide Type "C" specimen



**FIG. 3.12 TYPICAL 7" WIDE "C" SERIES SPECIMEN
(WITH 2" DIA. WELDED PATCH)**

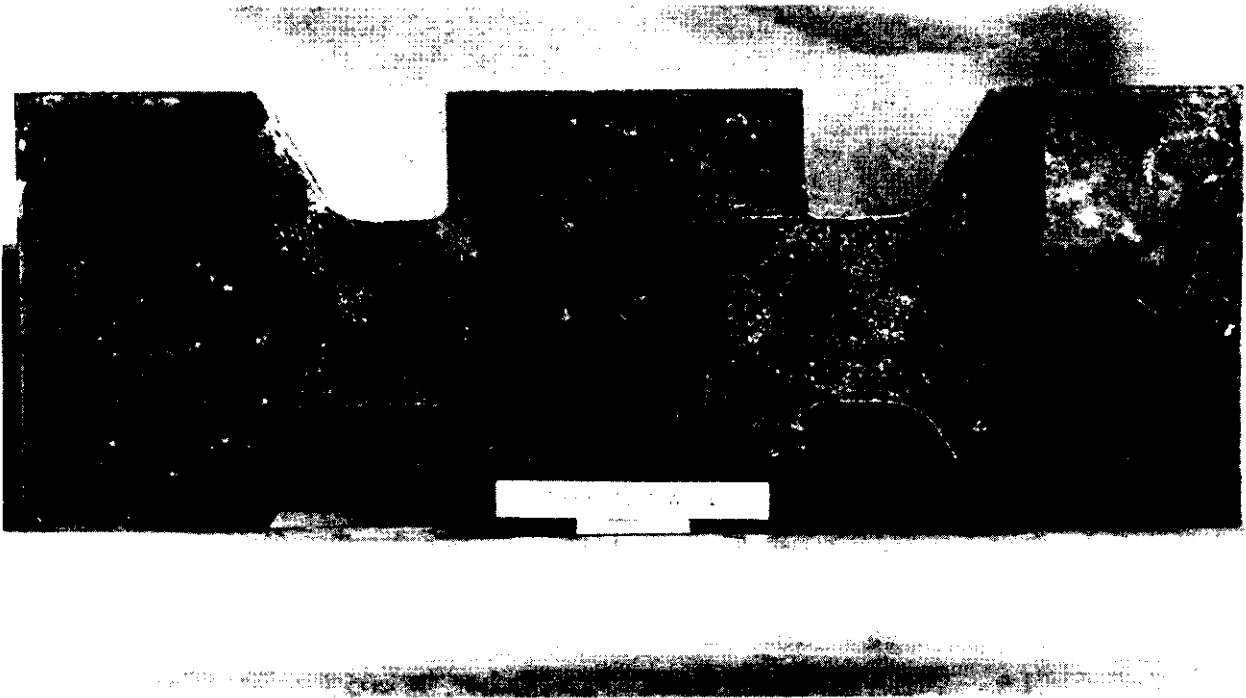


Fig. 3.13 - Photograph of 7-in. wide Type "C" specimen

was to make a specimen with a reproducible flaw in a field of residual stress, in order to have a suitable testing technique for determining the inter-relationships between applied static, dynamic, and residual stresses.

The first group of Type-C specimens consisted of specimens C-1 through C-19, each with a central full-thickness double-vee slot, 3/4-in. long at the mid-section. Root passes of hard-facing welding electrode were laid in the grooves from either side; these root passes cracked during cooling. The welds were completed with an E-6010 electrode, and the reinforcement was ground flush. The stresses locked in the weld metal after cooling were of yield-point magnitude.

The specimens were tested at approximately 0°F in the 460-lb drop-weight apparatus pictured in Fig. 3.3. The data for this test series are given in Table 3-III and shown graphically in Fig. 3.14. Only the results of the first blow are plotted since it is quite possible that subsequent plastic deformation partially relieves the residual stress. As a probable result of the lack of control over the welding flaw, the data from these initial tests were quite erratic. A typical fracture of a 3-in. wide Type-C specimen is shown in Fig. 3.15.

The second group of Type-C specimens, specimens C-21 through C-41, was an experimental group in which the type of controlled stress raiser and the method of inducing residual stresses were investigated as variables. The types of stress raisers tested experimentally included jeweler's hack saw notches 0.01-in. wide and of various lengths, drilled holes of various diameters, and jeweler's hack saw notches terminating in holes of various diameters. These data are summarized in Table 3-IV.

Another objective in studying this second group of specimens was to establish a reproducible method of introducing residual stresses. Some of the methods explored included (1) solid E-6010 weld metal in a double-vee groove, 3/4-in. long, ground flush and notched; (2) spot heating by an oxyacetylene torch; and (3) spot heating by electrical induction. The method that appeared to be most satisfactory was the circular-patch method devised by Levy and Kennedy.¹⁰

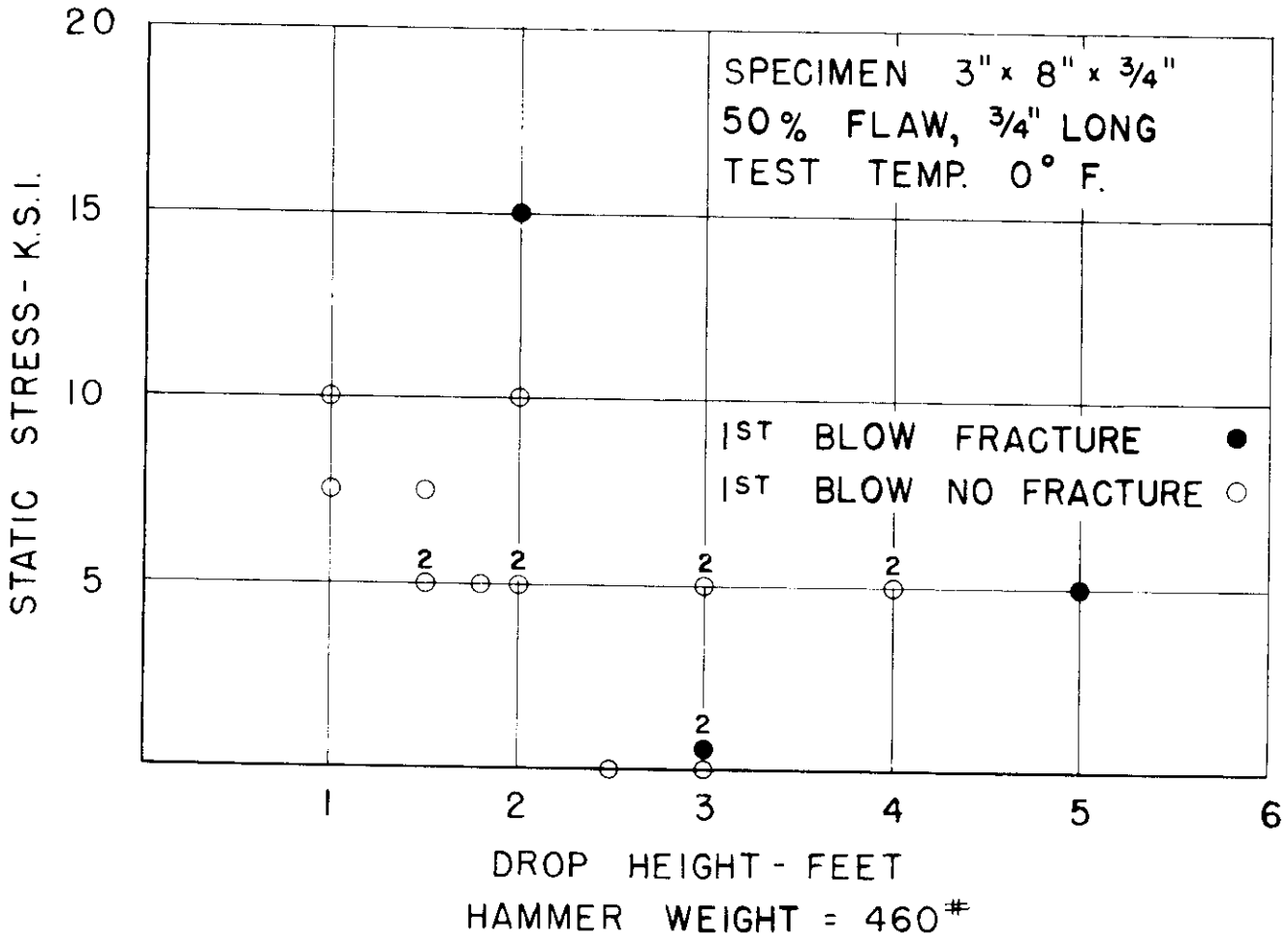


FIG. 3.14 DATA SUMMARY TYPE "C"
SPECIMENS

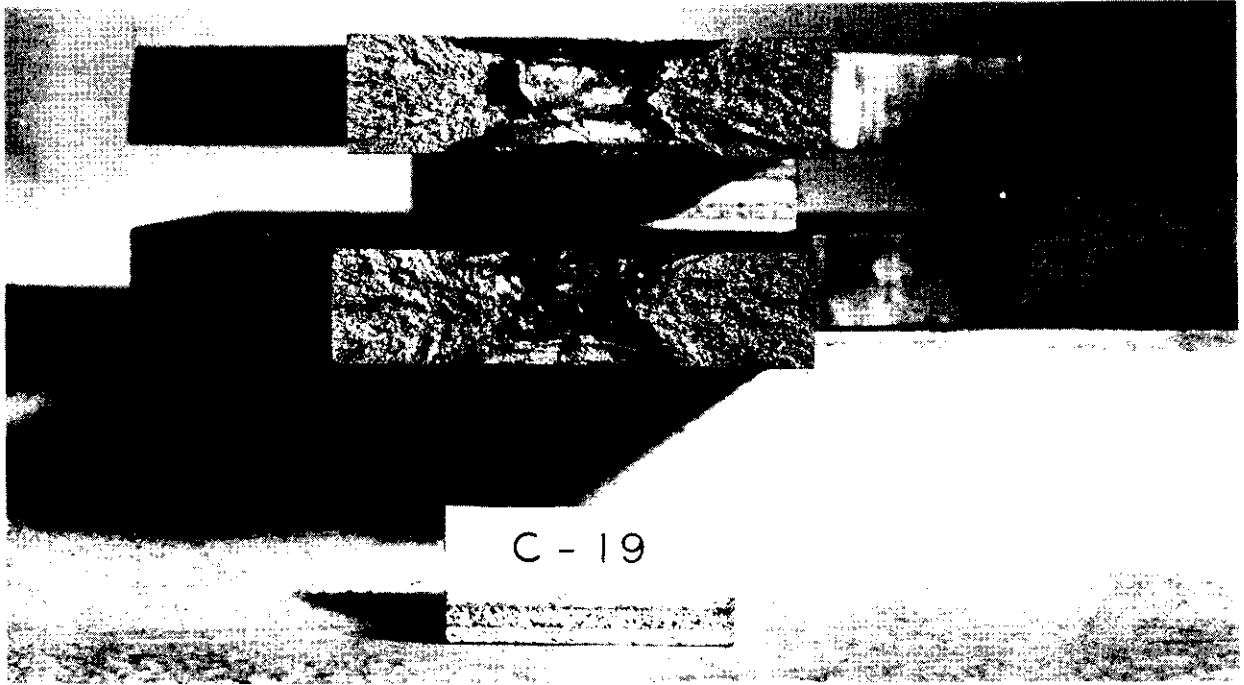


Fig. 3.15 - Photograph of fracture of Specimen C-19

The patch method consists of cutting out a circular patch at the mid-section of the specimen and fabricating the stress raiser in this patch. The patch is then welded back into the plate so that a biaxial residual stress field is created in the patch. The weld reinforcement around the patch is then ground flush. The proportions of a 2-in. diameter patch in a 7-in. wide test section permitted biaxial tensile stresses of approximately 35,000 psi, as determined from measurement of the strain released during removal of a 1-in. square patch at the center of the specimen.

A third group of Type-C specimens, all incorporating the welded patch, is represented by specimens C-43 through C-53. The data for these specimens are summarized in Table 3-V. The primary objective in investigating this experimental group was to determine a suitable hammer weight for the 7-in. wide specimen that contained a 2-in. diameter patch. The stress raiser consisted of a 1/4-in. diameter drilled hole with radial jeweler's hack-saw notches 1/32 in. in length. A hammer weight of 175 lb was selected as being suitable for testing specimens over the range of static stress desired in the program.

In testing a fourth group of Type-C specimens, C-54 through C-81, use was made of the data established by the preceding group. The specimen design was the same as that shown in Fig. 3.12 and in the photograph, Fig. 3.13, having a test section 7-in. wide, a residual stress field in a 2-in. diameter patch, and a stress raiser consisting of a 1/4-in. drilled hole with two jeweler's hack-saw notches 1/32-in. long. The 175-lb hammer was selected for the drop-weight apparatus. The data for this series of tests are summarized in Table 3-VI and shown graphically in Fig. 3.16. It can be seen that these data, with some scatter, indicate a general trend of lowered dynamic effect with increased static tensile stress required to produce fracture. It is interesting to note that at 15,000 psi static stress, it was impossible to obtain fracture even at the maximum height of the drop of the hammer. In this respect, the behavior of this series of specimens was similar to the furnace stress-relieved specimens C-80 and C-81, which

TABLE 3-III

Data summary - Type C specimens

Specimen size: 3 in x 8 in x 3/4 in.; Weld flaw: 3/4-in. long, 50% buried crack in double-V slot. All tests at 0°F.

Specimen	Static stress, ksi	1st blow drop height ft	1st blow fracture		Total blows	Ht. of last blow ft	Fracture		Hammer weight lb	Remarks
			yes	no			yes	no		
C-1	0	3		x	2	4	x		460	
C-2	0	3	x		1	3	x		460	
C-3	0	2.5		x	3	3 5	x		460	
C-4	5	1.5		x	2	2	x		460	
C-5	5	1.5		x	2	2	x		460	
C-6	5	2		x	8	9	x		460	
C-7	10	1		x	6	4	x		460	
C-8	7.5	1		x	5	3	x		460	
C-9	7.5	1.5		x	4	3	x		460	
C-10	10	2		x	5	7	x		460	
C-11	5	5	x		1	5	x		460	Stress relieved at 1150 F
C-12	15	2	x		1	2	x		460	
C-13	0	3	x		1	3	x		460	
C-14	5	1.75		x	8	10	x		460	
C-15	5	2		x	3	5	x		460	
C-16	5	3		x	2	4	x		460	
C-17	5	4		x	6	9	x		460	
C-18	5	3		x	5	9	x		460	
C-19	5	4		x	2	5	x		460	

TABLE 3-IV

Data summary - Type C specimens

Specimen size 3 in. x 22 in. x 3/4 in

Testing temperature as noted

Specimen	Static stress, ksi	1st blow drop ht ft	1st blow fracture		Total blows	Ht. of last blow, ft	Fracture		Hammer weight lb	Temp. F	Type of flaw
			yes	no			yes	no			
C-21	0	3	x		1	3	x		460	-10	3/4 in. JHC Notch
C-22	0	2	x		1	2	x		460	-10	" " " "
C-23	5	1/2		x	3	2	x		460	-5	" " " "
C-26	0	2		x	2	3	x		460	-6	" " " " term. in 3/64 in. holes
C-27	0	6		x	2	8	x		460	-4	3/4 in. JHC Notch term. in 1/8 in. holes
C-28	0	3		x	2	5	x		316	-6	3/4 in. JHC Notch term. in 3/64 in. holes
C-29	0	4		x	2	5	x		316	0	3/4 in. JHC Notch term. in 3/64 in. holes
C-30	0	6		x	3	9	x		316	+6	3/4 in. JHC Notch term. in 3/16 in. holes
C-31	0	8		x	3	13		x	316	0	1/8 in. hole only
C-32	0	8	x		1	8	x		316	-10	5/16 in. JHC
C-33	0	8	x		1	8	x		316	-10	" " "
C-34	0	8		x	3	13		x	316	0	2 - 1/16 in. holes, 1/4 in. c. to c.
C-35	0	10		x	2	13		x	316	0	3/64 in. hole
C-36	0	8	x		1	8	x		316	-10	7/32 in. hole + 2 - .040 in. holes
C-37	0	8	x		1	8	x		316	-10	1/8 in. hole + 2 - 3/32 in. side holes
C-38	0	8	x		1	8	x		316	-10	2 - 1/8 in. holes (Residual stress by spot heating)
C-39	0	8		x	2	13		x	316	0	2 - 1/8 in. holes (No resid. stress)
C-40	0	6		x	3	13		x	316	0	2 - 1/8 in. holes (2 in. dia welded patch)
C-41	0	13		x	1	13		x	316	-10	2 - 1/8 in. holes (2 in. dia welded patch)

-06-

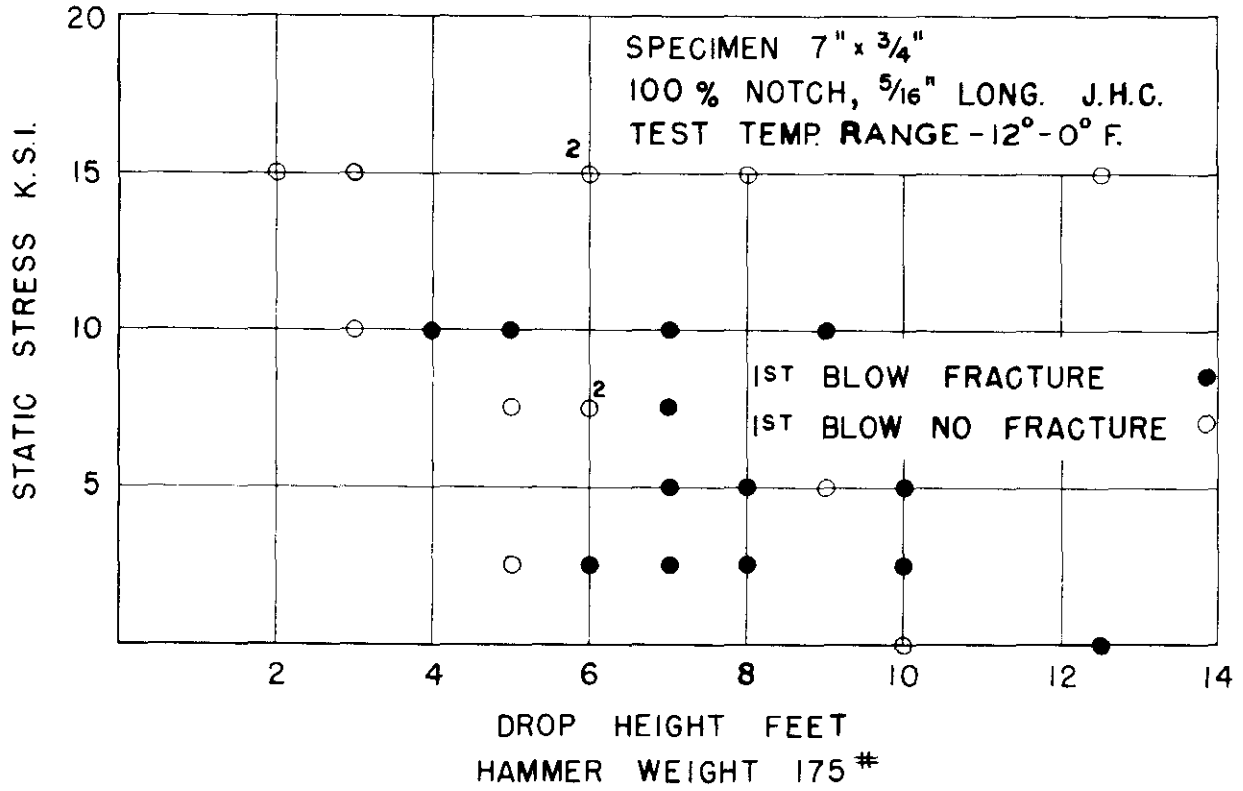


FIG. 3.16 DATA SUMMARY TYPE "C" SPECIMENS

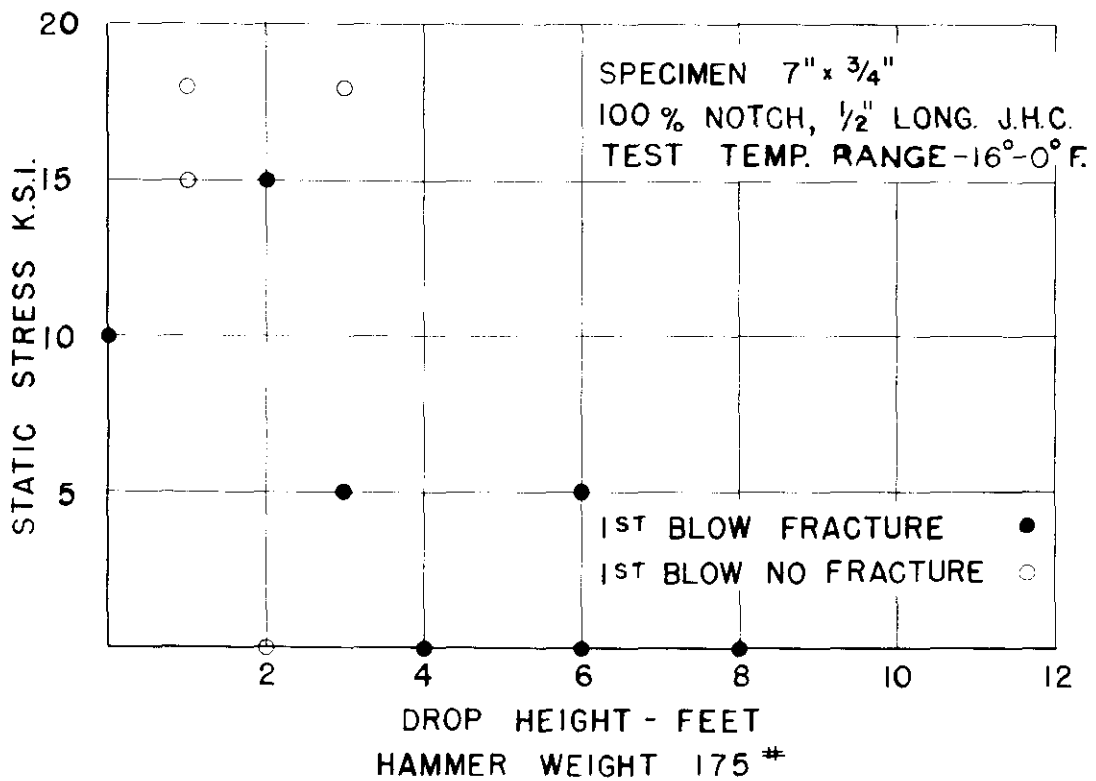


FIG. 3.17 DATA SUMMARY TYPE "C" SPECIMENS

would not fracture at the maximum hammer drop. This was discussed in the Summary of Type-B specimen tests and will also be discussed in the Summary of Part III.

At the suggestion of the Advisory Committee, specimens C-82, 85 and 86, were tested. The orientation of the notch in C-82 and C-85 was parallel to the axis of loading, rather than transverse as it had been in the preceding specimens. These specimens did not fracture at the maximum drop height of the 175-lb hammer, nor did specimen C-86, which had the notch oriented at 45° to the axis of loading.

The final group of specimens in the Type-C program, C-88 to C-98, were those having a notch 1/2-in. long, which was made by cutting two jeweler's hacksaw notches 1/8-in. long from a 1/4-in. diameter hole. The hammer weight remained at 175 lb. The data for these specimens are presented in Table 3-VII and are shown graphically in Fig. 3.17. A photograph of the fracture surface of a specimen of this group is shown in Fig. 3.18.

Summary, Type-C Specimens: The testing program for the Type-C specimens was an extension of the program described for the Type-B specimens. It represents an exploratory program designed to find the combinations of residual stress, impact stress, and static applied stress that would most likely superpose on a given flaw to produce low-nominal-stress brittle fractures at 0°F.

The data of Fig. 3.17 illustrate the fact that superposition of these stresses can take place under appropriate conditions. These specimens contained 1/2-in. long, 100% full-thickness flaws in a field of residual stress. The data indicate that these Type-C specimens would fracture at drop heights of 4 ft with no static stress, at 3 ft with 5000 psi static stress, and with no dynamic effect necessary, at 10,000 psi static stress. The following tabulation indicates the estimated stress levels at fracture for these specimens:

TABLE 3-V

Data summary - Type C specimens

Specimen size: 7 in x 19 in x 3/4 in. with 2-in. dia. welded patch.

Testing temperatures as noted.

Specimen	Static stress, ksi	1st blow drop ht. ft	1st blow fracture		Total blows	Ht. of last blow ft	Fracture		Hammer weight lb	Temp. F	Type of flaw
			yes	no			yes	no			
C-43	0	6	x		1	6	x		316	-10	1/4 in. hole, two - 1/32 in. JHC
C-44	0	7		x	3	13		x	468	0	Two - 1/8 in. holes
C-45	0	6		x	3	13		x	468	0	1/4 in. hole, two - 1/32 in. JHC, stress relieved
C-46	0	6	x		1	6	x		316	-10	1/4 in. hole, two - 1/32 in. JHC
C-49	0	9	x		1	9	x		203	-10	1/4 in. hole, two - 1/32 in. JHC
C-50	0	9		x	2	13		x	164	-10	" " " " " " "
C-51	0	9		x	2	13		x	182.5	-10	" " " " " " "
C-52	0	10	x		1	10	x		182.5	-10	" " " " " " "
C-53	0	8	x		1	8	x		182.5	-12	" " " " " " "

TABLE 3-VI

Data summary - Type C specimens

Specimen size: 7 in. x 19 in. x 3/4 in. with 2-in. dia. welded patch.

Test temperatures as noted

Specimen	Static stress ksi	1st blow drop ht. ft	1st blow fracture		Total blows	Ht. of last blow ft	Fracture		Hammer weight lb	Temp. F	Type of flaw
			yes	no			yes	no			
C-54	0	10		x	3	12.5		x	175	0	1/4 in. hole, two - 1/32 in. JHC
C-55	0	12.5	x		1	12.5	x		175	-10	" " " " " " "
C-56	5	9		x	3	12.5		x	175	0	" " " " " " "
C-57	10	9	x		1	9	x		175	-10	" " " " " " "
C-58	10	7	x		1	7	x		175	-10	" " " " " " "
C-59	10	5	x		1	5	x		175	-10	" " " " " " "
C-60	10	3		x	4	9		x	175	0	" " " " " " "
C-61	10	4	x		1	4	x		175	-12	" " " " " " "
C-62	5	10	x		1	10	x		175	-12	" " " " " " "
C-63	5	8	x		1	8	x		175	-12	" " " " " " "
C-64	5	7	x		1	7	x		175	0	" " " " " " "
C-65	15	2		x	4	6		x	175	0	" " " " " " "
C-66	15	3		x	2	5		x	175	-5	" " " " " " "
C-67	15	6		x	2	8		x	175	-5	" " " " " " "
C-68	2.5	10	x		1	10	x		175	-8	" " " " " " "
C-69	2.5	8	x		1	8	x		175	-10	" " " " " " "
C-70	2.5	7	x		1	7	x		175	-10	" " " " " " "
C-71	2.5	6	x		1	6	x		175	-10	" " " " " " "
C-72	2.5	5		x	2	7		x	175	-6	" " " " " " "
C-73	7.5	5		x	2	8		x	175	-6	" " " " " " "
C-74	7.5	6		x	2	10		x	175	-8	" " " " " " "
C-75	7.5	7	x		1	7	x		175	-10	" " " " " " "
C-76	7.5	6		x	2	12		x	175	-5	" " " " " " "
C-77	15	6		x	2	12		x	175	-5	" " " " " " "
C-78	15	8		x	1	8		x	175	-10	" " " " " " "
C-79	15	12.5		x	1	12.5		x	175	-10	" " " " " " "

TABLE 3-VI (continued)

Data summary - Type C specimens

Specimen size: 7 in. x 19 in. x 3/4 in. with 2-in. dia. welded patch.

Test temperatures as noted

Specimen	Static stress ksi	1st blow drop ht ft	1st blow fracture		Total blows	Ht. of last blow ft	Fracture		Hammer weight lb	Temp. F	Type of flaw
			yes	no			yes	no			
C-80	5	12.5		x	1	12.5		x	175	-10	1/4 in. hole, two - 1/32 in. JHC (Stress relieved)
C-81	10	12.5		x	1	12.5		x	175	-10	1/4 in. hole, two - 1/32 in. JHC (Stress relieved)
C-82	0	12.5		x	1	12.5		x	175	-10	1/4 in. hole, two - 1/32 in. JHC (Longitudinal orientation)
C-85	10	12.5		x	1	12.5		x	175	-10	1/4 in. hole, two - 1/32 in. JHC (Longitudinal orientation)
C-86	10	12.5		x	1	12.5		x	175	-10	1/4 in. hole, two - 1/32 in. JHC (45° orientation)
C-87	0	12.5		x	1	12.5		x	175	-10	1/4 in. hole, two - 1/4 in. JHC (45° orientation)

TABLE 3-VII

Data summary - Type C specimens

Specimen size 7 in x 1³/₄ in x 3/4 in with 2-in dia welded patch

Test temperatures as noted

Specimen	Static stress, ksi	1st blow drop ht., ft	1st blow fracture		Total blows	Ht. of last blow ft	Fracture		Hammer weight lb	Temp. F	Type of flaw
			yes	no			yes	no			
C-88	5	6	x		1	6	x		175	-10	1/4 in. hole, two - 1/8 in. JHC
C-89	10	0	-	-	-	-	x		-	-16	1/4 in. hole, two - 1/8 in. JHC
C-90	15	2	x		1	2	x		175	-8	1/4 in. hole, two - 1/8 in. JHC
C-91	18	1		x	3	12.5	x		175	0	1/4 in. hole, two - 1/8 in. JHC
C-92	18	3		x	3	10		x	175	0	1/4 in. hole, two - 1/8 in. JHC
C-93	0	8	x		1	8	x		175	-10	1/4 in. hole, two - 1/8 in. JHC
C-94	0	6	x		1	6	x		175	-10	1/4 in. hole, two - 1/8 in. JHC
C-95	0	4	x		1	4	x		175	-10	1/4 in. hole, two - 1/8 in. JHC
C-96	15	1		x	4	10		x	175	0	1/4 in. hole, two - 1/8 in. JHC
C-97	0	2		x	3	4	x		175	-5	1/4 in. hole, two - 1/8 in. JHC
C-98	5	3	x		1	3	x		175	-10	1/4 in. hole, two - 1/8 in. JHC

Residual stress, ksi	35	35	35
Static stress, ksi	0	5	10
Dynamic stress, ksi	<u>12</u>	<u>10.7</u>	<u>0</u>
Total estimated stress on gross area at frac- ture, ksi	47	50.7	45

The Griffith crack theory, with the strain-energy release rate nomenclature used by Irwin, would predict for these specimens having a 1/2-in. 100% full-depth, flaw, for an assumed "G" value of 100 in.-lb per sq in., a fracture stress of 60,500 psi based on the gross area at fracture. Since it is also likely that strain-energy release rates may be as low as 40 in.-lb per sq in., the stress might be found to be as low as 38,400 psi.

The specimens represented by the data of Figs. 3.14, 3.16, and 3.17 all indicate the difficulties of superposing a dynamic stress on a residual stress field in specimens that were loaded to a high level by an external static stress. This is the same difficulty that was observed in testing the Type-B specimens. Again, it probably holds true that the combination of the residual stress and the static stress is sufficient to cause significant plastic action in the mid-section of the plate. The hammer blow, then, rather than raising the stress level, provides plastic strain and some local increase of strain rate.

As further evidence of the plastic flow at the plate mid-section and the consequent relief of residual stress, the data in the tabular summaries of the Series C specimens indicate that, in most instances, the specimens that did not fracture under the first blow did not fracture under subsequent blows. In this respect, their behavior was similar to specimens that had been stress-relieved by annealing.

The greater severity under impact of short 100% flaws in comparison with short buried 50% flaws can be seen by comparing the data from Fig. 3.14, which

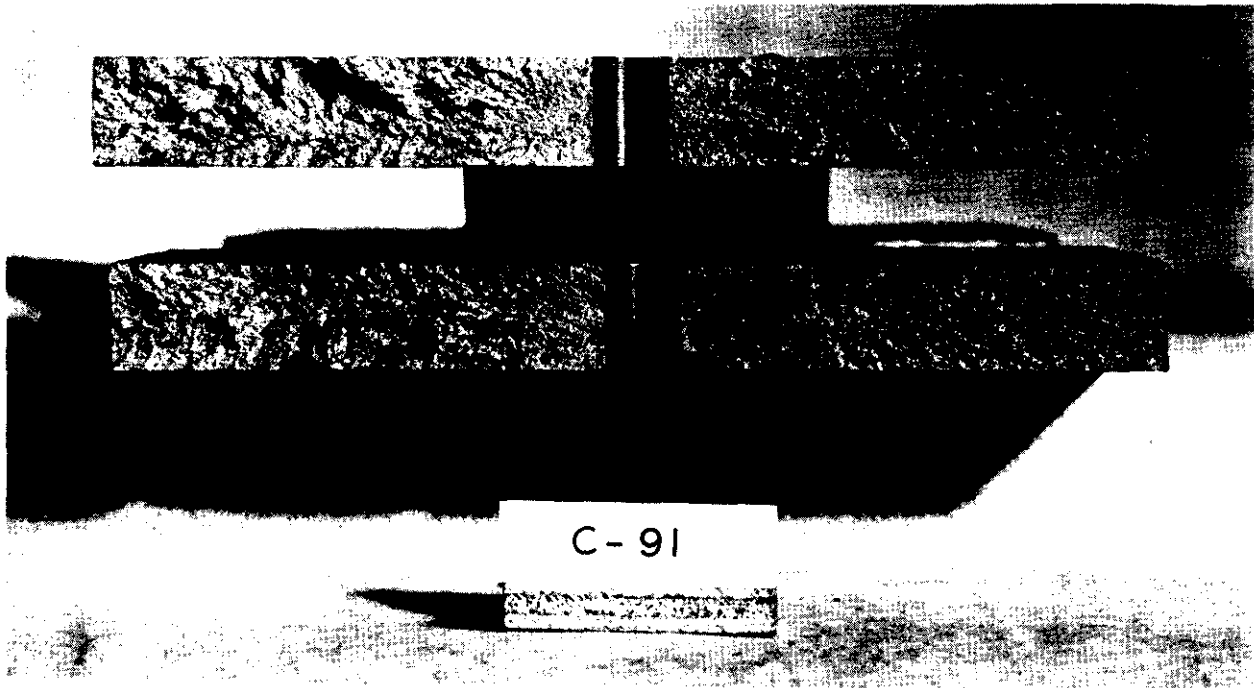


Fig. 3.18 - Photograph of fracture of Specimen C-91

represents 3/4-in. long, 50% flaws at the mid-thickness of a 3-in. wide plate, with the data from Figs. 3.16 and 3.17. For the former group of specimens, a 460-lb hammer was used. Subsequent testing of the Series D specimens of Part IV indicated that buried 50% flaws would not initiate low-stress fracture by static means alone, until they reached a length of approximately 1-1/2 in. This length limit for the shorter buried flaws is probably due to the restraint offered by the surrounding plate material, which prohibited the first break-through to the faces of the plate.

Also included in this investigation were 100% flaws, 5/16-in. long, which were either parallel to or at 45° to the axis of the static and impulsive loadings (Specimens 82, 85, and 86, Table 3-VI). In each instance, these specimens did not fracture at the maximum drop height of the hammer.

Summary of Part III

It is believed that the explanation for the behavior of the impact test specimens of Series A, B, and C, lies in the following hypothesis, proposed by Ludwik and summarized by Salmon:

Material in which the resistance to shear is relatively large, fails when the stress exceeds the cohesive force between the grains, there is little or no deformation, and the material is said to be brittle. In a ductile material resistance to shear is relatively small, deformation due to slip occurs when the shear exceeds that resistance. The resistance to slip increases with the rate of deformation; further, the relative values of cohesive and shear resistance can be modified by heat treatment, and depend on the temperature of the test.

In a notched-bar test a small volume of highly stressed material near the notch has to absorb the energy. This volume is surrounded by less highly stressed material which prevents plastic flow, i.e. it prevents the lateral distortion which accompanies the longitudinal strain, and, in consequence, a state of three-dimensional stress is set up. In one-dimensional stress the maximum shear stress is one-half the direct stress, but in three-dimensional stress the maximum shear stress is one-half the difference between the greatest and least principal

stresses. These stresses may therefore have large values before the resistance to shear is reached, and ere that the cohesion may be overcome. Not only so, but since the highly stressed volume which absorbs the energy is small, the rate of deformation will be large, even at relatively low impact velocities; this will raise the resistance to shear, enhancing the tendency to cohesion failure. Apparently brittle fractures in ductile materials are thus explained.

The type of fracture depends therefore on (1) the amount of restriction to plastic flow, (2) the rate of deformation, and (3) the temperature of the test.¹¹

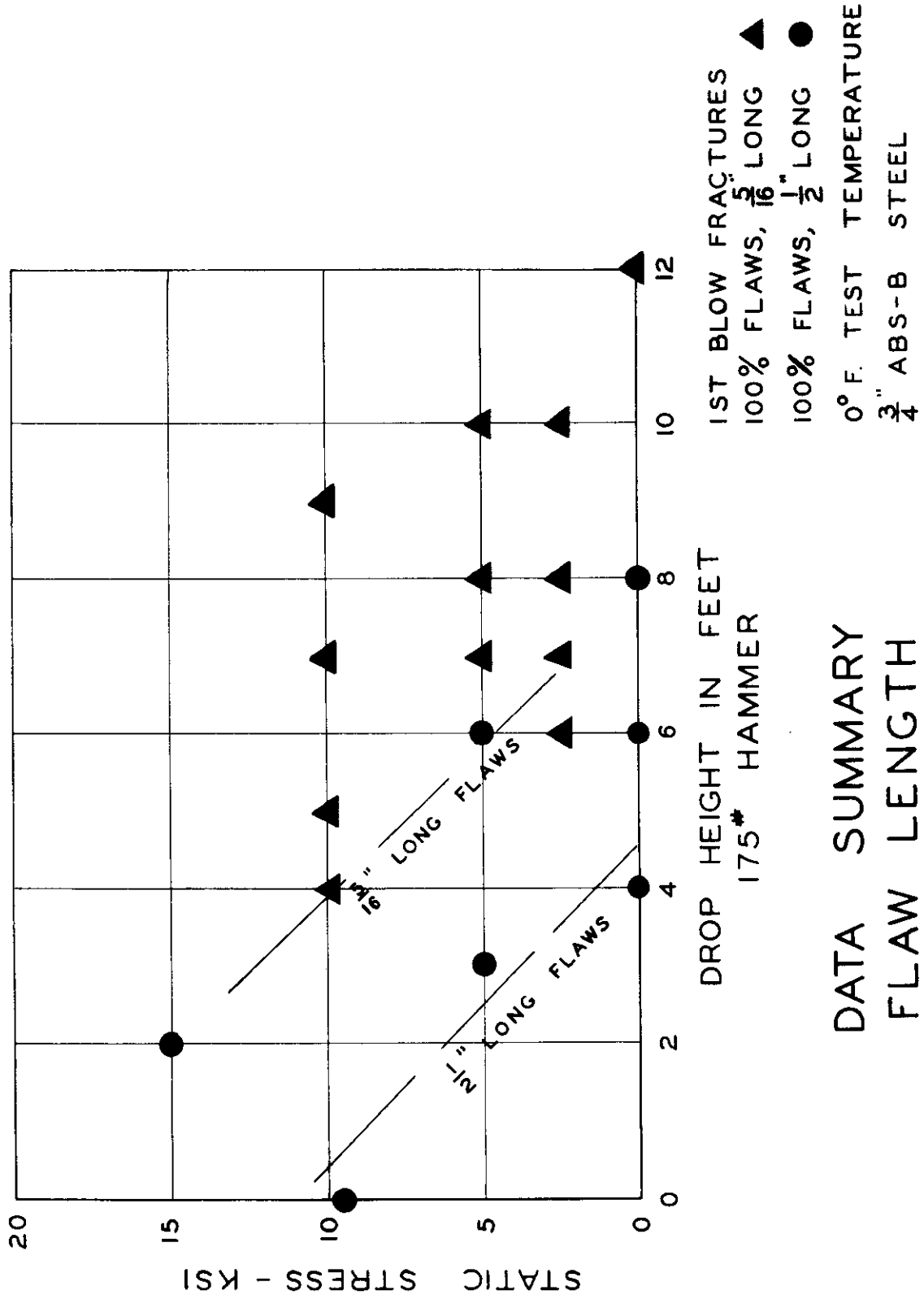
The fractures under impact loading, as well as the non-fractures under impact loading, can be explained on the basis of the foregoing reasoning.

Specimens that did not exhibit first-blow fractures can be placed in two groups: (1) those for which the impact loading was too moderate to provide a high enough rate of deformation, and (2) those specimens for which the combination of residual and static stresses had provided gross plasticity prior to the impact, so that the rate of deformation at the notch was insufficient at impact.

Specimens that did exhibit fracture were those in which residual, static, and dynamic stresses were present with a sufficiently high rate of deformation. The dynamic energy in these cases was absorbed in small, plastically strained regions at the ends of the notches, so that the strain rate was sufficient to allow the stress to increase to the level required for fracture. Specimens that fractured under a single blow of the drop hammer exhibited no general plastic deformation. The thickness reductions at the fractured surfaces were too small to be measured; this was often the case with welded ship fractures.

The length of the notch is a factor in the dynamic stress required for brittle fracture (see Fig. 3.19), as can be seen by an examination of the Inglis relationship for maximum stress at the apex of the major semi-axis of an elliptic hole:

$$\sigma_{\max} = \sigma \left(1 + \frac{2a}{b} \right)$$



DATA SUMMARY
FLAW LENGTH

FIG. 3.19

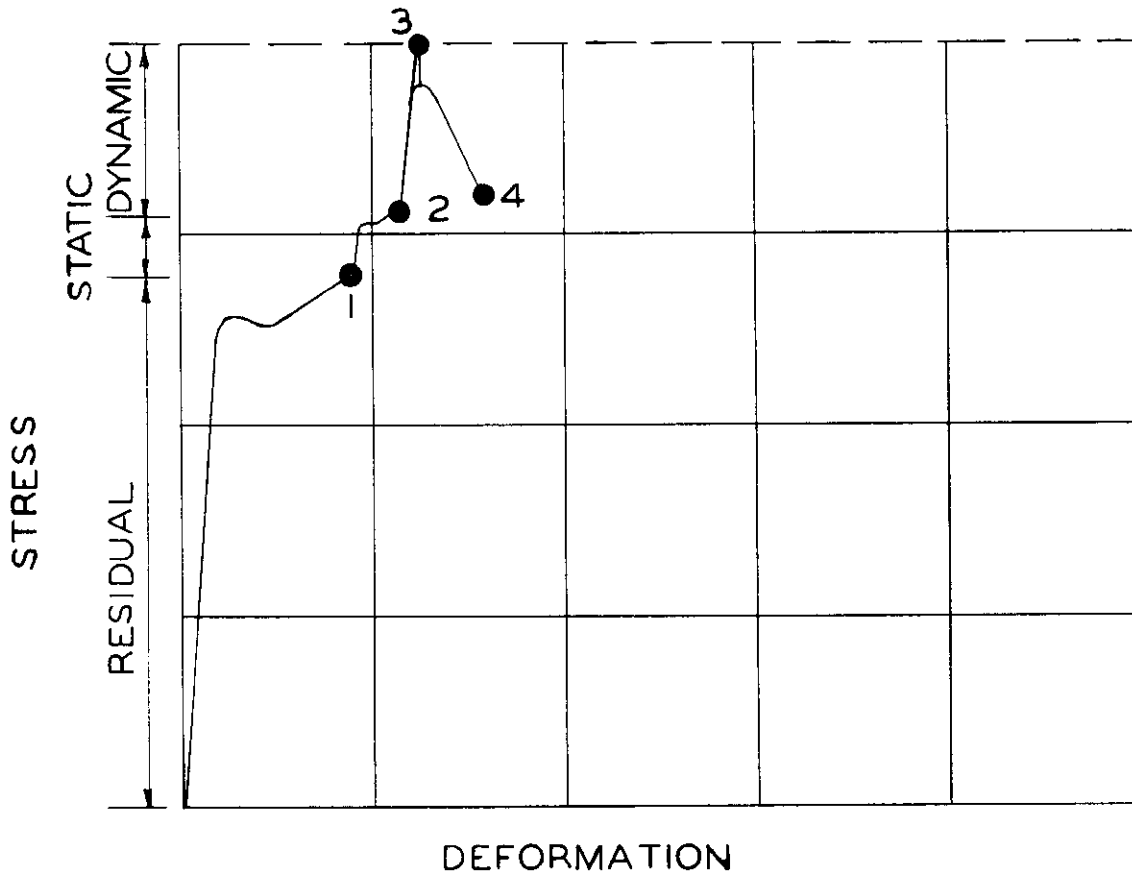
where a is the major semi-axis, perpendicular to the direction of tension σ , and b is the minor semi-axis. The radius of curvature at the apex of an ellipse is $\rho = \frac{b^2}{a}$. It follows that the maximum stress in a very flat ellipse or a crack having a length of $2c$ and radius ρ is approximately given by

$$\sigma_{\max} = 2\sigma \sqrt{\frac{c}{\rho}}$$

Thus it can be seen that the maximum stress (or plastic strain) at the apex of a crack would be a function of the length and sharpness of the crack. The Griffith theory for sharp cracks, as demonstrated in the summary of the Type-C specimens, also indicates that fracture stress decreases with an increase in crack length.

An indication of the amount of plastic straining at the apex of a notch has been shown by Wells' measurement of strain over a 0.038-in. gage length at the root of a saw-cut edge notch, which was 0.004-in. wide in 1/8-in. steel plate.¹² This measured strain was approximately 200 times greater than the average strain on the specimen cross section. The stress concentration factor, as calculated from the Inglis relationship, for a 1/2-in. long, 100% flaw in a Type-C specimen is 21.3; however, the plastic strain would be expected to be many times that value according to the measurements made by Dr. Wells.

As a part of the testing program on impact specimens, strain rates were estimated for various drop heights of the hammer. These strain rates, plotted against height of drop, are shown in Fig. 3.9. They were determined at the mid-section of un-notched specimens, and have a range of 0.154 in./in. sec. to 0.20 in./in. sec. It is not difficult to imagine that this strain rate at the apex of a sharp notch of molecular or even jeweler's saw-cut sharpness would be magnified to a critical value at the low temperature of the tests, 0°F. This effect, combined with the restriction to plastic flow at the root of the notch, probably results in cleavage failure before slip can take place.



1. STATE OF STRESS AND DEFORMATION AT APEX OF A NOTCH IN A FIELD OF RESIDUAL STRESS.
2. STRESS LEVEL AFTER THE ADDITION OF A SMALL EXTERNAL STATIC STRESS (STRAIN HARDENING HAS INCREASED THE YIELD POINT.)
3. FRACTURE STRESS RESULTING FROM DYNAMIC STRESS OF SUFFICIENTLY HIGH STRAIN RATE.
4. ADDITIONAL PLASTIC DEFORMATION IF THE STRAIN RATE WAS OF INSUFFICIENT MAGNITUDE TO REACH FRACTURE STRESS.

**SCHEMATIC REPRESENTATION
OF STRESS SUPERPOSITION
IN IMPACT TESTS**

FIG. 3.20

Another factor that could aid in the initiation of brittle fracture is the influence of a certain amount of strain hardening. When the patch welds were made in the specimens, or when the grooves were welded, high nominal residual stresses resulted. At the apex of the notches, plastic strains resulting from concentrations would occur to produce a significant amount of strain hardening. The yield-point stress at the notches would then be raised to the stress level required for brittle separation.

A graphical interpretation of these principles as applied to the specimens subjected to impact is shown in Fig. 3.20.

Part IV

WELD FLAWS IN RESIDUAL AND STATIC STRESS FIELDS

Introduction

This study of weld flaws has indicated the importance of residual stresses in the initiation and propagation of brittle fracture. Although it has been demonstrated that residual stress may not have an effect in a flawless system, this is not the case when weld cracks or submerged flaws exist. The energy reservoir created by the residual stress field has been shown to be sufficient to initiate spontaneous brittle fracture, without superimposed external load, if a flaw of critical size is present. Furthermore, if the fracture is not spontaneous, it has been found that an additional superimposed static tension as low as 4000 psi could initiate the fracture. Flaws similar to those that have been critical under residual stress conditions were stress relieved and found not to be critical.

The flaws used in this phase of the program were of both the buried and full-plate-thickness types simulating weld cracks. To provide laboratory control, the simulated cracks were all made with a jeweler's hack-saw cut 0.010-in. wide. A

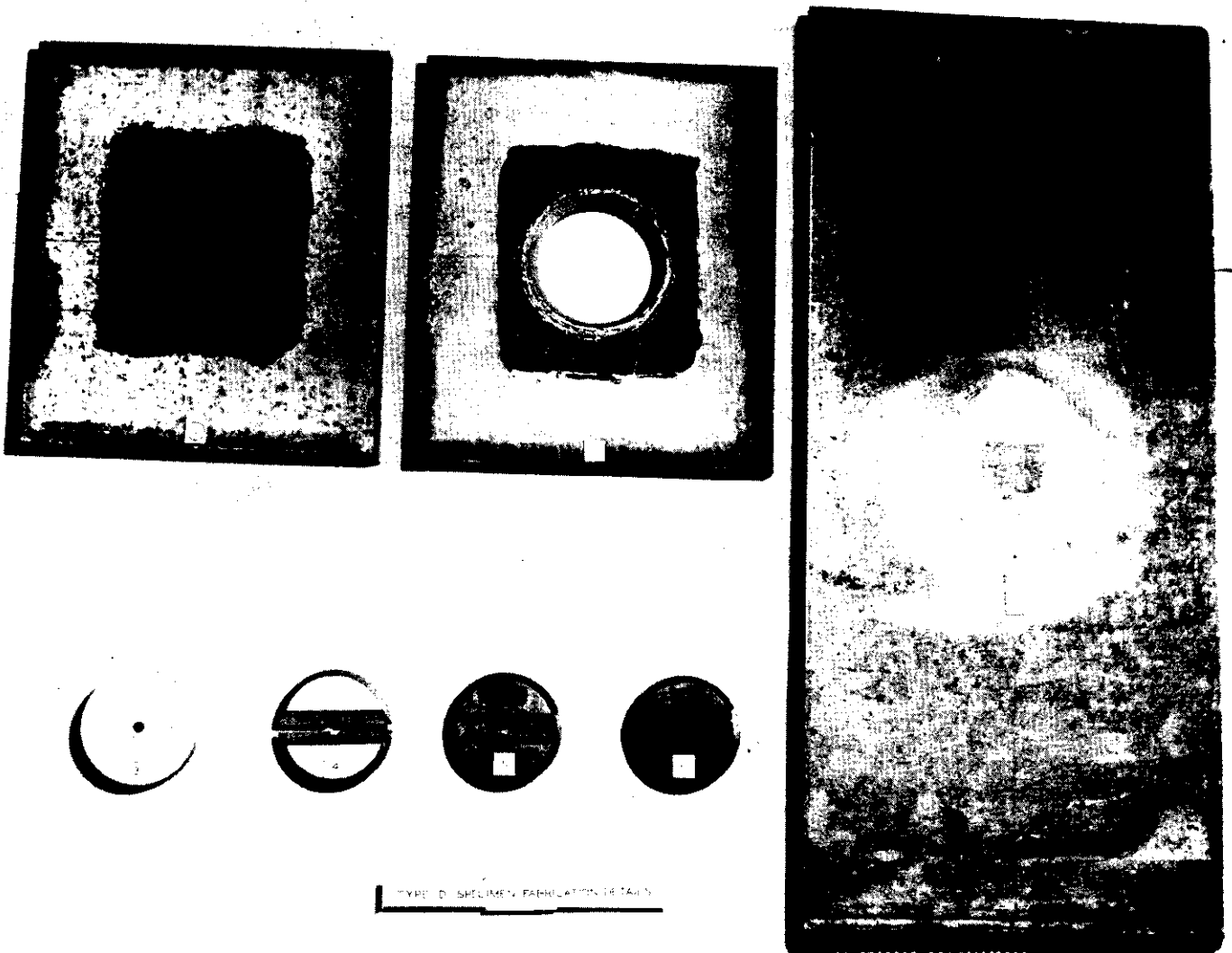


Fig. 4.1 - Fabrication of "D" specimen

1. Layout of circular patch
2. Circular patch cut out
3. Unprepared circular patch of plate material
4. Patch grooved for welding of test weld
5. Groove welded 50% and saw cut made to represent flaw
6. Test weld fully made
7. Final "D" Specimen with patch containing test weld welded into test plate.

flaw is classified by its length and its total depth in the plate-thickness direction. A 100% flaw indicates a flaw of full plate thickness, a 75% flaw is a buried flaw with the crack occupying the center 75% of the plate thickness, and a 50% flaw is a buried flaw occupying the mid-half of the plate thickness.

The weld flaws were always tested with the length of the flaw normal to the applied external static tension. A majority of weld flaws investigated were in weld metal placed in double-vee grooves; therefore initiation occurred in the weld metal of the butt weld and not in the plate. This examination of weld flaws was later extended to cover the case of weld flaws transverse to the butt weld, the flaw terminating in the heat-affected zone (HAZ) of the plate. Only limited data, however, are available at present for this type of flaw.

Type of Specimen: Fig. 4.1 is a photograph of a 3/4-in. thick ABS-Class B steel specimen, of the type used throughout Series D. The methods of fabrication can be noted in the photograph of Fig. 4.1. In the Type-D specimen, use was made of the shrinkage in the double-vee groove weld, which had been placed around the circular patch to induce a residual stress field. This use of the circular patch for the control of residual stress follows from the suggestions of Levy and Kennedy.¹⁰ The circular patch was generally sawed from the 3/4-in. thick plate to a given diameter, with a 3-in. diameter patch in a 10-1/2-in. wide plate most frequently used. The residual stress magnitude can be varied by varying the ratio of patch diameter to plate width. The periphery of the patch and the adjoining plate were then machined to form a 90° double-vee groove. Similarly, the patch was grooved across a diameter to prepare for the placing of the test weld that contained the flaw. The test weld with its flaw was made in the unrestrained patch and ground flush, after which the circular patch was replaced in the test plate and the circumferential welds made and ground flush.

The residual stress field was measured across a transverse section by means of SR-4 gages and a relaxation method, as shown in Fig. 4.2. Fig. 4.3 represents

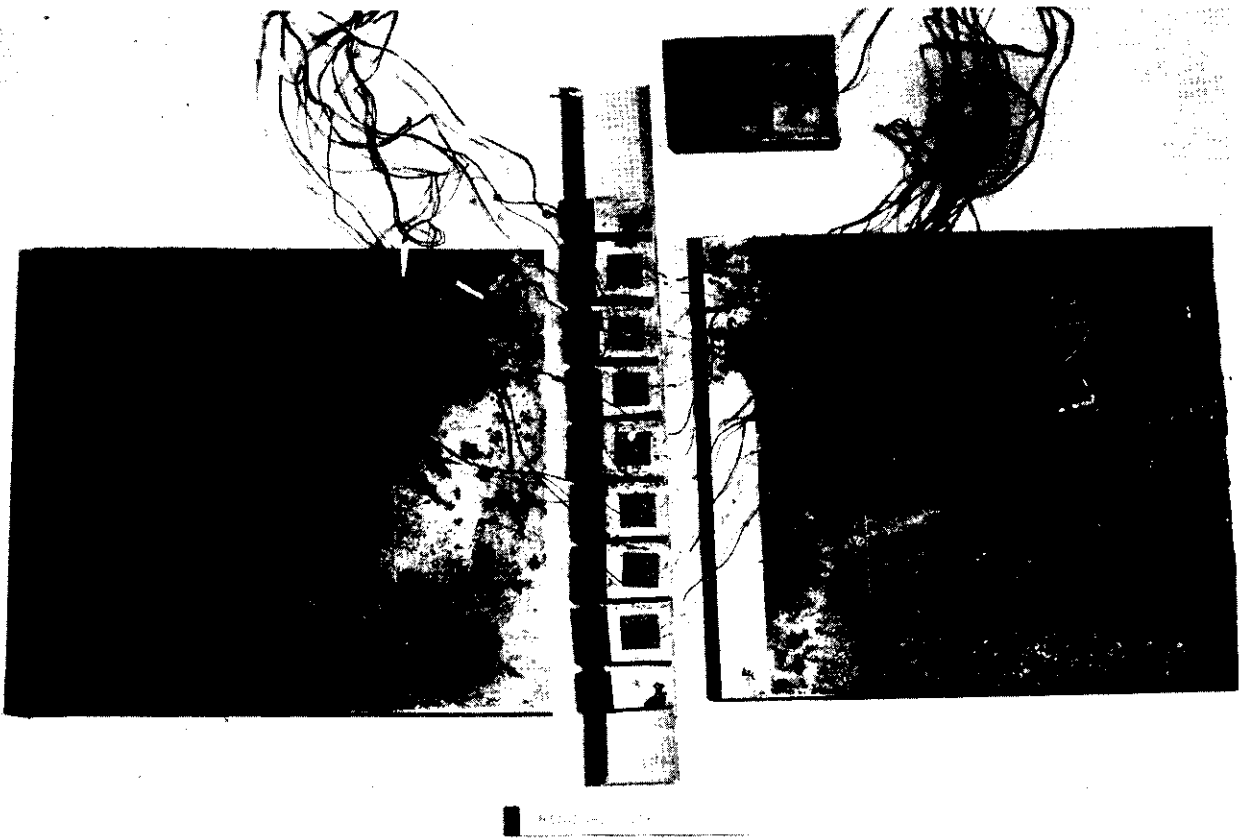


Fig. 4.2 - Residual stress measurements

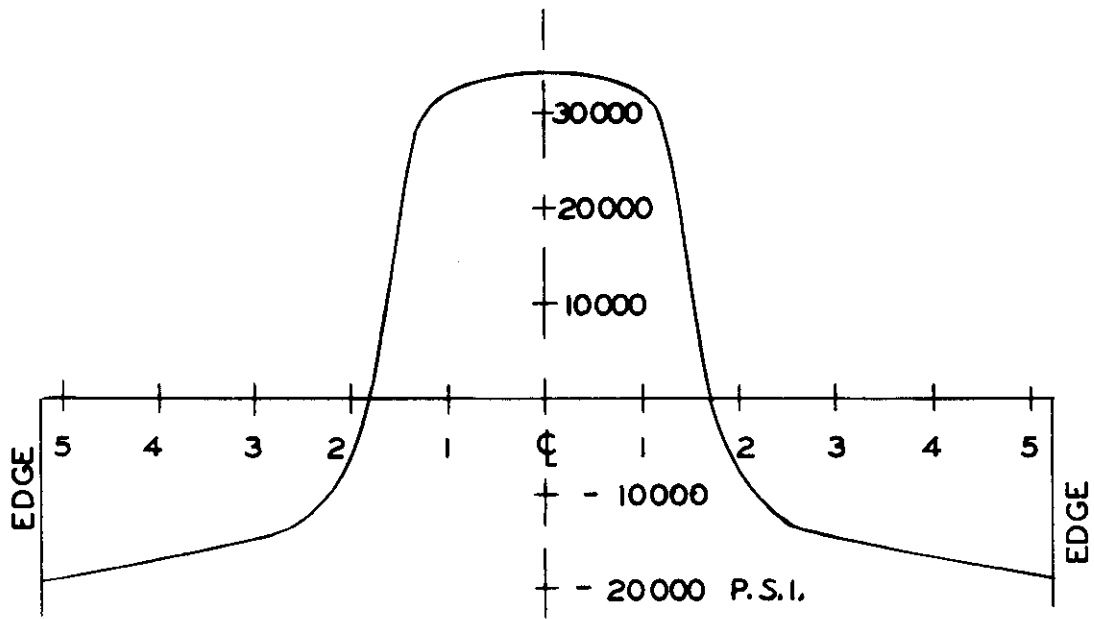


FIG. 4.3 RESIDUAL STRESSES FOR
 $10\frac{1}{2}$ " WIDE TYPE D
SPECIMEN - PATCH 3" DIA.

the residual stress distribution for a 10-1/2-in. wide specimen with a 3-in. diameter patch. When the patch was a solid disc, the residual stress field in the center was biaxial and 35,000 psi in intensity.

The authors are aware of the controversy that has existed in naming such internal stress patterns.¹³ They have been termed residual stresses here to avoid an unprofitable academic discussion of the various terms and distinctions that have arisen, such as "locked-in" or "reaction" stresses.

In general each flaw was made to simulate a sharp weld crack in E-6010 weld metal and is classified by the length of the crack and the per cent of the central thickness the crack occupies. For example, a crack entirely through the weld throat is termed a 100% flaw, whereas a 50% flaw occupies only the mid one-half of the weld throat and is spoken of as a buried flaw. These induced flaws were always tested so that length of flaw was transverse to the static tensile loading. A 50% buried flaw (see Fig. 4.1) was made by (1) making a weld in the mid 50% thickness of the plate, (2) drilling a pilot hole and (3), cutting the weld with a jeweler's hack saw to the required length of flaw. The pilot hole was then plugged with a split plug and the remaining 25% thickness on each side of the plate was welded. Accompanying photographs (Figs. 4.4--4.6) show these rectangular flawed areas in fractured specimens.

No difficulty was encountered in fabrication other than with the 75% flaws. Here the residual stresses were often large enough to cause premature full-depth cracking. In that event, the flaws became examples of the 100% flaw and were tested as such.

In one of the few specimens made to date to study the effect of weld crack extension into the heat-affected zone of the plate, a one-inch long, 100% crack extended spontaneously to a crack 10-1/2-in. long in a 14-in. wide plate while being cooled to -17 F. This is the most dramatic example experienced at this laboratory of the effect of residual stress, as the specimen was unloaded and entirely

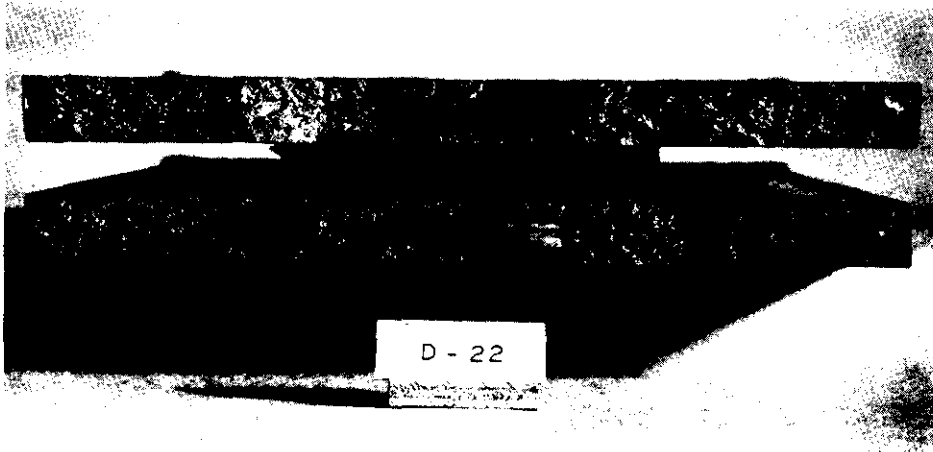


Fig. 4.4 - Specimen D-22 - 50% flaw - 2 1/4 in. long

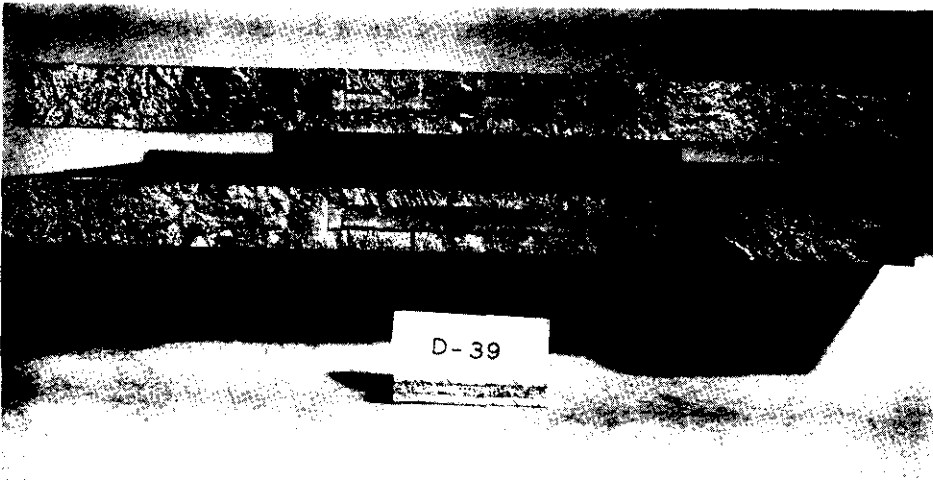


Fig. 4.5 - Specimen D-39 - 50% flaw - 3 in. long

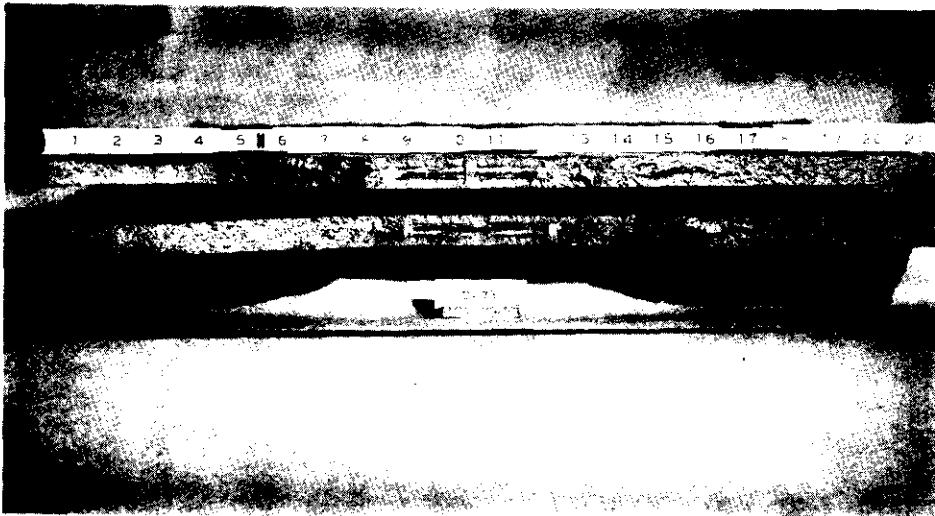


Fig. 4.6 - Specimen D-73 - 50% flaw - 3 1/2 in. long in 21 in. wide plate

unrestrained at the time. Other similar specimens had spontaneous cracks 4 in. in length produced at room temperature.

The flaws to be discussed are thus seen to be highly idealized sharp notches, selected because of their reproducibility for research purposes.

Test Results--50% Buried Flaw: The test results for the 50% buried flaw or crack are given in Table 4-I. The size of specimen, length of weld flaw, and the test temperatures are recorded. Essentially all fractures were of the brittle type without the thumb-nail (ductile) start so characteristic of many of the notched plate tests. Photographs of typical fractured specimens are shown in Figs. 4.4--4.6. The average unit stress reported is the average static tension stress computed over the gross sectional area of the plate, with no deduction for material removed by the flaw. This practice in reporting unit stresses was adhered to even in the event that a partial or arrested fracture occurred before final fracture. In this way, observed data could be compared with the brittle crack propagation theory of Griffith and the energy release rate concept of Irwin. It should be pointed out, however, that once an arrested fracture occurs, the unit stress (on the net remaining cross section) required to complete the fracture approaches or generally exceeds the yield stress of the material.

These major points of interest may be easily seen in Fig. 4.7 where the results of the 50% submerged flaw are plotted: first, flaws of less than 1 in. in length did not act as initiators of low-stress brittle fractures, for in these cases, unit stresses of from 45,000 to 62,000 psi were required for fracture; and second, flaws of 1 in. to 2-1/2 in. in length initiated fracture at both high and low levels of stress. Although initiation was obtained for static applied stresses ranging from 4500 psi to 20,000 psi, fracture at high stress levels also occurred. The 1-1/2 in. 50% buried flaw is thus capable of initiating fracture under low stress. High stress was always necessary to fracture stress-relieved specimens. It may be stated further that, for many specimens, flaws 1-1/2 in. in length or longer

NOTES:

ALL SPECIMENS OF D-SERIES
TEMPERATURES VARIABLE, SEE
TABULATED DATA.

ALL FRACTURES CLEAVAGE MODE

ALL FRACTURES SUDDEN AND OVER
COMPLETE PLATE WIDTH EXCEPT
FOR 5 TESTS SHOWN WITH
ARRESTED FRACTURE.

ALL TESTS WITH ORIGINAL FLAW
SUBJECT TO INITIAL RESIDUAL STRESS
OF 35,000 PSI, EXCEPT TWO
INDICATED S.R., (STRESS RELIEVED).

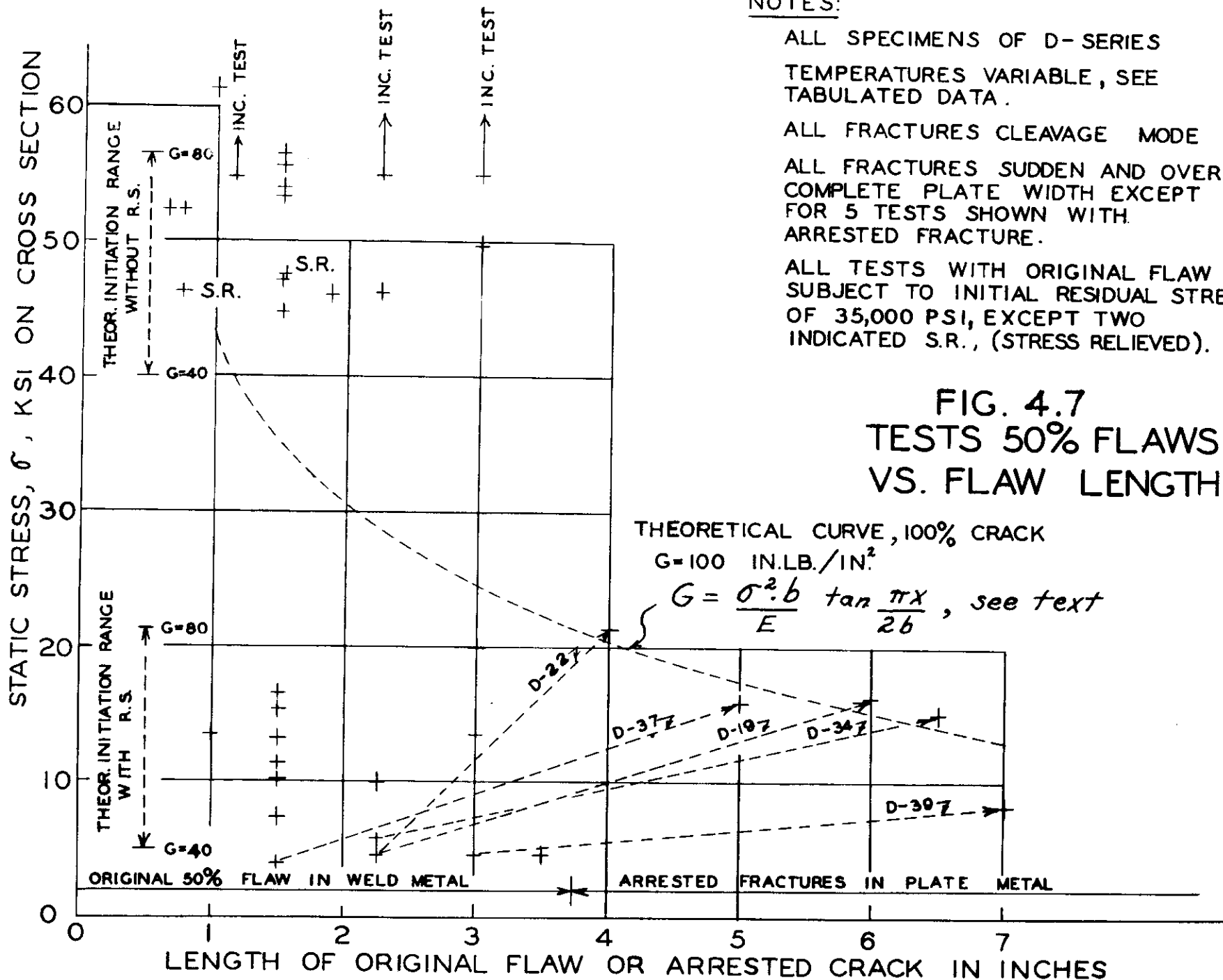


FIG. 4.7
TESTS 50% FLAWS
VS. FLAW LENGTH

TABLE 4-I
D-Series
50% Flaw

Internal flaw simulated by jeweler's hack saw

Specimen No.	Temp. F	<u>Description</u>			Fracture initiation stress on gross area, psi
		Width, in.	Dia. of welded patch in.	Original crack length, in.	
D-11	-60	7	2	5/8	52,600
D-32	-80	10-1/2	3	3/4	52,500
D-50	-80	10-1/2	3	3/4	46,600 (stress relieved)
D-14	-80	7	2-1/2	1-1/2	15,200
D-18	-40	7	2-1/2	1-1/2	Incomplete test - failed at headers
D-17	-30	7	2-1/2	1-1/2	" " " " "
D-27	-30	7	2-1/2	1-1/2	16,500
D-31	-80	10-1/2	3	1-1/2	7,300
D-33	-30	10-1/2	3	1-1/2	53,300
D-37	-85	10-1/2	3	1-1/2	{ 4,000 5 in. crack formed (bare rod) 15,900 5 in. crack - 100% (bare rod)
D-41	0	10-1/2	3	1-1/2	47,200 (bare rod)
D-51	-80	10-1/2	3	1-1/2	47,400 (stress relieved)
D-35	-70	10-1/2	3	1-1/8	Incomplete, failed at headers
D-36	-30	10-1/2	3	1-7/8	46,200
D-19	-100	10-1/2	3	2-1/4	{ 4,500 6 in. crack formed 16,200 6 in. crack - 100%
D-22	0	10-1/2	3	2-1/4	{ 4,300 4 in. crack formed 21,400 4 in. crack - 100%
D-34	-80	10-1/2	3	2-1/4	{ 5,800 6-1/2 in. crack formed 15,000 6-1/2 in. crack - 100%
D-21	-30	10-1/2	3	2-1/4	10,000
D-26	+30	10-1/2	3	2-1/4	Incomplete, failed at headers
D-20	-95	14	4	3	13,300
D-24	-40	14	4	3	20,000
D-29	-40	14	4	3	Incomplete, failed at headers
D-28	-30	14	4	3	49,800

TABLE 4-I D-Series, 50% Flaw (continued)

Specimen No.	Temp. F	Description			Fracture initiation stress on gross area, psi
		Width, in.	Dia. of welded patch in.	Original crack length, in.	
D-25	0	14	4	3	4,800 7 in. crack formed
D-39	-80	10-1/2	4	3	8,100 7 in. crack - 100%
D-93	+30	10-1/2	3	2-1/4	46,600
D-85	-30	10-1/2	3	1	61,500
D-83	-30	10-1/2	3	1	Fracture outside of flaw at 55,900
D-77	0	10-1/2	3	1-1/2	54,000
D-78	0	10-1/2	3	1-1/2	44,800
D-76	-80	10-1/2	3	1	13,700
D-79	-80	10-1/2	3	1-1/2	7,100
D-68	-90	21	6	4	21,800
D-73	-80	21	5	3-1/2	4,600
D-105	+50	10-1/2	3	1-1/2	56,000 (Note: Flaw opened, ductile through patch weld, then brittle)
D-104	-50	10-1/2	3	1-1/2	11,400
D-103	-15	10-1/2	3	1-1/2	56,400
D-102	-15	10-1/2	3	1-1/2	10,200
D-101	-50	10-1/2	3	1-1/2	13,300

initiated fracture in the weld at stresses of about 4000 psi, with the crack spontaneously extending upward to 6-1/2 in. in length before being arrested. After this primary initiation in weld metal, testing continued with the fracture progressing into the plate material. Figs. 4.4 and 4.5 are selected examples of arrested fracture.

The specimen behavior for the arrested brittle fractures noted above is one of the most interesting and valuable results of these tests. Because the initial fracture was arrested, an opportunity was provided for energy release studies (discussed below). For specimens completely severed without arrest, the opportunity to account for all strain energy is lost, since a surplus of energy (over that required for fracture) has been furnished.

The specimen with 50% flaw also provides an opportunity to speculate on the matter of the mechanics of initiation, particularly since it appears that length of the buried initial flaw beyond 1-1/2 in. may not be an important parameter. That is, 50% flaws shorter than 1-1/2 in. did not initiate low-stress fracture, but 50% flaws longer than 1-1/2 in. could initiate fracture at a low applied stress level. This suggests that initiation may be independent of flaw length greater than 1-1/2 in. This hypothesis appears to be further justified by the fact that a short buried flaw can expand in size only by fracturing all around its periphery, while a long buried flaw fractures along a preferential initial path to the faces of the plate. The exercise of this preference causes the submerged weld-flaw cavity to expand rapidly and extend to the surfaces of the plate, creating a complete 100% full-plate depth flaw. With the flaw expanding to a shape to fit this new, completely cracked-through situation, strain energy is further released with a total fracture or with fracture extending until arrested. This may be an oversimplified view of this mechanism, since it is also likely that the flaw in individual specimens may open up by progressive transverse fracture of the outer metal until the 100% crack exists. In any event, a rapid change in form exists. (This mechanism is more fully described in Part I of this report.)

It should be recognized that the rapid transformation from the buried flaw to an open crack is accompanied by a small but quick release of strain energy and a rapid increase in the stress at the tips of the crack. This creates a highly localized strain rate which results in a brittle separation. This mechanism may be likened to an internal self-induced impact and may be a feature distinguishing buried flaws from full-depth flaws. Calculations of this quick energy release for a 1-1/2 in. long buried flaw indicate that approximately 50 in.-lb of strain energy is released.

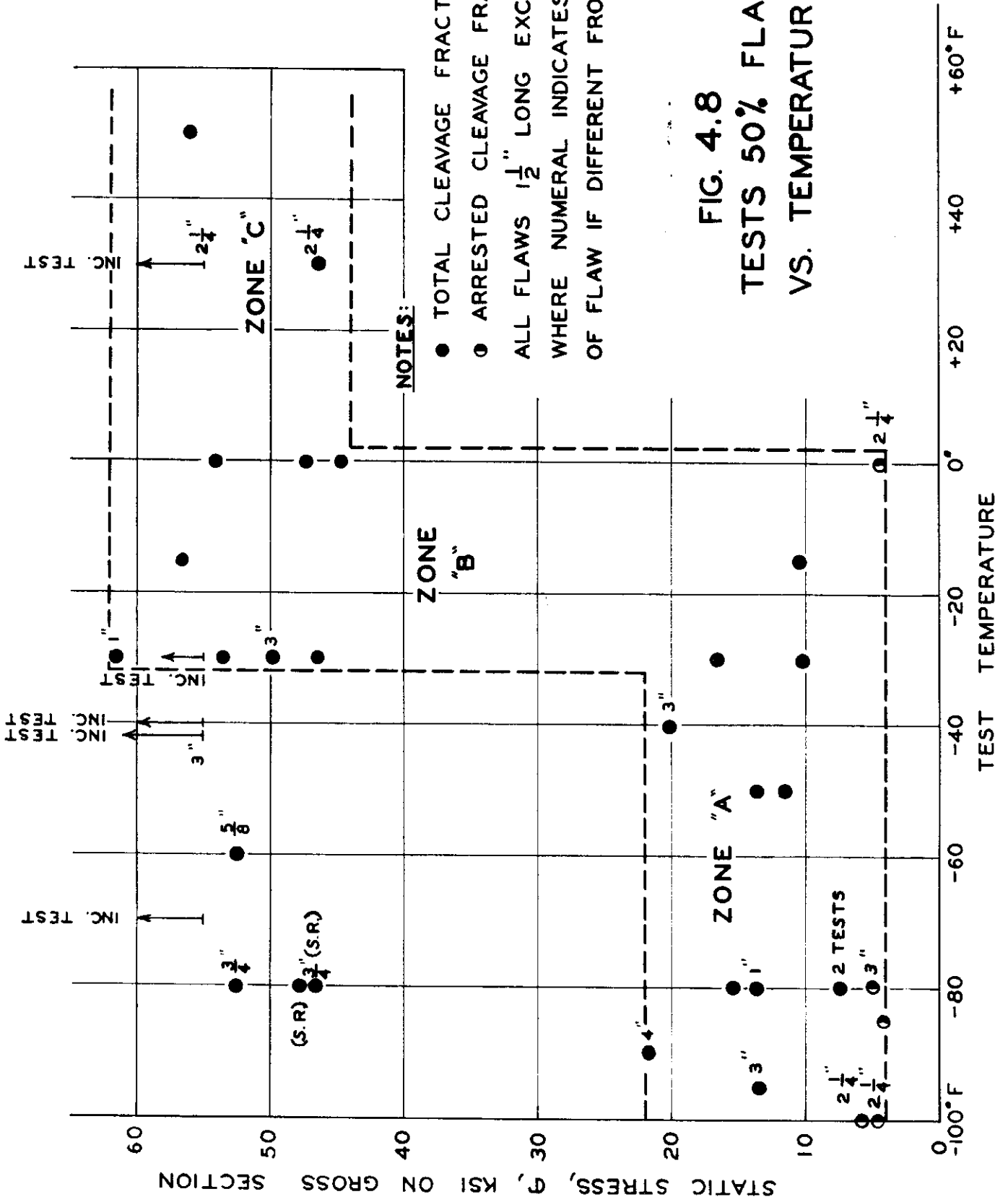
The one disappointing aspect of the tests, from the point of view of their bearing on structural failure, has been the fact that temperatures of about -30 F have been necessary for low-stress initiation from 50% buried flaws. To insure low-stress initiation with the critical flaw, temperatures as low as -80 F were required. In only one instance, specimen D-22, did the low-stress initiation occur at 0°F. Statistically speaking, fracture can occur at 0°F, but with less probability than at -30 F.

In the graphical representation of Fig. 4.7, the theoretical line for the 100% cracks formed by the arrested fractures is based on the energy-release concept as devised by Irwin. This theory relates the gross stress on cross-section and the crack length to an energy release rate. The data in this report are in close agreement with theory when the energy release rate is taken as 150 in.-lb per sq in.

Comparisons between theory and laboratory observations of the buried flaw may be made from the Irwin equation for force tendency (see Part I for definition of symbols):

$$G = \frac{\sigma^2 b}{E} \tan \frac{\pi x}{2 b}$$

Considering that the 50% flaw is represented by a 3/8-in. crack in the thickness direction, and letting $G = 40$ in.-lb per sq in., as determined from tests reported in Part I,



$$40 = \frac{\sigma^2 (3/4)}{30 \times 10^6} \tan \frac{(3/8) \pi}{2 (3/4)}$$

$$\sigma = 40,000 \text{ psi}$$

On Fig. 4.7, this value for σ is shown as the lower limit of the theoretical range of static stress for fracture initiation. Assuming superposition to apply, σ may also be accounted for by combining the residual stress with a static stress. If the residual stress is 35,000 psi, the static stress would be 5000 psi. Fig. 4.7 shows this as the lower limit of the theoretical range of static stress when residual stress is effective. The upper limits of these two theoretical ranges may be computed by assuming that "G" may approach a value of 80 in.-lb per sq in. Although "G" is certainly affected by material, notch, and size factors, substantial agreement of the "G" values with the observed data can be seen. It should be particularly noted that the observed data also group into a high and a low static stress range with no intervening observations. This agreement between theory and observed data indicates the probability that the mechanism of fracture from a buried flaw is subject to theoretical analysis

An examination of the results of static stress versus temperature for the 50% flaw can best be made by referring to Fig. 4.8, which plots all of the tests listed in Table 4-I. The ordinate is σ , the unit stress on the gross cross section. The numerals opposite a plotted point refer to the length of the flaw. The heavy dotted lines partition the data into three zones in accordance with the stress and temperature ranges required to initiate and propagate fracture.

Zone A, extending from -100 to -30 F, is a zone in which flaws 1 in., 1-1/2 in., or longer are conducive to the initiation and propagation of complete brittle fractures at average static stress levels ranging from 7000 to 22,000 psi. It is also the zone in which arrested fractures were initiated at stress levels of 4000 psi. Flaws shorter than 1 in. do not fall in Zone A. In this zone, the total environment of the flaw is favorable for low-stress fracture, as indicated by the temperature,

superposition of static and residual stress, stress concentration, and the mechanism of quick energy release from the expanding internal flaw. The crack retains its sharpness and its influence on stress concentration in this zone in spite of small deformations. At these lower temperatures, plastic constraint factors remain high, and brittle strength is reached.

Zone B, from -30 to 0°F , is a zone of uncertainty concerning total environment. It is to be noted that although low-stress fracture occurred, as well as one arrested fracture, over half of the specimens fractured at stress levels above the yield stress. It might be said, therefore, that it is an inherent property of a specimen that determines the stress level for fracture or arrest. The environment of Zone A must hold for the lower levels of stress, but is likely to be altered for the higher levels of stress because of the loss in the residual stress effects with increasing deformation. The stress concentrations are also limited by the changed acuity of the flaw produced by deformation. This is no doubt due to the higher temperature and the consequential lower yield-point stress which permit the specimen to yield.

Zone C, from 0° up in temperature, with stress ranging from 44,000 to 62,000 psi, is a zone of certainty in which none of the essential environment of Zone A is present. Fractures in this zone are still classified as fast and brittle, although evidence of local yielding is apparent through reduction in thickness and scaling. This action greatly modifies the stress concentrations at the flaw.

It can be stated, therefore, that the potential of a flaw to initiate a low-stress fracture is greatly influenced by temperature through its control of local deformation at the flaw tip and through the temperature-dependence of the "cohesive strength." In a sense, the range of temperature for Zone B may be likened to a transition-temperature range. While the term "transition temperature" has often been used to indicate a transition point between cleavage and ductile fracture appearance for a given type of specimen, no such interpretation is possible here since the fractures were essentially all brittle. It would be best to interpret

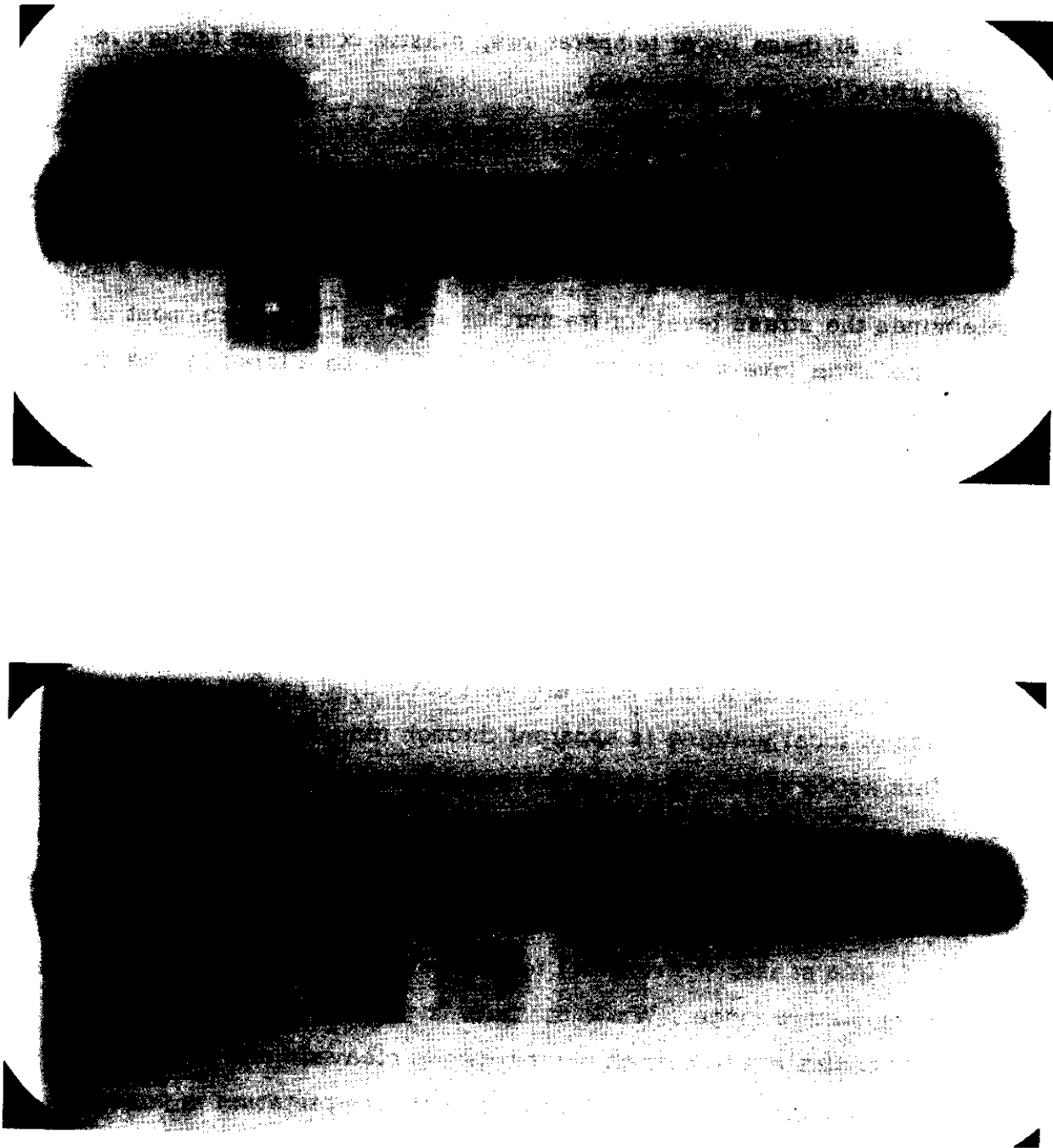


Fig. 4.9 - X-rays of Specimens D-62 and D-63

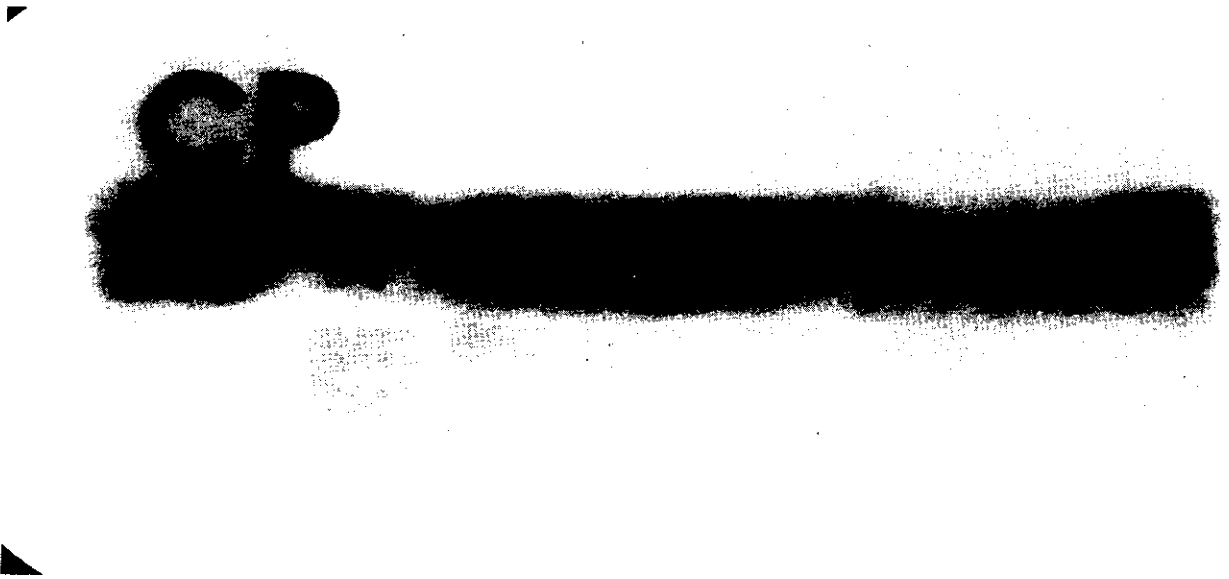


Fig. 4.10 - X-rays of Specimens D-64 and D-65

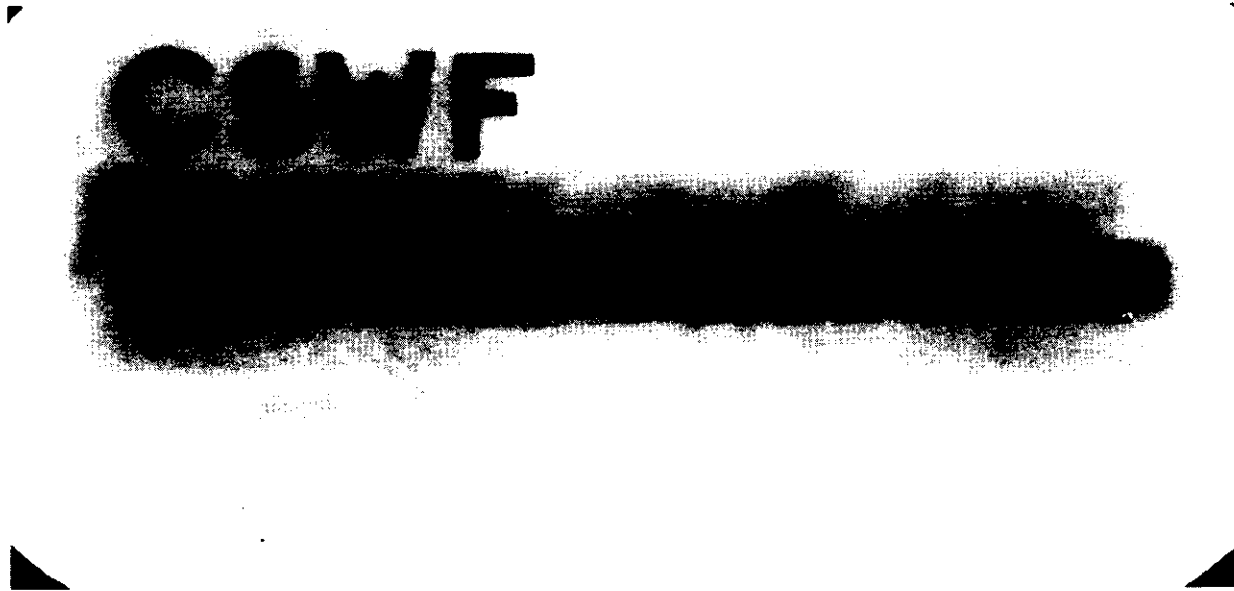


Fig. 4.11 - X-rays of Specimens D-66 and D-67

Zone B as a critical temperature zone in which the combined effects of notch and internally high strain rates are in a transient state.

T. S. Robertson has pointed out that a minimum critical stress level exists for brittle crack propagation.¹⁴ In the Robertson tests, the fracture was initiated by external static means alone. The range of average static stress in Zone A (low temperature and nil ductility) is apparently such that the higher values of stress produce continuous propagation and total fracture. The low-static-stress fractures (4000 psi) are generally arrested because the running crack encounters a low tension or compression stress field and the energy release rate decreases. The fact that the fractures are arrested in a low tension field agrees with the Robertson concept that critical stress maintains fracture propagation at a given temperature.

Additional tests and test results were obtained from six specimens containing weld flaws prepared at New York Naval Shipyard under the direction of Noah Kahn. This laboratory prepared a 3-in. diameter circular patch circumscribing these flaws. After the weld reinforcement was removed, the patch was welded into 10-1/2-in. wide by 3/4-in. thick plates to make the Type-D specimens. The prepared specimens were then tested under static tension at -80 F.

Figs. 4.9--4.11 are prints of the X-ray negatives furnished by the New York Naval Shipyard, which show the flaws with weld reinforcement. Figs. 4.12 and 4.13 are photographs of the brittle fracture surfaces of the four specimens that fractured through these flaws. Representative of the 1-1/2-in. long flaws of over 50% of the plate thickness, these flaws may be roughly classified as representing lack of root penetration in a double-vee butt weld. The two specimens that fractured through the test plate instead of the flaw were representative of lack of side-wall fusion in a single-vee butt weld over a length of about 1-1/2 in. These two specimens (D-66 and D-67) eventually broke through the flaw after they were edge-notched. The lack of side-wall fusion was barely detectable.

The test results are given in the following table. The specimen numbers are designated by this laboratory's code as well as by the code of the New York Naval Shipyard.

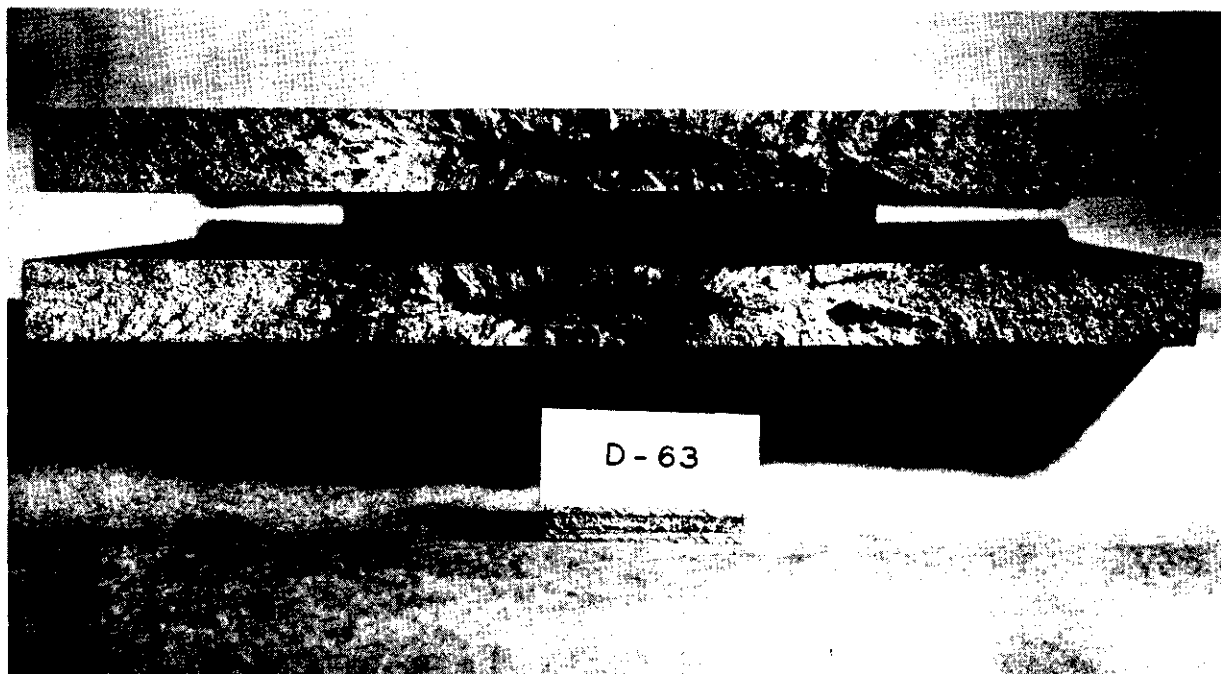
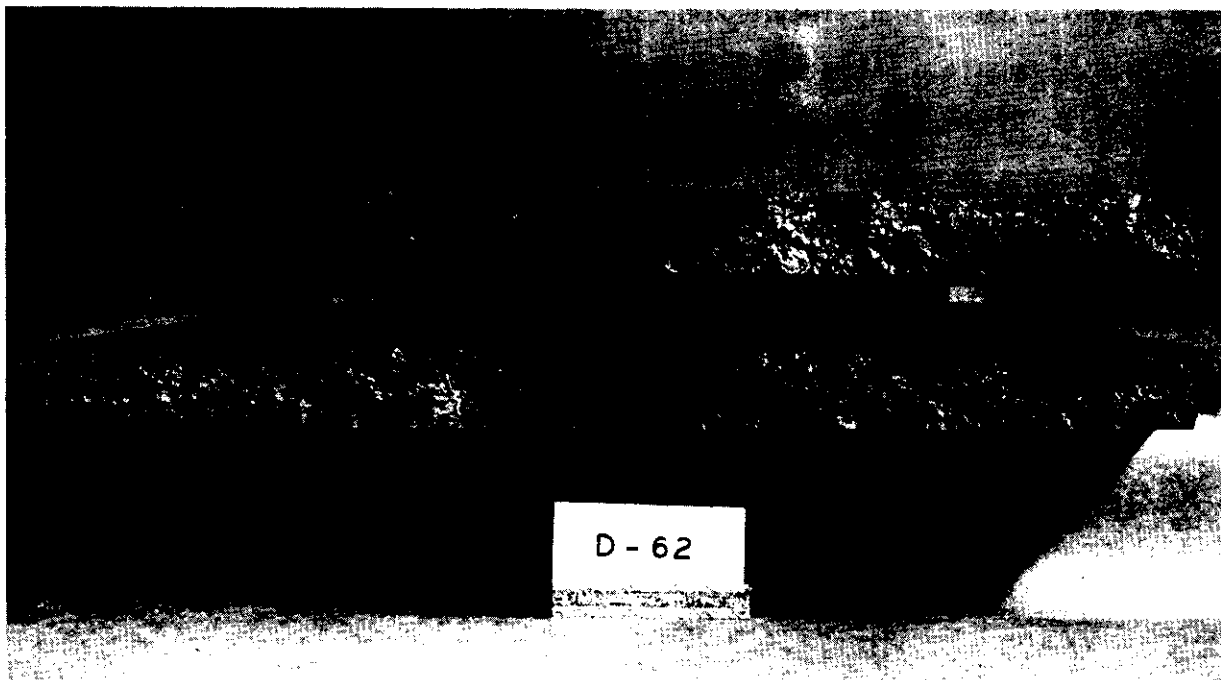


Fig. 4.12 - Fracture and flaw, Specimens D-62 and D-63

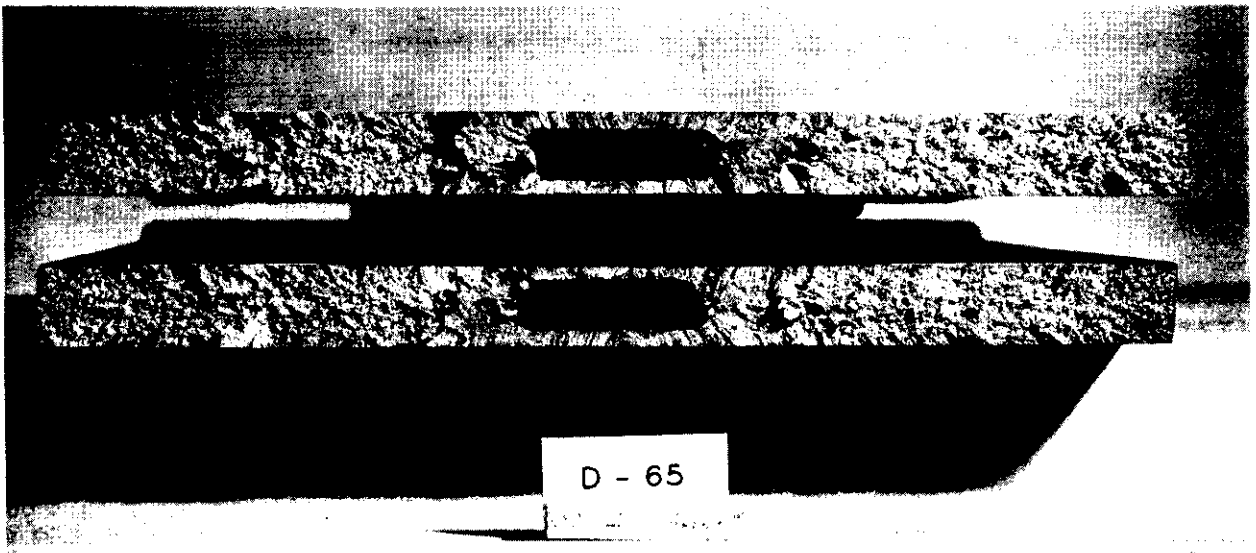
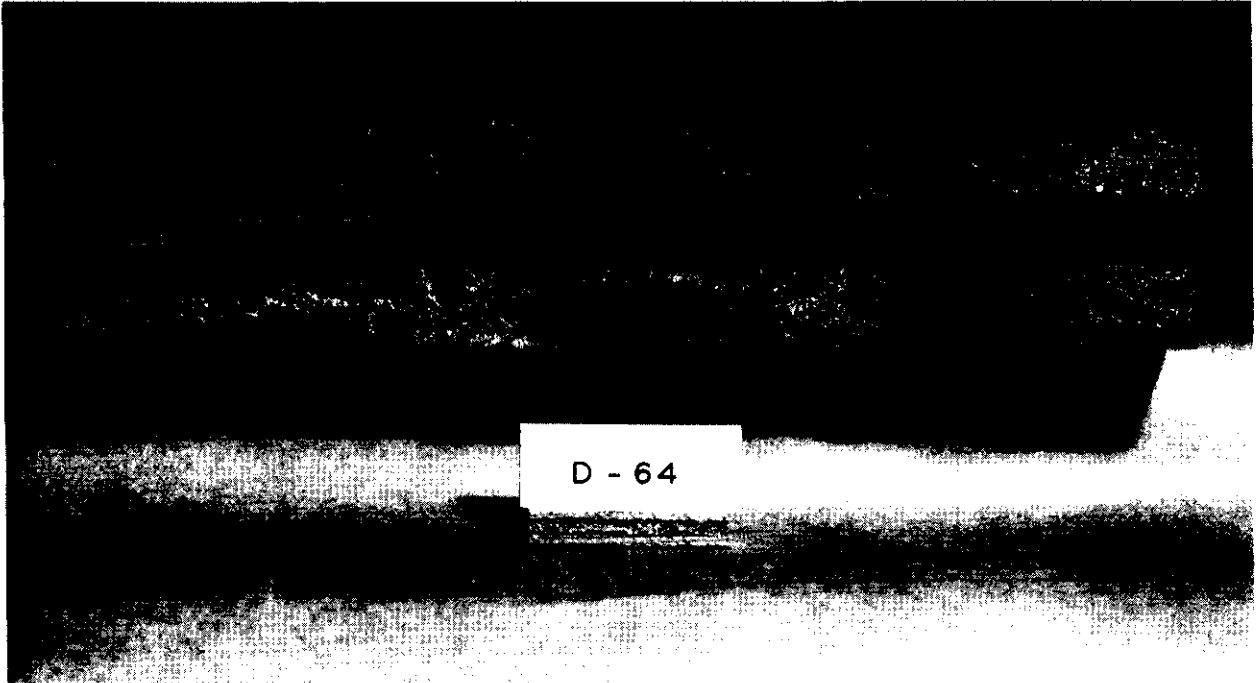


Fig. 4.13 - Fracture and flaw, Specimens D-64 and D-65

<u>Our Laboratory No.</u>	<u>Specimen No.</u> New York Naval Shipyard No.	<u>Static fracture stress on gross section, psi</u>
D-62	MF	51,400
D-63	CF	7,900
D-64	SWM	10,700
D-65	CP	48,600
D-66	MSWF	Fractured outside of flawed zone
D-67	CSWF	at 60,000 psi

The results from the most severe of these internal flaws are similar to the results obtained using flaws made by the jeweler's hack-saw cut, which indicates that this general laboratory flaw is about as severe as the internal flaw.

Test Results--75% Buried Flaw: The test results for the 75% buried flaw and a description of the test specimens are given in Table 4-II. Configuration of the specimen with its welded patch to create the residual stress field has been described previously. A 75% flaw occupies the middle three fourths of the plate thickness and is made with a jeweler's hack-saw cut. The photographs of Fig. 4.14 show typical fractures through flaw. Specimen D-61 had reinforcement left on; Specimen D-87 is an example of an arrested fracture.

The results of these tests are shown plotted in Fig. 4.15, with the stresses again representing the average static and externally applied stress on the gross-cross-section. With a flaw length of 3/4 in. and temperatures of -30 F and -80 F, total fracture occurred when the gross stress was 16,000 psi and 13,000 psi, respectively, at temperatures of 0°F, fracture occurred at approximately 52,000 psi.

A change in behavior was noted when the crack length was 1-1/2 in. and longer: the majority of the low-stress fractures created a 100% crack which was arrested after extending from 3-1/2 in. to 6 in. in length. It is also significant to note that this occurred at temperatures of +15 F and +30 F, instead of at the low

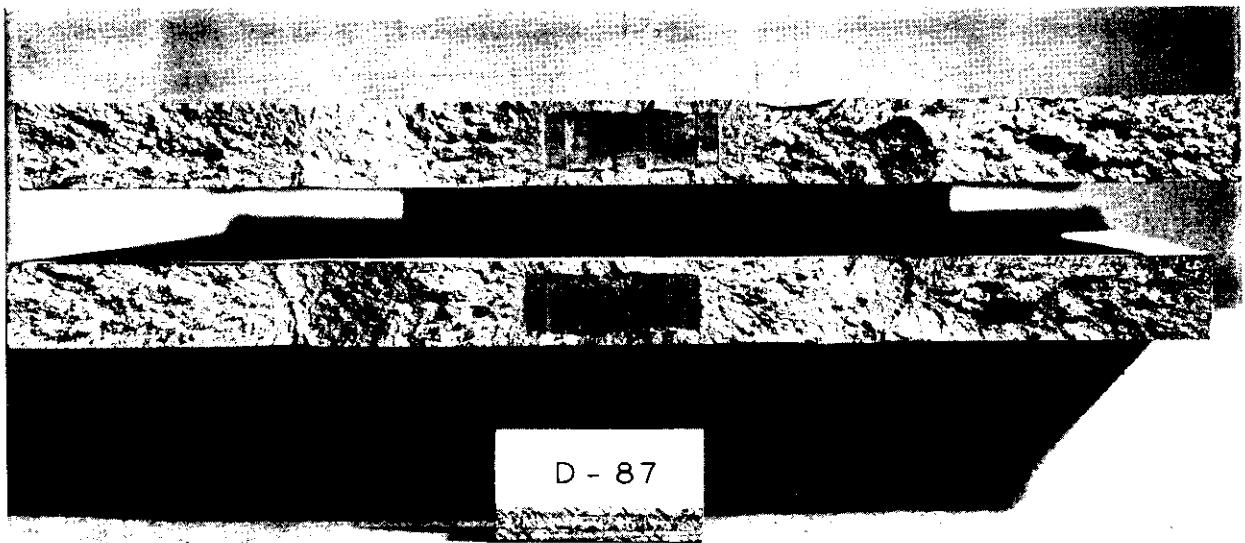
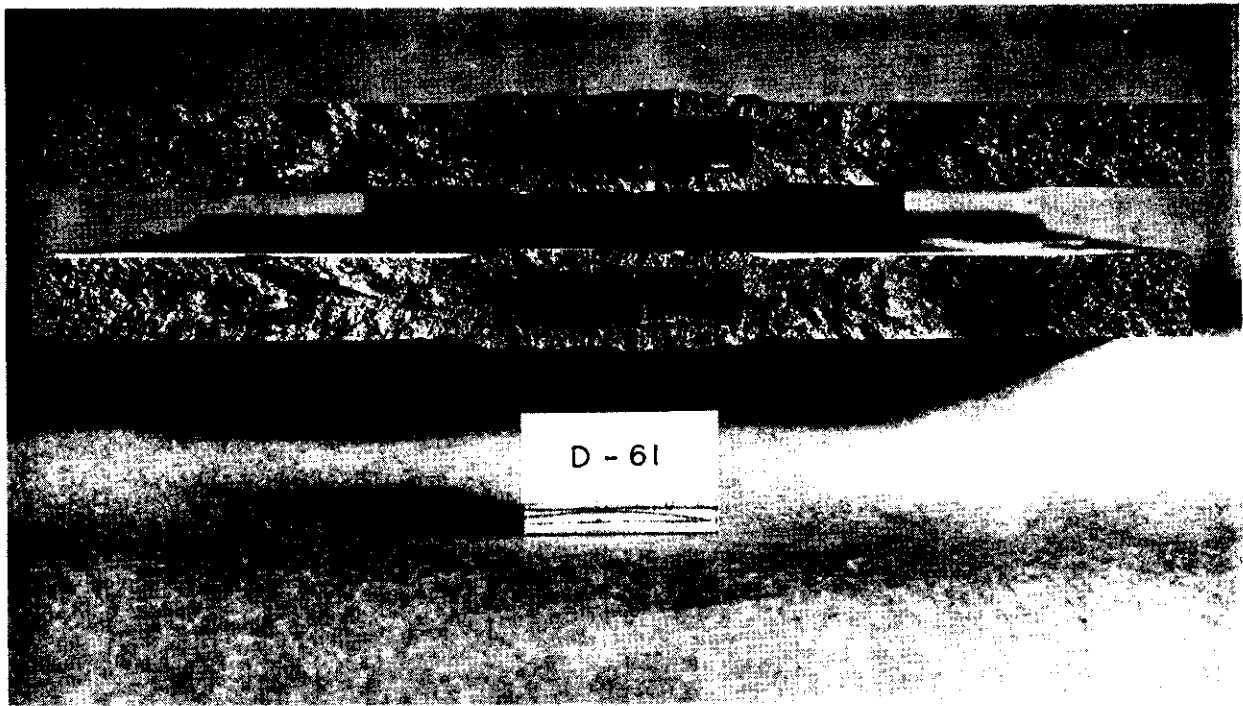


Fig. 4.14 - Fracture and flaw, Specimens D-61 and D-87

NOTES:

- ALL SPECIMENS OF D-SERIES
- TEMPERATURES VARIABLE SEE TABULATED DATA.
- ALL FRACTURES CLEAVAGE MODE.
- ALL FRACTURES SUDDEN AND OVER ENTIRE PLATE WIDTH EXCEPT FOR 6 TESTS SHOWN WITH ARRESTED FRACTURES.
- ALL TESTS WITH ORIGINAL FLAW SUBJECT TO INITIAL RESIDUAL STRESS OF 35000 PSI.
- R INDICATES REINFORCED WELD - ALL OTHER TESTS WELD IS FLUSH

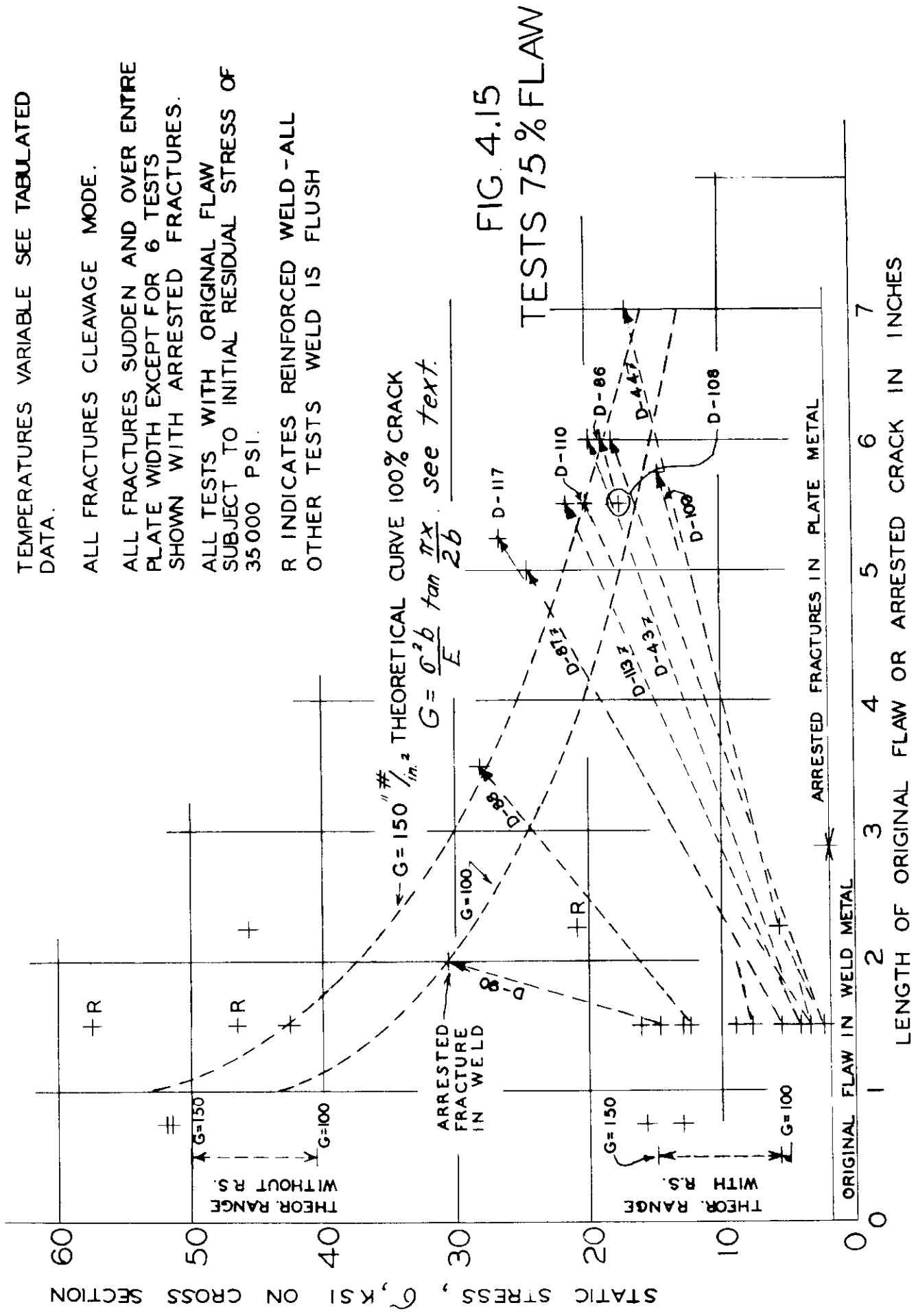


TABLE 4-II
D-Series
75% Flaw

Internal flaw simulated by jeweler's hack saw

Specimen No.	Temp. F	Description		Original crack length, in.	Fracture initiation stress on gross area, psi
		Width, in.	Dia. of welded patch in.		
D-81	-80	10-1/2	3	3/4	12,900
D-57	-80	10-1/2	3	1-1/2	8,900
D-91	-80	10-1/2	3	1-1/2	16,200 Representing incomplete fusion
D-108	-55	10-1/2	3	1-1/2	{ 3,200 5-1/2 in. crack formed
					{ 17,600 5-1/2 in. crack - 100% flaw
D-109	-55	10-1/2	3	1-1/2	{ 3,900 5-3/4 in. crack formed
					{ 14,300 5-3/4 in. crack - 100% flaw
D-42	-30	10-1/2	3	3/4	15,700
D-43	-30	10-1/2	3	1-1/2	{ 4,100 6 in. crack formed
					{ 19,700 6 in. crack - 100% flaw
D-58	-30	10-1/2	3	1-1/2	57,600 Reinforcement over flaw
D-44	-30	10-1/2	3	2-1/4	{ 5,600 7 in. crack formed
					{ 16,900 7 in. crack - 100% flaw
D-60	-30	10-1/2	3	2-1/4	21,000 Reinforcement over flaw
D-110	-15	10-1/2	3	1-1/2	{ 2,500 5-1/2 in. crack formed
					{ 20,000 5-1/2 in. crack - 100% flaw
D-111	-15	10-1/2	3	1-1/2	{ 2,900 6 in. crack formed
					{ 18,000 6 in. crack - 100% flaw
D-47	0	10-1/2	3	3/4	51,400
D-84	0	10-1/2	3	3/4	51,700
D-82	0	10-1/2	3	1-1/2	12,900
D-86	0	10-1/2	3	1-1/2	{ 7,800 6 in. crack formed
					{ 18,800 6 in. crack - 100% flaw
D-90	0	10-1/2	3	1-1/2	{ 14,800 2 in. crack formed
					{ 30,400 2 in. crack - 100% flaw
D-61	0	10-1/2	3	2-1/4	45,600 Reinforcement over flaw
D-87	+15	10-1/2	3	1-1/2	{ 5,500 5 in. crack formed
					{ 24,400 5 in. crack - 100% flaw

TABLE 4-II. D Series 75% Flaw (continued)

Specimen No.	Temp. F	Description			Fracture initiation stress on gross area, psi
		Width, in.	Dia. of welded patch in	Original crack length, in	
D-113	+15	10-1/2	3	1-1/2	{ 3,800 5-1/2 in. crack formed 21,400 5-1/2 in. crack = 100% flaw
D-117	+15	10-1/2	3	1-1/2	{ 3,400 5-1/4 in. crack formed 26,600 5-1/4 in. crack = 100% flaw
D-88	+30	10-1/2	3	1-1/2	{ 12,500 3-1/2 in. crack formed 28,200 3-1/2 in. crack = 100% flaw
D-116	+30	10-1/2	3	1-1/2	42,500
D-99	+50	10-1/2	3	1-1/2	46,400 Ductile

temperatures required for the 50% flaw. For complete and unarrested fracture, temperatures of -30 F and -80 F were required. However, in one test of a 1-1/2 in. flaw at 50 F, ductile shear fracture occurred at a high stress level. This is one of the few specimens to show fully ductile action. In a single test, a 2-1/4 in. long flaw initiated fracture at a low stress value of 5500 psi. It is not possible to state that this ductile action is entirely independent of flaw length, since sufficient test results were not available. It is apparent, however, that the same initiating mechanism that was discussed with reference to the 50% flaw applies here.

Fig 4. 15 also shows the theoretical curves for fracture initiation from 100% arrested cracks, based upon strain energy release rates of 100 and 150 in.-lb per sq in. It should be noted that the higher value furnishes the best agreement with observed data for these flaws, in contrast to the close approximation obtained by letting $G = 100$ for the 50% flaws. Applying the theory in a manner similar to that demonstrated in the discussion of fracture initiation from a 50% buried flaw, the two theoretical ranges shown in Fig. 4. 15 are determined. The values of "G" are 100 and 150 for the upper and lower bounds of these ranges, while for the 50% flaw the values of "G" are 40 and 80. Considering our present knowledge, these differences may be attributed to size effect.

An examination of the results of static stress versus temperature for the 75% flaw can be made by referring to Fig 4 16. The ordinate is the unit stress on the gross cross-section. The numerals opposite a plotted point refer to the length of flaw. The heavy dotted lines partition the data into three zones in accordance with the stress and temperature ranges required to initiate and propagate fracture.

Zone A, extending from -80 F to 0°F, is a zone in which flaws 3/4 in or longer are conducive to the initiation and propagation of complete brittle fractures, while flaws 1-1/2 in. or longer initiated and propagated arrested brittle fractures. The stress range of Zone A is from about 2000 psi to 21,000 psi. In Zone B, from 0°F to +30 F, the fractures were predominantly arrested fractures at low stress

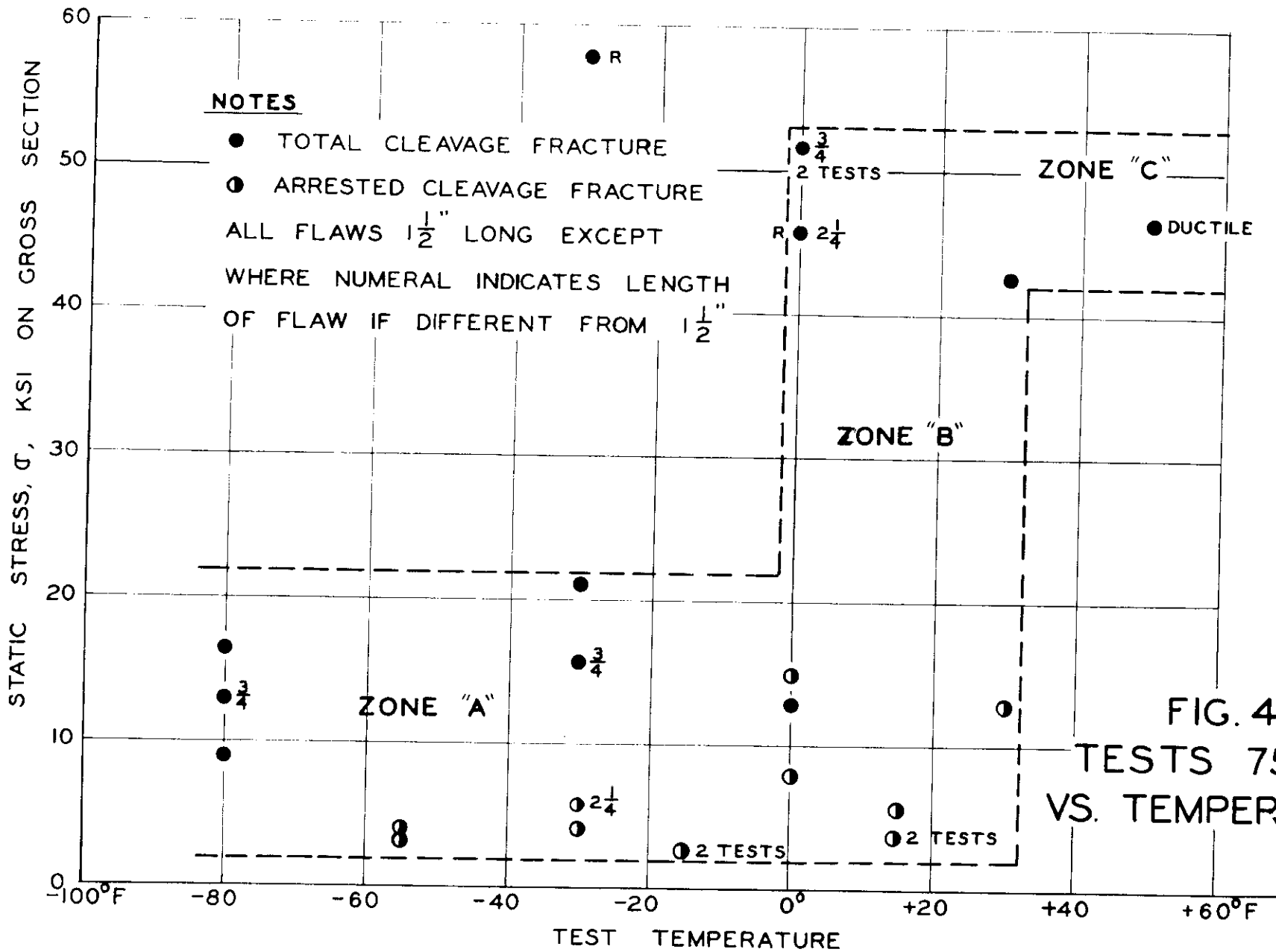


FIG. 4.16
TESTS 75% FLAW
VS. TEMPERATURE

levels but a few brittle fractures occurred at a high level of stress. This may be referred to as a transition range, since in Zone C, for temperatures +30 F and above, a high stress is required to fracture with probable shear or ductile action.

A comparison of the results of the 50% and 75% flaws indicates that low-stress fracture can be initiated from a 75% flaw that is shorter than the minimum required 50% flaw. It is also apparent that dangerous brittle fracture will occur with 75% flaws at a temperature +30 F higher than that necessary for the 50% flaw.

Test Results--100% (Full Thickness) Flaw: Test results for the 100% flaw (a full thickness crack made in a butt weld with a jeweler's hack saw) are given in Table 4-III and plotted in Fig. 4.17. These specimens were all of Type-D, incorporating a circular patch to induce residual stress; however, unless the flaw was short, a high level of residual stress could not be developed because of the opening of the crack. Hence, for flaws 1-1/2 in. or longer, negligible residual stress resulted.

Although the 100% flaw results are presented last in this section of the report, they were among the first flaws investigated in the Type-D specimen. The first few specimens listed in Table 4-III were of value in determining the degree of superposition of static and residual stress. It is to be noted that as the ratio of the diameter of the welded patch to the width of plate increases, the residual stress decreases. This provided a device for varying the residual stress. One specimen (D-6) was subjected to high-temperature stress relieving* to check the efficacy of this treatment. The following tabulation compares the results of superposition for four specimens tested at a temperature of -80 F and having a 1/2-in. long jeweler's hack saw notch. All fractures were of the fast brittle type.

Although certainly of limited nature, these tests do indicate that it is practicable at these low test temperatures to superimpose static and residual stress fields for short flaws in the absence of yielding influences.

*Specimen held at 1150 F for one hour and then furnace cooled.

TABLE 4-III

D-Series
100% Flaw

Original crack length induced by jeweler's hack saw.
Test crack length due to premature cracking from
cut of original per cent shown, becoming 100%.

E-6010 welding electrode
Cracks longer than 3 in. end
in ABS-Grade B base plate

Specimen No.	Temp. F	Description		Original crack %	Original crack length, in.	Test crack length, in.	Fracture initiation stress on gross area, psi
		Width, in	Dia. of welded patch, in.				
D-1	-80	7	2	100	1/2	1/2	11,600
D-3	-80	7	2	100	3/4	3/4	11,600
D-4	0	7	2	100	1/2	1/2	39,000
D-5	-80	7	4	100	1/2	1/2	45,600
D-6	-80	7	2	100	1/2	1/2	41,500 Stress relieved
D-10	-80	7	3	100	1/2	1/2	21,100
D-12	-60	7	2	100	1/2	1/2	42,600
D-13	-70	7	2	100	1-1/2	1-1/2	30,000
D-45	-30	10-1/2	3	100	1-1/2	1-1/2	10,100
D-46	-30	10-1/2	3	100	2-1/4	2-1/4	40,600
D-52	0	10-1/2	3	100	1-1/2	1-1/2	39,900
D-48	0	10-1/2	3	75	1-1/2	2-1/2	40,400
D-49	0	10-1/2	3	75	2-1/4	2-1/4	40,000
D-94	+50	10-1/2	3	75	1-1/2	2-1/2	42,800 Ductile
D-95	+30	10-1/2	3	75	1-1/2	2-1/2	44,000 Ductile in patch welds
D-89	-30	10-1/2	3	75	1-1/2	2-1/4	43,700

The following are specimens of 50% or 75% type flaws that had an arrested fracture in plate.

Arrested fracture length shown as test crack length.

Stress recorded as gross stress on total cross-section

D-19	-100	10-1/2	3	50	2-1/4	6	16,200
D-22	0	10-1/2	3	50	2-1/4	4	21,400
D-34	-80	10-1/2	3	50	2-1/4	6-1/2	15,000
D-37	-85	10-1/2	3	50	1-1/2	5	15,900
D-39	-80	10-1/2	4	50	3	6	8,100

TABLE 4-III D-Series 100% Flaw (continued)

Specimen No.	Temp. F	Description		Original crack %	Original crack length, in.	Test crack length, in.	Fracture initiation stress on gross area, psi
		Width, in.	Dia. of welded patch, in.				
D-108	-55	10-1/2	3	75	1-1/2	5-1/2	17,600
D-109	-55	10-1/2	3	75	1-1/2	5-3/4	14,300
D-43	-30	10-1/2	3	75	1-1/2	6	19,700
D-44	-30	10-1/2	3	75	2-1/4	7	16,900
D-110	-15	10-1/2	3	75	1-1/2	5-1/2	20,000
D-111	-15	10-1/2	3	75	1-1/2	6	18,000
D-86	0	10-1/2	3	75	1-1/2	6	18,800
D-87	+15	10-1/2	3	75	1-1/2	5	24,400
D-113	+15	10-1/2	3	75	1-1/2	5-1/2	21,400
D-117	+15	10-1/2	3	75	1-1/2	5-1/4	26,600
D-88	+30	10-1/2	3	75	1-1/2	3-1/2	28,200

	Specimen			
	<u>D-1</u>	<u>D-10</u>	<u>D-5</u>	<u>D-6</u>
Residual stress, psi	35,000	22,000	negligible	stress relieved
Static stress, psi, gross section	<u>11,600</u>	<u>21,100</u>	<u>45,700</u>	<u>41,500</u>
Sum by direct super- position, psi	46,600	43,100	45,700	41,500

Because of the importance of residual stress to the evaluation of flaws and the difficulty of developing it in longer flaws, only a few of the 100% 1-1/2 in. long cracks were specially fabricated. Additional 100% flaw specimens were obtained from two different sources:

- 1) Cooling a specimen containing a 75% flaw would often cause a premature cracking through to the surfaces of the plate and often extend the crack length.
- 2) Testing a specimen that originally represented a 50% or 75% flaw would sometimes produce an arrested full-thickness fracture.

Therefore, the series of tests used random crack lengths ending in the plate material and the results are plotted in Fig. 4.17 with an identifying symbol.

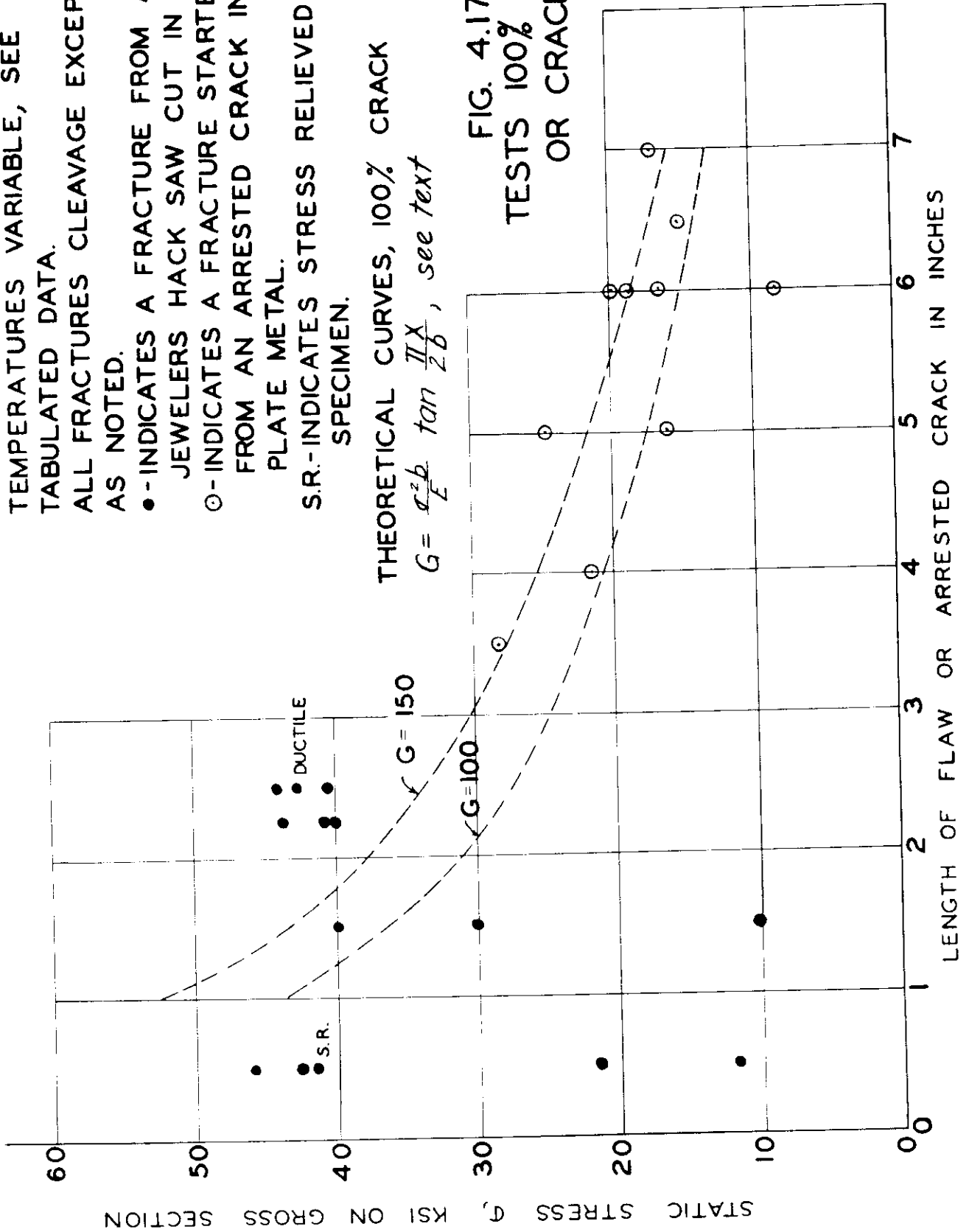
As shown previously, the 1/2-in. long flaws under high residual stress initiated brittle fracture at a static stress of about 12,000 psi at -80 F. A test on the same flaw at 0°F initiated brittle fracture at a static stress of 39,000 psi. Although not conclusive, this is an indication of the effect of temperature, which was also noticed with other flaws. With a 1-1/2-in. long flaw three specimens tested at -70 F, -30 F, and 0°F fractured at static stress levels

NOTES:

- ALL SPECIMENS OF D-SERIES
- TEMPERATURES VARIABLE, SEE
- TABULATED DATA.
- ALL FRACTURES CLEAVAGE EXCEPT
- AS NOTED.
- - INDICATES A FRACTURE FROM A
- JEWELERS HACK SAW CUT IN WELD.
- - INDICATES A FRACTURE STARTED
- FROM AN ARRESTED CRACK IN
- PLATE METAL.
- S.R. - INDICATES STRESS RELIEVED
- SPECIMEN.

THEORETICAL CURVES, 100% CRACK

$$G = \frac{\sigma^2 b}{E} \tan \frac{\pi X}{2b}, \text{ see text}$$



of 30,000, 10,100, and 39,900 psi, respectively. Thus it would appear that a large scatter of test results can be expected, as has been the case in other tests on notched specimens. Enough tests were not performed to permit a statistical study of the temperature effects.

Tests with the flaw length at 2-1/4 in. or 2-1/2 in. all indicated that yield-point stresses or higher were necessary for brittle fracture, while one specimen failed in shear mode at +50 F.

In Fig. 4 17, two theoretical curves are drawn with "G" values of 100 and 150 in.-lb per sq in. These curves encompass the general trend of the plotted data, except that for the extremely short cracks, a "G" value equal to either 50 or 200 in.-lb per sq in. would provide better agreement. The important point is, however, that the strength impairment and potential for initiating brittle fracture caused by full-thickness sharp cracks in plates of the widths tested appears to be subject to theoretical prediction.

Determination of Force Tendency--Slotted Plate: A Type-D specimen 3/4 in. thick, 10-1/2 in. wide, with a 3 in. diameter welded patch was used to determine experimentally the force tendency ("G") discussed in Part I. The plate was successively slotted with full-thickness central slots of 1 in., 1-1/2 in., 2 in., 2-1/2 in., 3 in., 4 in., 5 in., 6 in., and 7 in. After each slot length was sawed by a jeweler's hack saw, its opening was determined by using a series of 1-in. strain-gage readings over the slot. The total slot openings represented the elastic opening for different lengths, owing to relaxation of residual stress. This specimen is shown in Fig. 4 18.

Following the basic Griffith development outlined in Part I, the rate of strain-energy release, "G", was determined. This was accomplished by first finding the area of the elastic opening of the slot and the volume of this opening. These data were then incorporated with the residual stress data of Fig. 4.3, assuming that these stresses would, if applied to the open slot, close it. The volume of the opening times the average values of such stress was taken to represent the total strain energy

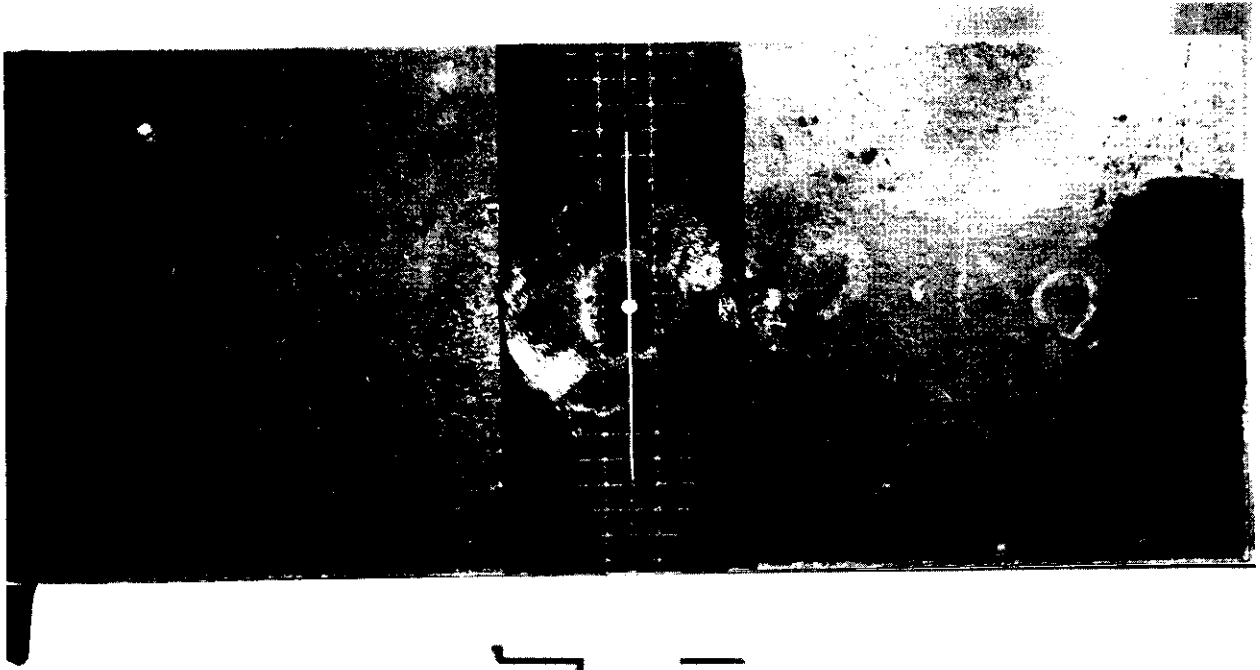


Fig. 4.18 - Slot opening study

released in the slotting operation. Each individual slot length was treated as a separate calculation, and proper finite summations of partial volumes times appropriate average unit stresses were used. The difference in computed strain energy released for any two successive crack or slot lengths was conceived to be the energy required to extend the slot over the incremental cross-sectional area. For example, for slot lengths of 1 in. and 1-1/2 in., the incremental area was $(1-1/2 - 1) \cdot 3/4 = 3/8$ sq in. The difference in energy released divided by this area was then taken to equal the strain-energy release rate for crack or flaw extension. This is "G," and its value was considered to hold for the average slot length of 1-1/4 in.

A repetition of the above methods enables the lower curve of Fig. 4.19 to be plotted. It is to be noted that "G" rises to a maximum of 210 in.-lb per sq in., and then it falls to a low of 20 in.-lb per sq in. at a crack length of 7 in. This fact will be useful in interpreting arrested fractures.

To complete Fig. 4.19, the "G" values were also determined for external static tensions representing 5000 and 10,000 psi over the gross section and superimposed upon the residual stresses. This necessitated the adjustment of the stress pattern of Fig. 4.3 to agree with static equilibrium and the assumption that the yield point stress was 40,000 psi. A calculation was also made for the additional opening of the slot under the influence of the static load. Following previous methods, the strain energy released was computed and "G" calculated. The results given by the two upper curves of Fig. 4.19 disclose that, while only small changes in "G" take place for the short slot lengths, the differences become greater as the crack progressively extends. If the static stresses had been increased beyond 10,000 psi, there would be only small increases in the value of "G" for crack lengths up to 3 in., but beyond this length, the increases would be larger. Successively increasing the external load would force the high point on the "G" curve to rise and move to the right.

G - ENERGY RELEASE RATE - IN. LBS / SQ. IN.

ARRESTED FRACTURES
 ● FROM 50% FLAW
 ✱ FROM 75% FLAW

RANGE OF G FOR PLATE

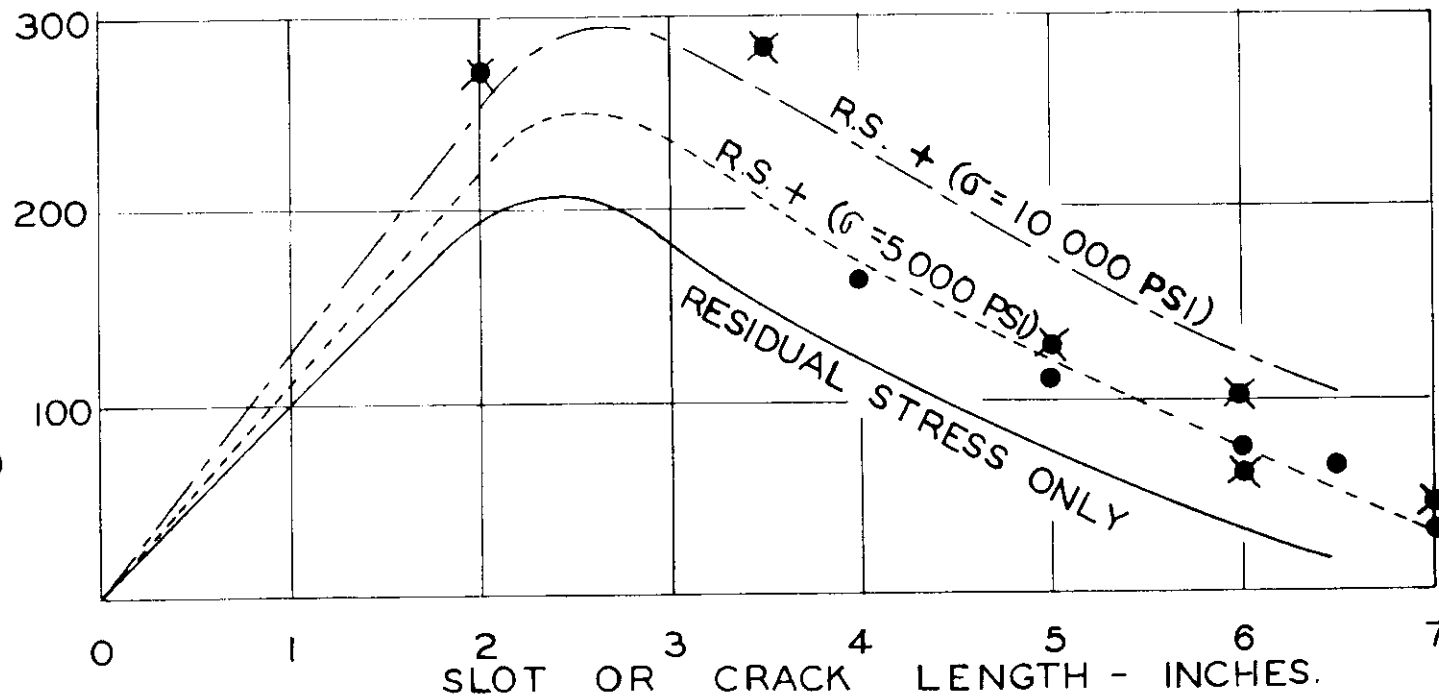


FIG. 4.19 ENERGY RELEASE RATES - 10 1/2" WIDE D-SPECIMEN

The curves of Fig. 4.19 permit an examination of the arrested fractures noted for the 50% and 75% flaws. The arrested length of the crack is taken as the abscissa and is plotted by interpolation to agree with the static stress level that initiated the original fracture. It may be noted that except for two cases, the fractures were arrested in zones where the fracturing work rate ("G") varied from 40 to 120 in.-lb per sq in. The two excepted fractures were arrested in the weld zone around the patch with fracture terminating in a shear zone. On this basis, these values may be excluded from theoretical comparison, because the criterion that a sharp crack be accompanied by brittle action is violated. These values provide some degree of check on the values of "G" previously determined and reported in Part I for weld metal and plate ranging from 40 to 100 in.-lb per sq in. It is also to be recalled that such arrested fractures were again tested to complete fracture as 100% cracks, and the theoretical comparison indicated a "G" value of about 100 to 150 in.-lb per sq in. for plate material. It would thus appear that the energy release rate theory holds on a broad basis.

OVERALL SUMMARY STATEMENTS

The following statements summarize the findings from this investigation on simulated butt weld flaws, in which the welding was done with the E-6010 electrode in double-vee grooves in 3/4-in. thick ABS-Class B plate.

(1) Butt welds with less than a full-plate-thickness throat, made with an intentional lack of penetration by welding in specially prepared machined grooves, have a tensile load resistance at 0°F nearly proportional to the actual area of weld metal in the throat. The magnitude of the load is apparently predictable from normal strength properties of the weld metal.

(2) Butt welds in which no attempt was made to introduce high residual stress, fractured in the cleavage mode at 0°F these welds had a full thickness throat and

normal reinforcement but contained flaws representing internal and external cracks ranging from 5/8 in. to 6-1/4 in. long, of 10 in. in test width and between 25 and 50% of the throat thickness. The unit gross stress at fracture, calculated on the basis of full throat welds, ranged from 39,000 psi to 60,000 psi, with a general average low value of 45,000 psi. The short flaw required the higher stress for fracture, but flaw length beyond 3 in. was not a considerable factor.

The impairment in static strength is evident, and it can be broadly stated that these flawed welds can initiate a cleavage fracture at unit stress values close to the yield-point stress of the weld metal. However, such impairment is insufficient to explain the low-stress brittle fractures met in service structures.

(3) In view of limited tests, a positive statement can not be made at this time about the effect of butt weld flaws that represent slag inclusions and porosity. Such flaws do not appear to impair static strength to the same degree that crack-like flaws do.

(4) The preliminary tests that combined static and dynamic stress effects on specimens having a short buried flaw, and a high induced bi-axial residual stress indicated that the initiation of brittle fracture was greatly affected by residual stress and the local strain rates due to dynamic effect. It was particularly demonstrated that without the presence of residual stress, continued applications of dynamic blows to produce yielding at the flaw were necessary to effect a fracture initiation from these short buried flaws.

(5) Butt welds, incorporating sharp internal or buried cracks, 1 to 1-1/2 in. in length, were placed in a concentrated field of high bi-axial residual stress initiated brittle fracture under an additional superimposed influence of static stress as low as 4000 psi at temperatures ranging from -80 to +30 F. Sharp internal flaws shorter than 1 in. although impairing static strength, did not generally initiate brittle fracture at static stresses lower than 40,000 psi. While the incidence of low-stress brittle fracture initiation is more likely at low temperatures, sufficient low-stress arrested fractures have occurred at temperatures of 0°F, +15 F, and

+30 F, indicating that the probability of occurrence is high.

Arrested fractures frequently resulted from low-static-stress fracture initiation, the arrested length of the fracture being closely associated with the rate of strain-energy release in the zone of arrest.

A further finding was that the length of the internal weld crack, in the presence of high residual stress, had little or no effect on the amount of static stress required for fracture initiation of cracks 1-1/2 in. to 3 in. in length, the maximum length investigated

(6) In the presence of biaxial residual stress, full-thickness cracks in butt welds will not consistently initiate fracture at the low stress values reported for the buried flaws, unless the length of the flaw is as short as 1/2 in. and in the presence of a relatively high residual stress field. In general, a static stress of about 40,000 psi is required, although one full thickness crack (1-1/2 in. long) did initiate fracture at a static stress of 10,000 psi. This difference in action is mainly attributed to the difficulty of developing high residual stress because of the elastic separation of the longer full-thickness crack during fabrication

Test results are not yet complete in cracks ending in the heat affected zone, but there is an early indication that 1-in. cracks will be of sufficient length to produce low-stress fracture initiation

(7) Comparisons of the results obtained from the laboratory specimens with the brittle crack propagation theory as originally conceived by Griffith, and with the energy release rate concept of Irwin, have been quite satisfactory. From these correlations, it tentatively appears that the potential of full-plate-thickness sharp cracks as sources of brittle fracture initiation may be evaluated, whether or not such flaws are subject to residual stress

The theory is also tentatively applicable as a basis for evaluating the potential of buried flaws to serve as sources of brittle fracture initiation under static stress, with or without biaxial residual stress. The theoretical view of brittle

fracture initiation from a buried flaw involves a two-stage mechanism: (1) the rapid expansion of the internal flaw cavity as the fracture proceeds from the flaw to the faces of the plate; and (2) the continuous expansion of the full-depth crack opening created by the first stage. Owing to the extremely short time delay in the change from the buried flaw to a full-thickness crack opening, the material at the tip of the crack undergoes a high strain rate which causes material separation at the crack tip. This implies that the geometrical instability, associated with the mechanism of cavity expansion, creates a quick energy release or a self-induced impact. Considering this, and the fact that the buried flaw is ideal for the establishment of a full biaxial residual stress field, these short buried flaws appear to be potentially greater sources of low-static-stress fracture initiation than short full-thickness cracks. The foregoing discussion applies to 50% and 75% internal flaws, the percentage indicating the ratio of the depth of internal flaw to the thickness of the plate.

(8) These investigations point out that while any flaw is potentially dangerous and in general impairs strength, certain environments increase the potential for brittle fracture. A singularly important factor in this environment is the presence of residual stress. Temperature contributes strongly to the environment, as do strain rate and dynamic effects.

(9) In the interest of fundamental approach, the majority of flaws of this program were simulated, controlled flaws. Future work should further examine the natural flaws that occur by chance or by malpractice. Welds in thicker plates should be included.

ACKNOWLEDGMENTS

The project has been under the general supervision of Samuel T. Carpenter, Chairman of the Department of Civil Engineering, Swarthmore College, who collaborated with Professor Roy F. Linsenmeyer in the investigational aspects of the program. We are indebted to Professor Charles W. Newlin for his able assistance in the laboratory phase of Part II of this report.

The shop work and instrumentation was supervised by Ewald Kasten. Theodore Bartholomew, Gene Gicker, Malcolm McClay, and E. F. Kasten made all specimens and the necessary experimental set-ups. Drawings of the report are credited to Richard W. Heward, Jr., Robert W. McMinn, and Alexander S. Traub, students. Mrs. John Wills typed the original manuscript.

Finally, the investigators wish to acknowledge the encouragement and advice of the Advisory Committee. We also especially wish to thank Dr. G. R. Irwin for his helpful technical advice concerning fracture mechanics.

REFERENCES

1. Griffith, A. A., "The Phenomena of Rupture and Flow in Solids," Phil. Trans., Roy Soc. of London, vol. 221-A, pp. 163-198 (1920).
2. Irwin, G. R., "Fracture," Encyclopedia of Physics (Handbuch der Physik) 6, Berlin: Springer Verlag, 1958.
3. Irwin, G. R., "Analysis of Stresses and Strains Near the End of a Crack Transversing a Plate," Journal of Applied Mechanics, 24:3, pp. 361-364 (Sept., 1957).
4. Wells, A. A., Strain Energy Release Rates for Fractures Caused by Wedge Action (NRL Report 4705), Washington: Naval Research Laboratory, March 9, 1956.
5. Wells, A. A., The Brittle Fracture Strength of Welded Steel Plates (Paper No. 6), The Institution of Naval Architects, presented at March 22, 1956, meeting.
6. Westergaard, H. M., "Bearing Pressures and Cracks," Journal of Applied Mechanics, 6:2, pp. A 49-A 53 (June, 1939).
7. Brossman, M. W., and Kies, J. A., Energy Release Rates During Fracturing of Perforated Plates (NRL Memorandum Report No. 370), Washington: Naval Research Laboratory, November, 1954.
8. Manjoine, M. J., "The Influence of Rate of Strain and Temperature on Yield Stresses of Mild Steel," Journal of Applied Mechanics, 11:4, pp. A 211-A 218 (1944).
9. Sneddon, I. N., "The Distribution of Stress in the Neighborhood of a Crack in an Elastic Solid," Royal Society of London Proceedings, Series A, vol. 187, pp. 229-260 (1946).
10. Levy, A. V., and Kennedy, Harry E., "Stresses in Circular-Patch Weld-Test Specimens," The Welding Journal, 31:9, Research Supplement, pp. 402s-405s (Sept., 1952).
11. Salmon, E. H., Materials and Structures (1), p. 525, London: Longmans, Green and Company, 1931.
12. Wells, A. A., "The Mechanics of Notch Brittle Fracture," Welding Research, 7:2, 34r-56r (1953).
13. Osgood, W. R., ed., Residual Stresses in Metals and Metal Construction. New York: Reinhold Publishing Corporation, 1954.
14. Robertson, T. S., "Propagation of Brittle Fracture in Steel," Journal of the Iron and Steel Institute, vol. 175, pp. 361-374 (1953).